

ABSTRACT

Title of Dissertation: **Self-Degrading Soft Materials: From Molecular Gels to Gel-Foams**

Faraz A. Burni, Doctor of Philosophy, 2024

Directed By: Professor Srinivasa R. Raghavan
Department of Chemical and Biomolecular Engineering

This dissertation introduces the concept of self-degrading soft materials and demonstrates three distinct platforms for such materials. Self-degrading materials autonomously transform from solids to thin liquids after a preset ‘degradation time’ without the need for external triggers or stimuli. The degradation time is programmed into the initial material through composition, allowing for precise control over the instant when the solid-liquid transformation occurs.

In the first study, we develop self-degrading molecular organogels based on dibenzylidene sorbitol (DBS) in polar organic solvents. DBS molecules self-assemble into a nanofibrous network in these gels. In the presence of an aqueous acid, the gels slowly transform from robust solids (with shear moduli $> 10,000$ Pa) to thin sols. The degradation time can be tuned from hours to days through the acid concentration and temperature. Using NMR spectroscopy and mass spectrometry, we show that degradation occurs through the acid-catalyzed hydrolysis of DBS to form benzaldehyde and sorbitol. We demonstrate applications for these self-degrading gels in time-activated valves and flow diversion devices.

The second study extends the above concept to non-aqueous systems (oils) suitable for oilfield applications, specifically addressing the critical problem of lost circulation

during oil drilling. We show that DBS organogels containing organic acids like hexanoic acid degrade in a controlled manner through esterification rather than hydrolysis. These gels exhibit unique “shrinking core” behavior where their rheological properties remain constant even as the gel mass decreases linearly with time. The degradation kinetics can be tuned through multiple parameters: acid chain length (butanoic to octanoic), acid concentration (20–80 wt%), temperature (30–75°C), and DBS concentration (0.5–2 wt%).

In the third study, we create self-degrading “gel-foams” based on polyethylene glycol diacrylate (PEGDA) and polyethyleneimine (PEI). We start with solutions of PEGDA and PEI and foam their mixture, generating bubbles of oxygen gas. Within seconds, PEGDA and PEI react to form a gel around the bubbles. Thus, the liquid foam transforms into a solid gel foam that can be lifted up by hand (bubbles remain trapped in the gel). Thereafter, the gel degrades into a thin liquid and this is because the crosslinks are cleaved by hydrolysis. The degradation time can be tuned from minutes to days based on the polymer composition. We show that such gel foams can slowly release solutes (such as dyes or antibiotics) into water over long time periods — thereby, such materials could be useful for environmental remediation of contaminated water bodies.

Collectively, this work establishes self-degradation as a versatile concept that can be implemented across multiple chemical platforms and length scales. The ability to program materials to autonomously transform after a set time opens new possibilities across various fields, from oilfield operations to environmental remediation and controlled release applications.

Self-Degrading Soft Materials: From Molecular Gels to Gel-Foams

by

Faraz A. Burni

Dissertation submitted to the Faculty of the Graduate School of the
University of Maryland, College Park, in partial fulfillment
of the requirements for the degree of
Doctor of Philosophy
2024

Advisory Committee:

Prof. Srinivasa R. Raghavan, Dept. of Chemical & Biomolecular Engineering, Chair

Prof. Peter Kofinas, Dept. of Chemical & Biomolecular Engineering

Prof. Jeffery Klauda, Dept. of Chemical & Biomolecular Engineering

Prof. Chen Zhang, Dept. of Chemical & Biomolecular Engineering

Prof. Siddhartha Das, Dept. of Mechanical Engineering, Dean's Representative

© Copyright by
Faraz A. Burni
2024

*This dissertation is dedicated to my mother,
who taught me to see the wonder
in everything around us.*

Acknowledgements

I express my deepest gratitude to my advisor Prof. Srinivasa R. Raghavan for guiding me through my doctoral studies in the Complex Fluids and Nanomaterials group. This successful endeavor would not have existed without his continual encouragement to explore new research directions. His approach to science, ability to think creatively about challenging problems, and emphasis on clear scientific communication have profoundly influenced my development as a researcher. He has truly groomed me into a scientist, and the lessons learned under his mentorship will stay with me throughout my career. I could not have asked for a better advisor and mentor for my doctoral studies.

I would like to thank my committee members: Prof. Peter Kofinas, Prof. Jeffery Klauda, Prof. Chen Zhang, and Prof. Siddhartha Das for their insightful feedback and valuable suggestions that have strengthened this work. Their diverse perspectives and expertise have helped shape this research in meaningful ways.

I am grateful to all my colleagues and friends in the Complex Fluids and Nanomaterials group, both past and present, for creating a collaborative and supportive research environment. I would like to thank Dr. Nikhil Subraveti for our enlightening discussions about both science and life that helped broaden my perspective. Special thanks to Dr. Wenhao Xu for sharing his wisdom and teaching me valuable chemistry concepts that were crucial for this work. I am particularly grateful to Morine Nader and Mahima Srivastava not only for their productive suggestions and discussions but also for making

the lab a more enjoyable place. I would also like to thank Dr. Medha Rath, Dr. Leah Borden, Dr. Hema Choudhary, Amir Hossein Mohammadi, Hannah Cho, Eylul Utlü, Ireen Philip, Irene Orueta Ortega, Paula Montero Atienza, Samantha Grasso, and Briahnah Streeter. The collaborative spirit within our group has been instrumental in bringing this research to fruition.

I am grateful to my undergraduate mentees, especially Reuben Spencer, Evan Bergstrom, Jillian Schwartz, Max Walker, Ilham Kabir, Jefferson Von, Benjamin Raufman and Abhishek Malhotra, for their enthusiasm and contributions to this research.

Finally, I would like to express my deepest gratitude to my family. To my uncle and aunt, Zafar Iqbal and Roqaiya Iqbal, who generously opened their home to me during my studies - your support made this journey possible. To my sisters, whose encouragement and faith in me never wavered. And most importantly, to my mother, whose endless love and emphasis on education laid the foundation for everything I have achieved. Her ability to nurture curiosity and wonder has shaped not just my scientific career but my entire approach to life. Words cannot express my thankfulness for her love, support, and sacrifices that have brought me to where I am today.

Table of Contents

Acknowledgements.....	iii
Table of Contents.....	v
Chapter 1 Introduction and Overview.....	1
1.1 Self-Degrading Molecular Organogels	1
1.2 Proposed Approach	2
1.2.1 Self-Degrading Molecular Organogels	2
1.2.2 Non-Aqueous Self-Degrading Gels for Oilfield Applications	3
1.2.3 Self-Degrading Gel Foams	4
1.3 Significance of This Work	5
Chapter 2 Background	7
2.1 Introduction to Gels	7
2.2 Rheology of Gels	11
2.3 Molecular Gels	14
2.4 Introduction to Foams	18
Chapter 3 Self-Degrading Molecular Organogels	21
3.1 Introduction	21
3.2 Results and Discussion	26
3.2.1 DBS Gel Synthesis and Characterization	26
3.2.2 Self-Degradation of DBS Gels	31
3.2.3 Mechanism for Self-Degradation	38
3.2.4 Applications for Self-Degrading Gels	42
3.3 Conclusions.....	47
3.4 Experimental Section.....	48
Chapter 4 Organogels that Degrade Slowly at High Temperature	51
4.1 Introduction	51
4.2 Results and Discussion	57
4.2.1 Self Degradation of DBS Gels.....	57
4.2.2 Rheological Properties During Gel Degradation	64
4.2.3 Mechanism of Degradation	66
4.2.4 Mechanistic Insights from Comparative Degradation Behavior	70
4.3 Conclusions.....	71
4.4 Experimental Section	73
Chapter 5 Self-Degrading Gel-Foams	75
5.1 Introduction.....	75
5.2 Results and Discussion	79
5.2.1 PEGDA/PEI Gel System	79
5.2.2 Self-Degrading Behavior of PEGDA/PEI Gel System	83
5.2.3 Self-Degrading Gel Foams	89

5.2.4 Demonstration of Self-degrading Foams	92
5.3 Conclusions.....	97
Chapter 6 Recommendations and Future Work.....	99
6.1 Project Summary.....	99
6.2 Recommendations for Future Work.....	103
6.2.1 Triggered and Delayed Degradation Systems.....	103
6.2.2 Extension to New Chemical Platforms	104
6.2.3 Development of Temperature-Independent Degradation Systems	105
6.2.4 Sequential Release from a Multi-Compartment Self-Degrading System	105
List of Publications	108
List of Presentations	113
References.....	113

Chapter 1

Introduction and Overview

1.1 Problem Description and Motivation

Gels are a ubiquitous class of soft materials that combine liquid-like and solid-like properties in unique ways.¹ Despite being predominantly liquid in composition (often >90% liquid), gels exhibit solid-like mechanical behavior due to the presence of a three-dimensional (3-D) network structure that entraps the liquid phase.¹⁻³ This network can be formed through various mechanisms, including polymer crosslinking, colloidal assembly, or molecular self-assembly.⁴ Gels are used in countless applications ranging from consumer products (e.g., personal care items, foods)⁵⁻⁷ to advanced technologies (e.g., drug delivery systems, tissue scaffolds).^{8,9}

While the solid-like properties of gels are crucial for many applications, there are scenarios where it would be advantageous for a gel to transform into a liquid after a specific period. Traditional approaches to trigger such gel-to-sol transitions rely on external stimuli like temperature,^{10,11} light,¹² or chemical triggers.^{13,14} However, applying such stimuli may be impractical in many real-world situations. For example, if a gel is to be used deep underground, it may be impossible to deliver light or chemical triggers. Similarly, in large-scale environmental applications, applying external stimuli across large areas would be prohibitively expensive and logistically challenging.

We therefore see a need for gels that can autonomously transform to sols after a predetermined time *without external intervention*. To our knowledge, there has been little attention on this topic, whereas gels that respond to stimuli have garnered much attention. We believe that self-degrading gels would enable new applications while eliminating the need for post-treatment cleanup or removal. Developing such gels that can be used practically is indeed challenging. How can we cause the spontaneous degradation? Can we ensure that the gel properties are maintained over the initial period while ensuring that the gel completely liquefies afterwards? Can we tune the time after which the degradation occurs? Can we ensure that the degradation products are benign and compatible with the intended use environment? These are the questions that we will address in this work.

1.2 Proposed Approach

This dissertation introduces the concept of self-degrading soft materials (gels) and demonstrates the implementation of this concept across three distinct platforms:

1.2.1 Self-Degrading Molecular Organogels

In Chapter 3, we demonstrate the first example of self-degrading molecular organogels (Figure 1.1). The gels are formed by the self-assembly of dibenzylidene sorbitol (DBS) molecules into nanoscale fibrils that create a 3-D network. In the presence of an aqueous acid, the gels degrade because the acid hydrolyzes the acetal groups in DBS. Thereby, the robust gel transforms into a liquid after a predetermined time that can be tuned from hours to days through acid concentration and temperature. Using NMR spectroscopy and mass spectrometry, we conclusively show that degradation occurs through the acid-

catalyzed hydrolysis of DBS to form benzaldehyde and sorbitol. Since these degradation products cannot self-assemble into fibrils, the nanofibrillar network gradually breaks down. We demonstrate applications for these self-degrading gels in time-activated valves and flow diversion devices.

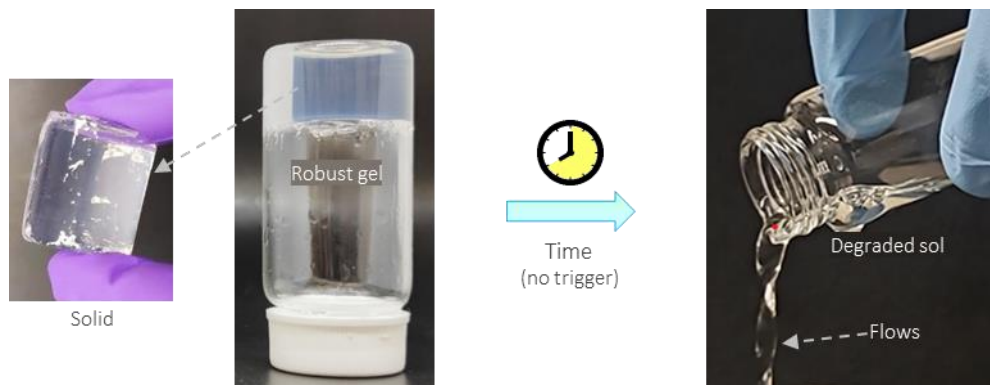


Figure 1.1. Self-degrading molecular organogels. The gel initially exhibits robust mechanical properties but spontaneously transforms into a flowing liquid (sol) after a predetermined time.

1.2.2 Non-Aqueous Self-Degrading Gels for Oilfield Applications

In Chapter 4, we extend the above concept to completely non-aqueous systems (oils) suitable for oilfield applications. We show that DBS organogels containing organic acids like hexanoic acid degrade in a controlled manner through esterification rather than hydrolysis. These gels exhibit unique “shrinking core” behavior where their rheological properties remain constant even as the gel mass decreases linearly with time. The degradation kinetics can be tuned through multiple parameters: acid chain length (butanoic to octanoic), acid concentration (20–80 wt%), temperature (30–75°C), and DBS concentration (0.5–2 wt%). These gels are particularly suitable for addressing the problem of lost circulation during oil drilling (Figure 1.2). That is, the gels will be placed in rock

fractures during drilling operations (Figure 1.2A), temporarily sealing the fractures and preventing the loss of drilling fluid. After several days, the gels will autonomously degrade (Figure 1.2B), thus restoring the permeability of the fractures and allowing oil to be extracted through these fractures (Figure 1.2C).

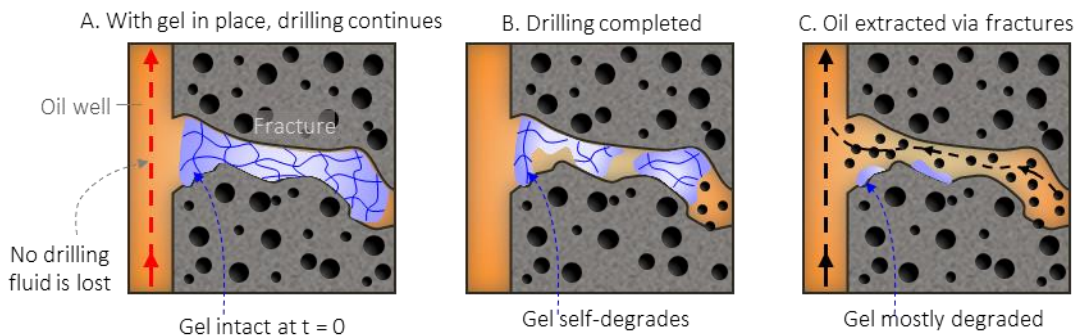


Figure 1.2. Self-degrading organogels for lost circulation control. (A) The gel temporarily seals fractures in rock during drilling operations. (B) The gel then self-degrades to a sol after several days. (C) The degradation restores permeability to the fractures, allowing oil to be extracted through the fractures.

1.2.3 Self-Degrading Gel-Foams

In Chapter 5, we create self-degrading “gel-foams” based on polyethylene glycol diacrylate (PEGDA) and polyethyleneimine (PEI). For this, we start with solutions of PEGDA and PEI and foam their mixture, generating bubbles of oxygen gas (Figure 1.3A). Within seconds, the acrylates on PEGDA and the amines on PEI react to form chemical bonds (crosslinks) and thereby a gel around the bubbles. Thus, the liquid foam transforms into a solid gel-foam that can be lifted up by hand (bubbles remain trapped in the gel) (Figure 1.3B). Thereafter, the gel-foam degrades into a thin liquid (Figure 1.3C) and this is because the crosslinks degrade by hydrolysis. The degradation time can be tuned from

minutes to days based on the polymer composition. We show that gel-foams can release solutes (such as dyes, drugs, or antibiotics) into water in a sustained manner over days. For comparison, a conventional (non-gelling) foam releases the same solutes instantly. Thus, gel-foams could be useful for environmental remediation of contaminated water bodies.

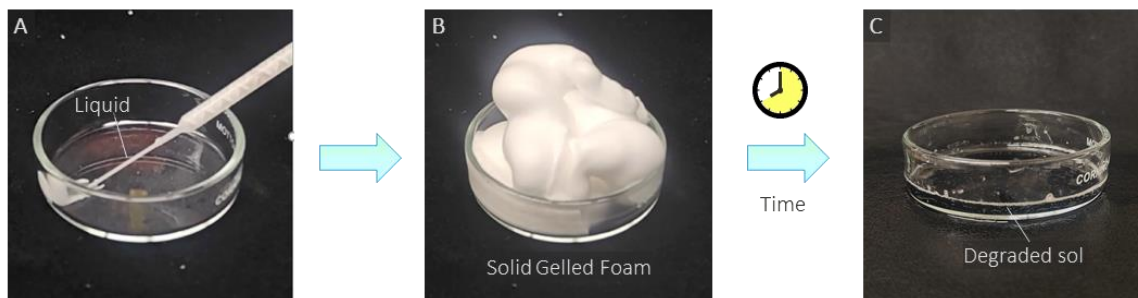


Figure 1.3. Self-degrading gel-foams. (A) The system starts as a liquid that gets foamed (i.e., bubbles of O₂ are entrapped in the liquid). (B) Within seconds, polymers in the liquid react to form a gel around the bubbles, and the sample becomes a gel-foam. (C) After a preset time, the gel-foam degrades into a thin liquid (sol) due to hydrolysis of the crosslinks in the gel.

1.3 Significance of This Work

In this dissertation, we describe new approaches for creating self-degrading soft materials. Each part of our work addresses specific practical problems while advancing material design strategies. Significant points pertaining to Chapters 3-5 are:

- In Chapter 3, we demonstrate the first example of self-degrading molecular organogels that overcome key limitations of current degradable gels. The system is robust, yet degrades completely to a thin liquid *without external triggers*. By incorporating the degradation trigger directly into the gel matrix, we eliminate the need for external stimuli (like heat or light) or harsh chemical degrading agents (that may not mix well

with the original gel). The degradation time can be precisely engineered from hours to days through the composition. We show applications for these gels in time-activated valves and programmable flow control devices.

- In Chapter 4, we propose a solution to a critical problem in oil drilling operations through non-aqueous self-degrading gels. The system addresses multiple engineering challenges: it is completely water-free, functions at elevated temperatures ($\sim 70^{\circ}\text{C}$), and maintains strong mechanical properties even during degradation. These features make the gel particularly effective for eliminating the problem of ‘lost circulation’, where the gel can temporarily seal rock fractures during drilling before autonomously degrading to restore formation permeability. The technology could significantly reduce drilling costs and improve the environmental profile of the drilling operation.
- Finally, in Chapter 5, we create self-degrading gel-foams that enable new approaches to treatment and environmental remediation of water bodies. The system solves several engineering challenges: a small volume of initial solution expands to cover a large surface area, forms a robust gel within seconds, and degrades completely after a predetermined time. These properties make it particularly suitable for delivering treatment agents to water surfaces for applications like harmful algal bloom control, where the foam can deliver algaecides that eliminate the algae before disappearing from the water surface and eliminating the need for any cleanup operations.

Chapter 2

Background

2.1 Introduction to Gels

This dissertation centers on the properties of soft materials, especially gels. The word ‘gel’ comes from the word gelatin, which is a common biopolymer that gels water.¹⁵ Gels are a fascinating class of soft materials that are common in everyday life. Many food products (e.g., Jell-O, ketchup), personal care products (e.g., toothpaste), and pharmaceutical products (e.g., gel capsules) are in the gel state.^{4,16} Beyond these everyday examples, gels play crucial roles in advanced technologies, including drug delivery systems, tissue engineering scaffolds, and oil recovery applications.^{2,17-19} What makes gels particularly interesting is their unique combination of properties: they exhibit the mechanical properties of a solid despite being mostly composed of liquid (often > 90% liquid by weight).¹⁶ Typically, gels are prepared by adding a gelling agent (gelator) to a liquid (sol).^{20,21} The gelator forms a 3-D network throughout the liquid volume, and this network immobilizes the liquid through capillary forces, causing the sample to behave like a solid.^{17,22} If the liquid is water, the resulting gel is called a hydrogel, whereas if the liquid is an organic solvent, the gel is termed an organogel.²³ This unique combination of a predominantly liquid composition with solid-like mechanical properties makes gels particularly interesting for a wide range of applications.

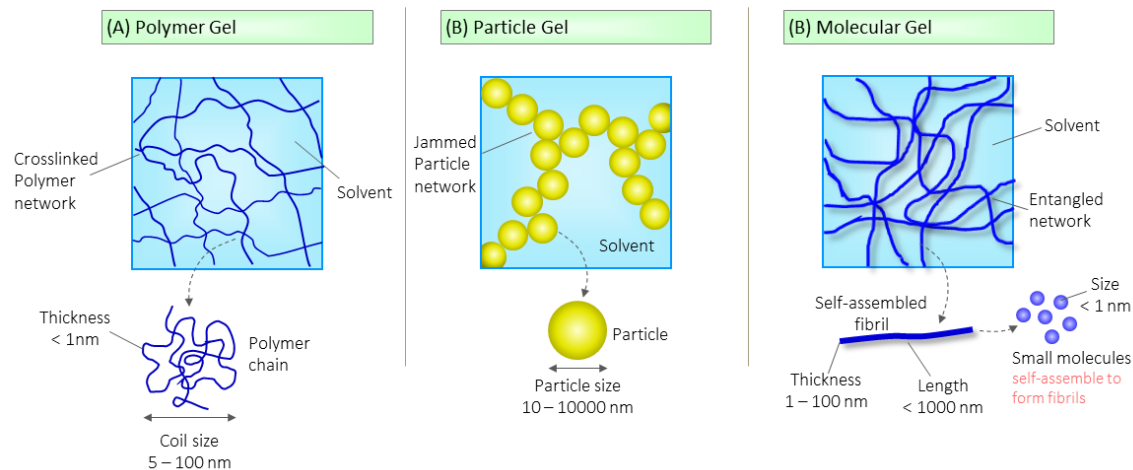


Figure 2.1. Three main types of gels classified by gelator type and network structure. In all cases, the network structure immobilizes the solvent, leading to solid-like mechanical properties. (A) Polymer gels form when long polymer chains are connected by crosslinks into a network. Individual polymer chains (shown in bottom panel) have sizes of 5-500 nm, while network mesh size can be $<1 \mu\text{m}$. (B) Particle gels arise from the aggregation of colloidal particles (10-10,000 nm) into a jammed network structure. (C) Molecular gels form through the self-assembly of small molecules ($<5000 \text{ Da}$) into long fibrils (1-100 nm thick) that entangle into a network. The fibrils form through non-covalent interactions between the molecules.

Three main classes of gels can be distinguished based on the nature of their gelator and network structure, as illustrated in Figure 2.1:

Polymer Gels: As shown in Figure 2.1A, polymers are long-chain molecules that exist as random coils when dissolved in a solvent. When these random coils are connected to each other by crosslinks, they form a sample-spanning network and the sample becomes a gel. Polymer gels can be classified into two categories based on the types of bonds that constitute their crosslinks: physical gels, where the bonds are non-covalent, and chemical gels, where the crosslinks are covalent. Examples of each are discussed below.

Chemical gels are typically formed by free-radical polymerization of a water-soluble monomer and a crosslinker.^{4,24} A classic example is the polymerization of acrylamide (AAm) with N,N'-methylenebisacrylamide (BIS). In this process, AAm (monomer with one double bond) and BIS (crosslinker with two double bonds) are mixed in water along with an initiator (e.g., ammonium persulfate, APS). Upon heating, APS generates free radicals that initiate polymerization. AAm molecules form growing polymer chains while BIS molecules connect multiple chains, creating a 3-D network.²⁵

Physical gels form through non-covalent interactions between polymer chains. One common example is gelatin, which is derived from collagen through alkaline or acidic hydrolysis.²⁶ When gelatin powder is dissolved in water above $\sim 40^{\circ}\text{C}$ and then cooled to room temperature, strands of gelatin bind to each other at junctions (where they form triple-helices) via weak non-covalent interactions. This creates a network structure in the gel.²⁷ Another important example of physical gels involves the biopolymer alginate, which is extracted from brown seaweed. Alginate is an anionic polysaccharide composed of mannuronic acid (M) and guluronic acid (G) residues. When multivalent cations (typically Ca^{2+}) are added to alginate solutions, the alginate chains become physically crosslinked through ionic gelation. The Ca^{2+} ions coordinate specifically with G-blocks on different alginate chains, creating "egg-box" junction zones that serve as physical crosslinks.²⁸ Alginate gels are widely used in biomedical applications due to their biocompatibility and their ability to form under mild conditions. Unlike gelatin gels which can be melted by heating, alginate gels are stable at high temperatures but can be reversed by removing the Ca^{2+} ions with a chelating agent.²⁹

Particle Gels: As shown in Figure 2.1B, these gels form when colloidal particles, especially anisotropic ones like rods,^{30,31} tubes,³² or platelets,³³ aggregate into a space-filling 3-D network. The network forms through particle-particle interactions, with particles typically ranging from 10-10,000 nm in size.³⁴ The particles are jammed in the network, leading to solid-like mechanical properties. Particle (colloidal) gels typically exhibit shear thinning, i.e., they behave as solids below a yield stress but flow (shear-thin) when this yield stress is exceeded.³⁵ The formation of particle gels can be understood as the opposite of particle stabilization — gelation arises when the particles attract whereas stabilization occurs when the particles repel.^{35,36} Attractive interactions between particles can include van der Waals forces, electrostatic, or steric interactions. During the process of gelation, the initial viscous liquid is converted into a self-supporting material which exhibits elastic character.^{36,37} While these systems present interesting opportunities, particle gels are not a focus of this dissertation.

Molecular Gels: As shown in Figure 2.1C, these gels form when small molecules (molecular weight < 5000 Da) self-assemble into long fibrils, which then entangle to create a 3-D network.^{20,22} The self-assembly is driven by non-covalent interactions like hydrogen bonding, π - π stacking, and van der Waals forces.³⁸ The fibril thickness is typically 1-100 nm, which is much smaller than the mesh size of the network.⁴ A key example relevant to this dissertation is dibenzylidene sorbitol (DBS), a sugar derivative that forms robust gels in many solvents through self-assembly into nanoscale fibrils.³⁸ We will discuss molecular gels of DBS in detail in Section 2.3.

This dissertation focuses primarily on molecular gels (Chapters 3-4) and chemical polymer gels (Chapter 5). Molecular gels are particularly interesting for creating self-degrading materials because their network structure relies entirely on non-covalent bonds, making them susceptible to controlled disruption through chemical triggers. The polymer gels we study involve chemical crosslinks that can be designed to hydrolyze under specific conditions, enabling programmed degradation of the network.

2.2 Rheology of Gels

Building on our understanding of gel structures from Section 2.1, we now turn to the characteristic properties that define gels and the methods used to measure them. The definitive signature of a gel is its elastic rheological response, specifically the presence of a non-zero equilibrium modulus.^{4,39} This means that a gel will not relax under a small mechanical stress even if given an infinite time, or equivalently, the gel will not flow under a mechanical stress (below a critical stress) even if the stress is imposed for an infinite period.³ The former implies an *infinite relaxation time* in a linear viscoelastic test (under dynamic rheology) while the latter indicates the existence of a yield stress below which no flow occurs (under steady shear rheology).

2.2.1 Dynamic (Oscillatory-Shear) Rheology

Rheological measurements are typically performed using a rheometer equipped with various geometries (e.g., parallel plates, cone-and-plate, or concentric cylinders) depending on the sample properties.⁴⁰ For gel characterization, parallel plate or cone-and-plate geometries are most common. Parallel plate measurements typically use gap sizes of

0.5-2 mm, while cone-and-plate geometry operates with a much smaller gap of around 50 μm at the cone tip, which helps ensure a uniform shear rate across the sample.^{40,41} In dynamic rheology, a small-amplitude oscillatory strain $\gamma = \gamma_0 \sin(\omega t)$ is applied to the sample, where γ_0 is the strain amplitude and ω is the frequency of oscillations.⁴² The sample response will be in the form of a sinusoidal stress $\sigma = \sigma_0 \sin(\omega t + \delta)$, which is shifted by a phase angle δ relative to the strain. This stress can be decomposed into two components: $\sigma = G' \gamma_0 \sin(\omega t) + G'' \gamma_0 \cos(\omega t)$, where G' is the elastic (storage) modulus and G'' is the viscous (loss) modulus.^{42,43}

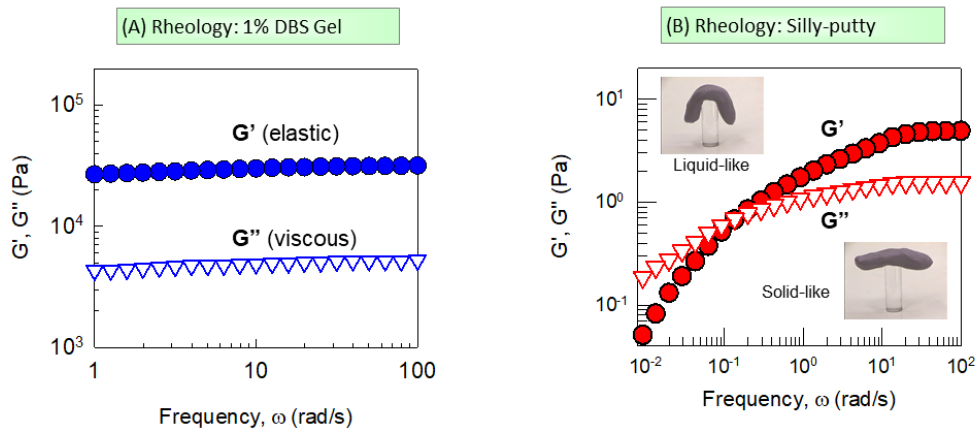


Figure 2.2. Rheological signatures of a gel and a viscoelastic material. Dynamic rheology showing the dependence of the elastic modulus G' (filled symbols) and viscous modulus G'' (open symbols) on frequency ω for two samples. (A) a true gel formed by 1% DBS: note the ω -independent G' plateau and that $G' > G''$ across all ω . (B) silly putty, which shows ω -dependent rheology, transitioning from liquid-like ($G'' > G'$) rheology at low ω to solid-like ($G' > G''$) at high ω . Inset photos in (B) show that silly putty is indeed solid-like at short times (high ω) but liquid-like at long times (low ω).

The rheological signature of a gel is shown in Figure 2.2A. Note that G' exceeds G'' over the range of frequencies ω and G' exhibits a plateau at low ω , indicating that the material does not relax over long timescales. The magnitude of G' provides a direct

measure of gel stiffness or gel strength.^{4,44} For example, robust molecular gels like those formed by DBS typically show $G' \sim 10^4$ to 10^6 Pa, while G'' is 10-100 times lower, indicating strong gel networks. In contrast, weak gels show $G' \sim 10$ to 1000 Pa. These measurements must be conducted in the linear viscoelastic regime where the moduli are independent of strain amplitude γ_0 . In contrast to gels, which are *elastic* materials, there are many materials that are *viscoelastic*. A classic example is silly putty (silicone polymer), the dynamic rheology of which is shown in Figure 2.2B. We find a crossover from solid-like behavior ($G' > G''$) at high ω to liquid-like behavior ($G'' > G'$) at low ω . This is typical of a viscoelastic material and it means that the material will flow given enough time.⁴⁵

2.2.2 Steady Shear Rheology

Under steady-shear, many gels (including particle gels and molecular gels) do not flow below a yield stress σ_y and their viscosity approaches infinity.^{3,22} Once the yield stress is exceeded, these gels show shear-thinning, where the viscosity η decreases with increasing shear rate $\dot{\gamma}$.³ This relationship often follows a power law model described by $\eta = K \dot{\gamma}^{n-1}$, where K is the consistency index and n is the power law index ($n < 1$ for shear-thinning materials).^{3,46} Many gels also exhibit thixotropy, which means that their structure and rheology recover slowly after shear is stopped.⁴⁷ Note also that crosslinked polymer gels will not show meaningful data in a steady-shear rheological experiment: the gels will splinter into pieces rather than flowing.

Dynamic rheology has several key advantages over steady shear measurements for characterizing gels. Most importantly, it allows examination of the gel structure in its at-

rest state since the small-amplitude oscillations do not disrupt the network structure. In contrast, steady shear measurements involve continuous flow and large deformations that typically destroy the gel network.⁴⁸ However, both types of measurements provide complementary information — dynamic rheology reveals the intrinsic gel structure, while steady shear measurements give insight into how the gel behaves under flow conditions relevant to processing and application.

2.3 Molecular Gels

Molecular gels are formed when small molecules (molecular weight < 5000 Da) self-assemble into 1-D supramolecular structures (i.e., chains, fibrils, filaments) that entangle to form a 3-D network.^{20,22} Small gelator molecules can gel solvents even at concentrations of 1 wt% or lower.⁸ The self-assembly of gelators is driven by non-covalent interactions including hydrogen bonding, π - π stacking, and van der Waals forces.³⁸ These directional interactions guide the molecules to stack in a specific manner, leading to the formation of long fibrils with diameters typically ranging from 1-100 nm.⁴ The fibrils can then physically wrap around one another, branch, or form insoluble structures that cannot flow past one another, creating a sample-spanning network.^{4,49,50} Unlike polymer gels where the network is held together by chemical crosslinks, molecular gels rely entirely on physical interactions, making them reversible.^{20,51}

Among the molecular gelators reported in the literature, (1,3:2,4)-dibenzylidene sorbitol (DBS) stands out as a particularly versatile and efficient gelator, capable of forming robust gels in a wide range of organic solvents.³⁸ Its structure consists of a sorbitol

backbone modified with two benzylidene groups, creating a butterfly-shaped molecule with a hydroxylated center and benzyl groups on either side (Figure 2.3). This unique molecular architecture enables DBS to self-assemble into nanoscale fibrils through a combination of non-covalent interactions, primarily hydrogen bonding through its hydroxyl groups and π - π stacking of its aromatic rings.^{38,52}

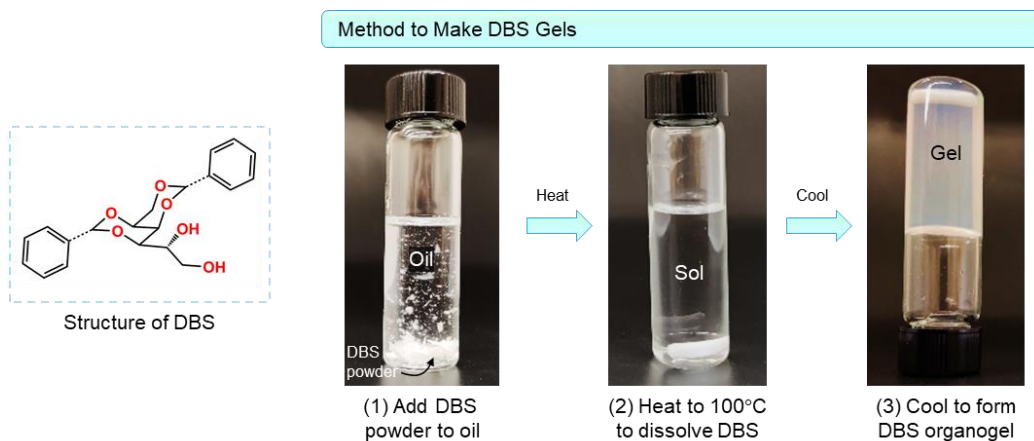


Figure 2.3. DBS and its organogels. (1) DBS (structure on left) powder is added to an oil (butanol) at a concentration of 1 wt%. (2) The mixture is heated to high temperatures ($\sim 100^\circ\text{C}$) to dissolve the DBS. At this stage, the sample is a low-viscosity sol. (3) The sample is cooled down to room temperature, whereupon it becomes an organogel.

What makes DBS particularly remarkable is its exceptional gelling efficiency — it can form robust gels at concentrations as low as 0.25 wt% in a range of solvents.⁵³ A common method to prepare DBS gels involves heating and cooling, as shown in Figure 2.3. First, DBS powder is added to the solvent and heated to $\sim 100^\circ\text{C}$ to dissolve the DBS, forming a low-viscosity sol. Upon cooling to room temperature, the DBS molecules self-assemble into long fibrils with diameters ranging from 5–50 nm. These fibrils then entangle and interconnect to create a three-dimensional network.

The rheological properties of DBS gels show a strong dependence on DBS concentration. As shown in Figure 2.4, the gel modulus G' follows a power-law: $G' \sim c^2$ with DBS concentration c .⁵⁴ Note also that the gel modulus can exceed 10^6 Pa for moderate c : this is much higher than for many other molecular gels at similar concentrations.

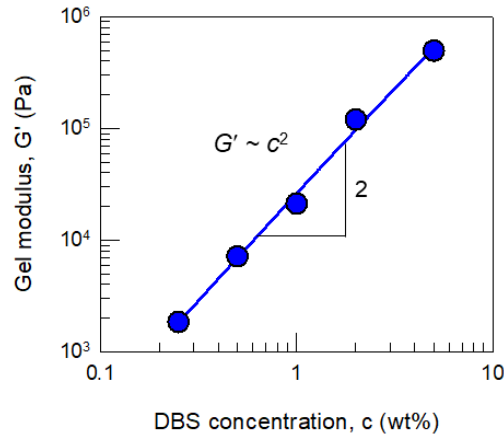


Figure 2.4. Rheology of DBS gels in hexanol as a function of DBS concentration. The gels can be characterized by the frequency-independent value of their elastic modulus G' , which can be termed the gel modulus. The log-log plot shows that $G' \sim c^2$, where c is the DBS concentration.

A distinctive feature of DBS gels is their shear-thinning behavior and rapid structural recovery, which are shown in Figure 2.5. Under steady-shear rheology (Figure 2.5A), the gel does not flow (i.e., its viscosity is infinite) at shear stresses below its yield stress (σ_y). Beyond σ_y , the viscosity drops rapidly with increasing shear-stress, indicating shear-thinning behavior. In dynamic rheology (Figure 2.5B), G' and G'' remain constant (with $G' > G''$) within the linear viscoelastic regime at low stresses. At high stresses, both moduli drop and G'' eventually exceeds G' , indicating a transition from solid-like to liquid-like behavior.

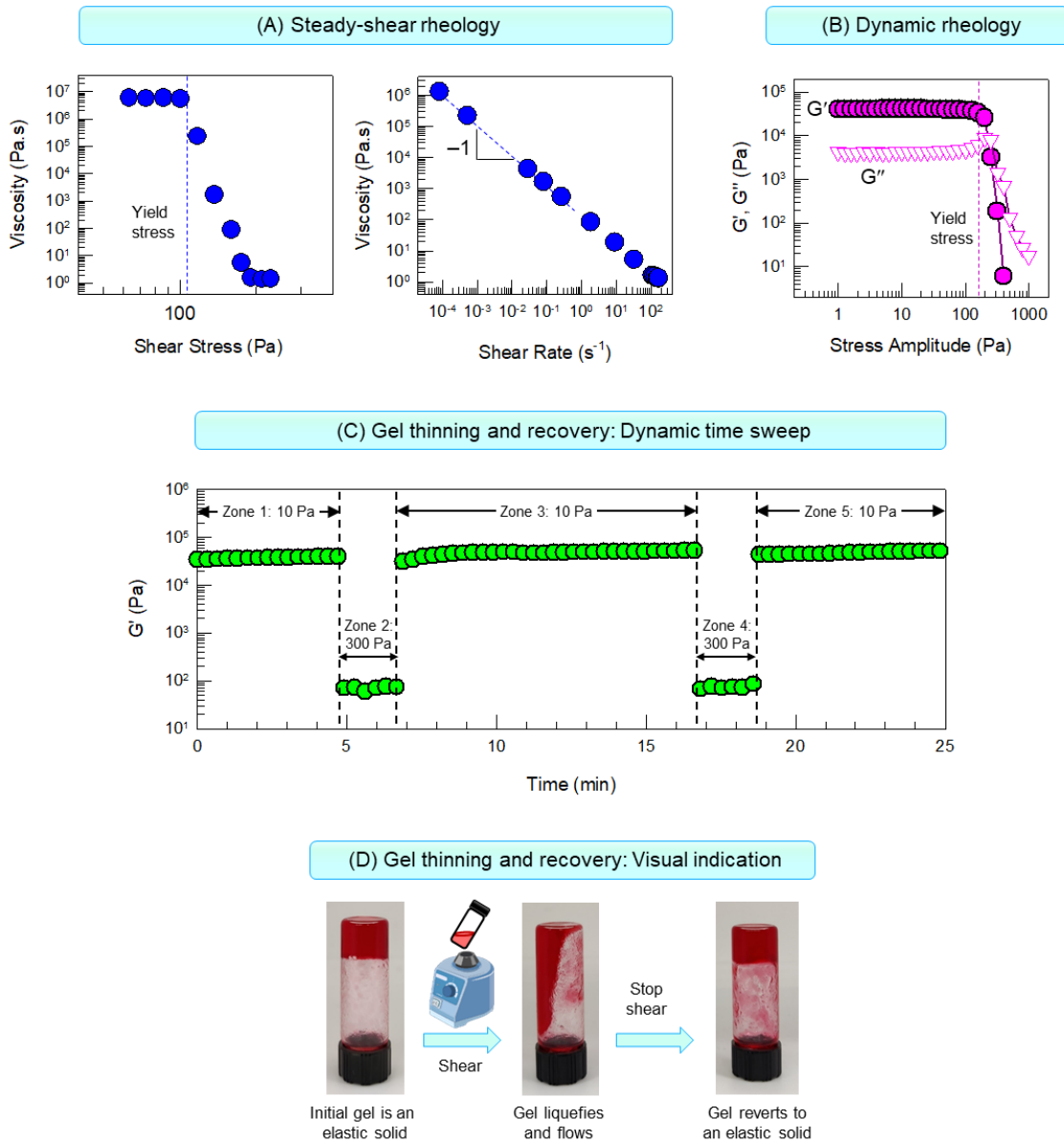


Figure 2.5. Shear-thinning behavior of DBS gels and their instant recovery after shear. The data are for a gel of 1% DBS in hexanol. (A) Data under steady-shear rheology. Above the yield stress, the viscosity decreases (i.e., the gel is shear-thinning). (B) Data under dynamic rheology showing the elastic (G') and viscous (G'') moduli vs. stress-amplitude. Beyond the yield stress, the gel shows liquid-like behavior ($G'' > G'$). (C) Gel thinning and recovery, probed by a dynamic time sweep. The elastic modulus G' is shown. In the linear regime (at a stress of 10 Pa), G' is high and the network is intact. When sheared at 300 Pa, G' drops to a low value because the network is disrupted. Thereafter, when the stress is again switched to 10 Pa, G' recovers within seconds to its initial extent, showing that the network is reformed rapidly. (D) Photos showing that the gel network is broken by shear on a vortex mixer (i.e., the sample flows) and quickly recovers after the shear is stopped. The photos are consistent with the time sweep in (C).

The breakdown and recovery of the gel structure is monitored through dynamic time sweeps (Figure 2.5C). Initially in Zone 1, the gel shows elastic behavior at low stress (10 Pa) with $G' \sim 30,000$ Pa. When subjected to high stress (300 Pa) in Zone 2, the structure breaks down and the material becomes liquid-like. Remarkably, upon returning to a low stress in Zone 3, the gel structure recovers within 30 s, with G' returning to its initial value. This cycle of breakdown and recovery can be repeated multiple times, as shown in Zones 4 and 5, demonstrating the reversible nature of the bonds in the DBS network. The practical implications of this behavior are visualized in Figure 2.5D. When a DBS gel is subjected to high shear (e.g., using a vortex mixer), it liquefies and flows. Once the shear is removed, the gel state recovers rapidly. This combination of shear-thinning and rapid recovery makes DBS gels particularly suitable for applications requiring injectable materials.

2.4 Introduction to Foams

We now discuss another class of soft materials — foams — that are relevant for Chapter 5. Foams are dispersions of gas bubbles in a liquid or solid phase.^{55,56} The stability and structure of these bubbles are governed by a balance between surface tension, which tries to minimize surface area and causes bubbles to coalesce, and the pressure difference (ΔP) between the bubble interior and exterior.^{57,58} This ΔP is given by the Young-Laplace equation: $\Delta P = 2\gamma/R$, where γ is the surface tension and R the bubble radius.^{59,60}

Foams are inherently unstable and require stabilizing agents to persist.⁶⁰ Surfactants are commonly used for this purpose — they are amphiphilic molecules with both hydrophobic and hydrophilic domains.⁵⁹⁻⁶¹ When added to a foam, surfactants adsorb at

the air-water interface, orienting their hydrophobic parts toward the air and hydrophilic domains toward water. This arrangement reduces surface tension and provides colloidal repulsion that helps prevent bubble coalescence.^{59,60} The stability of foams varies significantly with the type of stabilizer used — small molecule surfactants like sodium dodecyl sulfate (SDS) or Tween 80 provide stability for only minutes, while amphiphilic polymers can stabilize foams for hours.⁶²

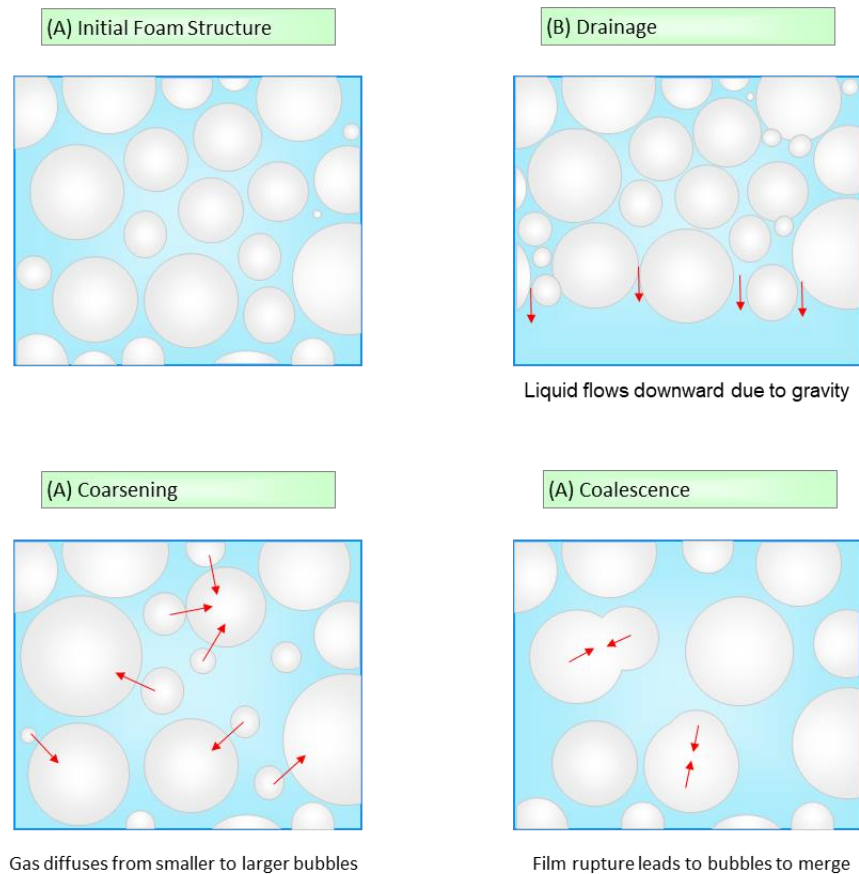


Figure 2.8. Mechanisms of foam destabilization. (A) Initial foam structure showing gas bubbles (white) dispersed in a continuous liquid phase (blue). (B) Drainage occurs as liquid flows downward through channels between bubbles due to gravity, leading to film thinning. (C) Coarsening (Ostwald ripening) involves gas diffusion from smaller to larger bubbles due to pressure differences. (D) Coalescence happens when the liquid film between adjacent bubbles ruptures, causing them to merge. Red arrows indicate the direction of liquid flow in drainage, gas diffusion in coarsening, and film rupture in coalescence.

Three main mechanisms contribute to foam instability (Figure 2.8). First, drainage occurs as liquid flows downward through channels between the bubbles due to gravity, leading to thinning of the liquid films.^{63,64} Second, coarsening (also known as Ostwald ripening) happens when gas diffuses from smaller bubbles to larger ones due to pressure differences, causing smaller bubbles to shrink while larger ones grow.⁶⁵⁻⁶⁷ Third, coalescence occurs when the liquid film between adjacent bubbles ruptures, causing them to merge into a larger bubble.⁶⁸ These processes occur simultaneously and eventually lead to complete foam collapse unless prevented by stabilizing agents.

There are several ways to generate foams. The simplest approach involves mechanical agitation to incorporate air bubbles, though this requires sufficiently viscous solutions to trap the bubbles.⁶⁹ More controlled approaches include microfluidic generation of uniform bubbles or chemical reactions that produce gas *in situ*.^{61,70} For example, mixing acetic acid (vinegar) and sodium bicarbonate (baking soda) generates bubbles of carbon dioxide (CO₂) gas.⁶¹ Similarly, the combination of hydrogen peroxide (H₂O₂) and a catalyst produces bubbles of oxygen (O₂) gas. In all cases, if stabilizers are present, the gas bubbles remain stable for a period of time ranging from minutes to several hours.

Chapter 3

Self-Degrading Molecular Organogels

The results presented in this chapter have been published in the following journal article: F. A. Burni, W. Xu, R. Spencer, E. Bergstrom, D. Chappell, J. K. Wee & S. R. Raghavan, “Self-degrading molecular organogels: Self-assembled gels designed to spontaneously liquefy after a set time.” *Advanced Functional Materials*, 34, 2403617 (2024)

3.1 Introduction

Gels are an intriguing class of soft materials that are an integral part of our everyday lives.^{4,16} Common items that we encounter routinely, including desserts like gelatin (Jell-O), consumer products like toothpaste, and pharmaceutical products like soft capsules are in the gel state — where the material exhibits solid-like (elastic) properties despite containing a high fraction of liquid.⁴ Gels are typically created by introducing a gelling agent (gelator) into a liquid.^{17,51,71-75} The gelator forms a three-dimensional (3-D) network throughout the volume, entrapping the liquid within it via capillary forces. Gelators can include polymers (long chains), which can be crosslinked into a network;^{17,71,72} colloidal particles that cluster into a network;⁷³ and small organic molecules (molecular weight < 5000 Da) that self-assemble into long fibrils and thereby into a fibrillar network.^{51,74,75} The latter will be the focus of the present study. The resulting gels are termed ‘molecular gels’ and they can be formed in water (hydrogels) or organic liquids (organogels).

In typical cases where gels are used, the gel state is critical for the success of the application or product. However, there are instances where it is advantageous for the gel to transform into a liquid of low viscosity (i.e., a sol) after a certain period. Three such

cases are illustrated in Figure 3.1. First, consider a gel that encapsulates a solute or payload within its matrix (Figure 3.1A). In some cases, delivery of the solute may require the gel to be degraded. Second, consider a gel that is being used as a fluidic valve (Figure 3.1B), with the solid gel blocking the gravity-driven flow of a liquid (i.e., the valve is closed). Subsequently, for the valve to be opened and the liquid to flow out, the gel must get transformed into a sol. Third, a variation of a valve is shown, where the gel is used to divert fluid flow (Figure 3.1C). In this case, the gel is placed in a side channel and blocks the entry of fluid into this channel. Thereby, all the fluid flows only through other channels. The scenario shown by Figure 3.1C is relevant during the extraction of oil from deep underground.^{18,76} Here, the blocking gel is introduced into fractures in oil-bearing rock and must stay in place for a period of days or weeks. After this time, it is important for the gel to get degraded, thereby allowing oil to be extracted (this application is discussed further later in Chapter 4).

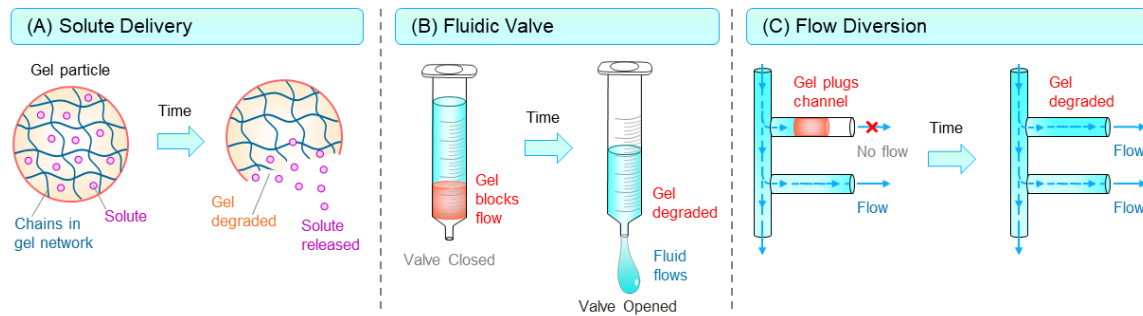


Figure 3.1. Self-degrading gels and their applications. The gels spontaneously transform into thin sols after a set time ($t = t_{\text{degr}}$). (A) A self-degrading gel particle releases encapsulated solute once the gel dissolves at $t = t_{\text{degr}}$. (B) In a fluidic valve, the downward flow of fluid is blocked as long as the gel at the bottom is intact. After $t = t_{\text{degr}}$, the gel liquefies and the valve opens. (C) The gel plugs the side channel and thus diverts flow away from this channel. After $t = t_{\text{degr}}$, the gel degrades, allowing flow to occur through the channel.

Faced with the challenges depicted by Figure 3.1, researchers have resorted to a few broad strategies. First, degradable gels have been developed that respond to external stimuli like temperature^{10,11} or light⁷⁷. For instance, the gel may be induced to degrade when exposed to UV light or when heated above a critical temperature. However, applying the relevant stimulus may be impractical in many scenarios, such as in an oilfield where the gel may be located in fractures several thousand feet underground. The second possibility is to use chemicals as ‘degrading agents’ to convert gels to sols. In this scenario, the gel is intact until it is contacted with the degrading moieties, which can include acids,¹³ bases,¹⁴ or enzymes⁷⁸. Degrading agents are widely used in oilfield applications, but they too can be problematic. One issue is that a solution of the degrading agent may only make contact with the *exterior* of the gel and thus the degradation may be confined to a small portion of the gel. In other words, the gel, being a solid, cannot be easily mixed with an external liquid. Also, if the degrading agent is a harsh chemical, it may cause undesired effects on the environment surrounding the gel. Thus, degrading agents may not be deployable in many cases.

The concept explored in this chapter is that of *self-degrading* gels, which will degrade even if left undisturbed under ambient conditions, i.e., without contact with either external stimuli or chemicals in the external medium. The key variable that dictates the degradation will then be *time*. In other words, the time t after which the gel degrades, i.e., $t = t_{\text{degr}}$, is *programmed* into the initial gel via the composition. This is indicated in Figure 3.1 for each of the three cases. For instance, in Figure 3.1B, over the duration that the gel

is intact ($t < t_{\text{degr}}$) the valve will be closed, but once $t = t_{\text{degr}}$ is reached, the gel will dissolve (i.e., convert to a sol) and the valve will open.

Our goal in this work is to make a self-degrading *molecular* gel, rather than one using polymers. After a polymeric gel degrades,^{19,79-84} the residue will still be long chains and the solution will remain viscous. However, after a molecular gel degrades, only the small gelator molecules will remain, i.e., the degradation will be *complete* and the solution will thus have a very low viscosity. Moreover, because molecular gels form fibrils via non-covalent bonds, the gels will be *shear-thinning*, i.e., shear will break the bonds and transform the gels into a flowing liquid. Hence, the gels can be pumped down an oil well or injected into a cavity using a syringe. Polymer gels held by covalent bonds will splinter into pieces when sheared rather than shear-thin.

To our knowledge, molecular gels with the ability to self-degrade have not been reported thus far. Here, we report for the first time a class of self-degrading organogels based on the self-assembly of small gelator molecules. The gels are (a) extremely strong and robust at the initial state, i.e., at time $t = 0$, the gel modulus G' is $> 10,000$ Pa; and (b) they are able to degrade spontaneously into thin sols ($G' \sim 0$) after a pre-determined period of time when left undisturbed. The degradation time t_{degr} can be set to be minutes, hours, or days at a given temperature. We make these gels using the organogelator (1,3:2,4)-dibenzylidene sorbitol (DBS).^{38,52,53,85-87} DBS is a derivative of the sugar-alcohol sorbitol and forms robust gels in a range of organic liquids, including both polar and non-polar ones. Gelation occurs because DBS self-assembles into nanoscale fibrils, which connect to

form a 3-D network.^{38,52,53,85,86} We will show that the key to self-degradation is to incorporate an acid (e.g., hydrochloric acid, HCl) into the DBS gel. The choice of acid and its concentration sets the kinetics of gel degradation and thereby the t_{degr} at a given temperature. We use NMR and mass spectrometry to pinpoint the degradation mechanism, which involves slow conversion of DBS into small molecules that cannot self-assemble. Self-degrading DBS gels are low-cost and environmentally benign. We have devised a way to prepare the gels easily in large quantities (> 1000 L) at room temperature. The use of these gels could be a game-changer for oil recovery, which could be done in a safer, more efficient and sustainable manner (due to reduced consumption of drilling fluids; see later in the chapter 4). The concept shown here could also facilitate delivery applications in the pharmaceutical, cosmetics, and agrochemical industries.

3.2 Results and Discussion

3.2.1 DBS Gel Synthesis and Characterization

We first discuss how we make molecular gels of DBS in different organic solvents. The structure of DBS (Figure 3.2) shows that it is a butterfly-shaped molecule with two aromatic rings on either side and a central rigid ring that contains hydroxyl (–OH) groups. Conventionally, gels of DBS,^{38,52,53,85,86} as with other molecular gels,^{51,74,75} are made by heat, which is depicted in Figure 2.3. DBS powder is added to the solvent and the mixture is heated to a high temperature ($> 100^{\circ}\text{C}$),^{38,53} whereupon the powder dissolves in the solvent and forms a thin, transparent sol. In this state, DBS molecules are either unaggregated or in small clusters. The sol is then slowly cooled to room temperature, and over that time (which can be a few hours), DBS molecules self-assemble into long nano-fibrils by non-covalent bonds: specifically, hydrogen-bonding (of the –OH groups) and pi-pi stacking of the aromatic rings.^{38,53} These nano-fibrils entangle with each other, forming a 3-D network, and accordingly, the sol transforms into a gel.

The above conventional method for synthesizing DBS gels (or any similar molecular gel) has its limitations due to the necessity for high heat followed by slow cooling. This method is both energy-intensive and time-consuming. In oilfield applications, gels will have to be prepared in the field at remote locations. Bulky heaters will be needed to achieve the high temperatures required, and these will also have to be transported to the field location. Heating large volumes of liquids on an operating platform imposes safety concerns as well as higher costs. To avoid these issues, we have devised a

novel and much simpler route for making DBS gels, which is shown by Figure 3.2. This route eliminates the need for heating and is entirely done at room temperature.



Figure 3.2. DBS organogels and their preparation by a simple new method at room temperature. The structure of DBS is shown in the box. To make the gel, a stock solution of 15% DBS in DMSO is first prepared by simply mixing the two at room temperature. (A) The oil to be gelled is then taken in a vial (here it is 2 g butanol). The stock solution (0.14 g) is added such that the DBS concentration in the mixture becomes 1%. (B) The sample is then mixed by hand or using a vortex mixer for a few seconds. (C) Right afterward, the sample becomes an organogel due to the self-assembly of DBS into a nanofibrillar network. This method to form DBS gels is simple, quick and does not require heat.

First, we dissolve DBS in dimethyl sulfoxide (DMSO). DMSO is known to be chemically similar to DBS. For example, in a previous study we showed that DBS and DMSO have very close solubility parameters.⁵³ Due to the chemical similarity, DBS does not gel DMSO and instead, it readily dissolves (up to 25% by weight) in DMSO without the need for heat. We can just add DBS powder to DMSO and gently stir the mixture to obtain a clear solution. Here, we prepare a stock solution of 15% DBS in DMSO. We then add measured quantities of this stock solution to the organic solvent to be gelled. In Figure 3.2, the solvent is butanol. DBS is an efficient gelator of this solvent, with just 0.25 to 1% of DBS enough to form a gel. This is because DBS and butanol are chemically dissimilar,

i.e., their solubility parameters are far apart.⁵³ To make the gel, we add 0.14 g of the DBS stock solution to 2 g of butanol in the vial (to achieve a DBS concentration of 1%) (Figure 3.2A). The resulting mixture is gently mixed, either by hand or using a vortex mixer (Figure 3.2B). Within seconds after the mixing is complete, we have a uniform and robust gel of 1% DBS in butanol. A photo of this gel holding its weight in an inverted vial is shown in Figure 3.2C — note the bluish tinge of the gel, which is due to light scattering from the DBS nano-fibrils.^{38,53}

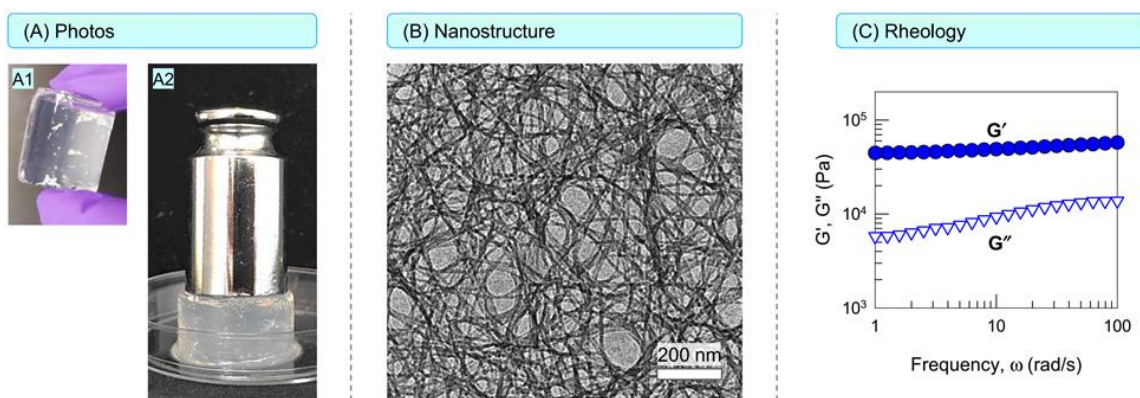


Figure 3.3. Photos, nanostructure, and rheology of a typical DBS gel. The gel is composed of 1% DBS in butanol. (A) Photos reveal that the gel is a free-standing solid that can support a weight of 100 g on top of it. (B) The nanostructure of the gel is shown via a TEM micrograph and it reveals a dense network of nano-fibrils. (C) Dynamic rheological data on the gel are shown in a plot of the elastic (G') and viscous (G'') moduli as functions of the angular frequency ω . The sample exhibits the expected rheology of a gel (i.e., $G' > G''$, G' independent of ω).

The above method of gel synthesis is simpler, faster, more convenient, and requires much less input of energy than the conventional method. Starting from the preparation of the stock solution, the entire process takes just 10 min at room temperature. This is a significant reduction in synthesis time compared to the conventional route, which can take

hours for heating and cooling (see also 2.3). We will show presently that DBS gels made by the two routes are nearly identical. Our method can also be extended to any other class of molecular gels. The one requirement is to know the solvent in which the gelator readily forms a thin solution (similar to DMSO in the case of DBS). The identity of such a solvent may either be known from experimental studies with the gelator or could be identified a priori from estimations of solubility parameters.^{53,74}

The nanostructure and rheology of the 1% DBS gel in butanol are presented in Figure 3.3. A representative image of the nanostructure from transmission electron microscopy (TEM) is shown in Figure 3.3B. As expected, a network of nano-fibrils is found in the gel, with the fibrils ranging in diameter from 5 to 50 nm. This is consistent with previous reports of the nanostructure in DBS gels.^{38,52,85,86} Next, the dynamic rheological response of the gel is shown in Figure 3.3C. This is a plot of the elastic (G') and viscous (G'') moduli as functions of the angular frequency ω . The rheology is that expected of a gel: i.e., G' surpasses G'' by an order of magnitude and both moduli are independent of ω .^{44,88} The frequency-independence of the moduli indicates that the network does not relax, i.e., the bonds between DBS molecules in the network are durable and do not dissipate over time. Gels can be characterized by their value of G' , which is the gel modulus. For the 1% DBS gel, G' is $\sim 20,000$ Pa, indicating a robust gel. Figure 3.4 plots G' and G'' vs. ω for the same DBS gel prepared using our simple (no-heat) method and the conventional (heat) method. The moduli are close for both the samples, indicating that the gels are comparable. Note that a very small amount of DMSO (from the stock solution) still remains in the butanol gel prepared by our simple method, but this DMSO

does not have any appreciable effect on the gel rheology. For the rest of the studies in this chapter, we will employ the simple method for making our gels.

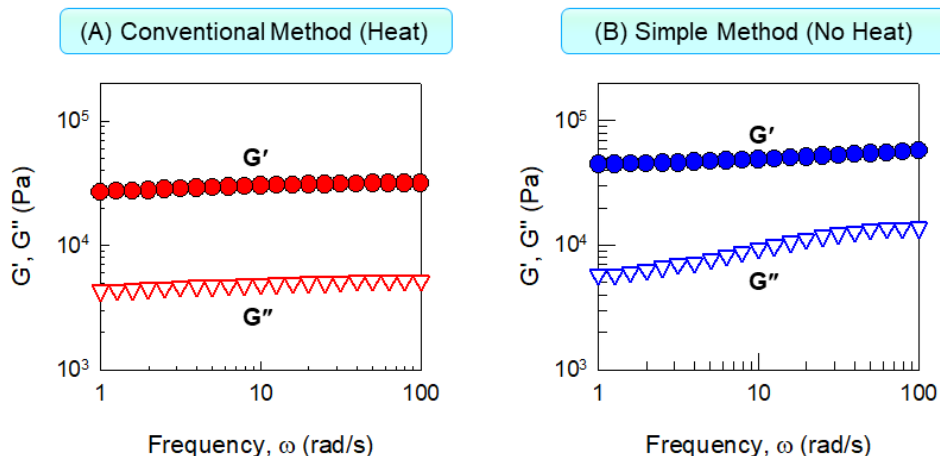


Figure 3.4. Comparing the dynamic rheology of DBS gels made by the conventional and simple methods. Plots of the elastic (G') and viscous (G'') moduli as functions of the angular frequency ω are shown for gels of 1% DBS in butanol prepared by (A) the conventional method, which involves heat (see Figure 2.3) and (B) the simple method, which involves no heat (see Figure 3.2). Both gels show similar rheology.

We emphasize that DBS gels are remarkably strong and robust. In fact, we are not aware of any molecular gels that exhibit similar strength at gelator loadings of just 1% by weight. This point is underscored by the photos in Figure 3.3A of the 1% DBS gel in butanol. We show that the gel can be taken out of the vial and held between one's fingers (A1) or placed on the countertop (A2). These observations indicate that the gel has ample rigidity — i.e., a sufficiently high gel modulus G' — to be a free-standing solid.^{44,88} Most molecular gels, on the other hand, have a paste-like consistency (akin to ketchup).^{51,74,75} While paste-like gels can hold their weight in inverted vials, they cannot be removed out of the vials and manipulated as discrete solids. Moreover, Photo A2 further highlights the

strength of the DBS gel on the countertop: on top of the gel weighing just 5 g, we place a 100 g steel weight — and the gel is able to withstand and support this load. Even free-standing polymer gels (e.g., gelatin gel desserts) will collapse under such a load.^{44,88} Thus, DBS gels are indeed very strong. At the same time, they are also shear-thinning, i.e., they transform into flowable liquids when sheared.^{38,53} We will return to this point later in the chapter.

3.2.2 Self-Degradation of DBS Gels

DBS organogels are very stable, remaining intact and unchanged over long periods (more than a year) under ambient conditions. They withstand contact with strong bases (e.g., sodium hydroxide, NaOH), powerful oxidizing agents (e.g., potassium permanganate, KMnO_4), or reducing agents (e.g. sodium thiosulfate, $\text{Na}_2\text{S}_2\text{O}_3$) without any signs of degradation. For example, Figure 3.5 shows a DBS gel in hexanol at the bottom of three vials. Above this gel, we add 5 g of 1 M KMnO_4 , $\text{Na}_2\text{S}_2\text{O}_3$, and NaOH respectively, in the three vials. After two weeks, the gel in each vial is unchanged in appearance and rheology from its initial state. However, our investigations revealed that strong acids did have an effect on DBS gels, causing their gradual transformation into thin sols. The degradation was slow enough that we could harness it for spontaneous self-degradation — where an initially robust DBS gel degrades over time.

The degradation of DBS gels can be accomplished with various kinds of acids and with gels formed in a variety of organic solvents. First, we will consider the simplest case of a *polar* organic solvent in which an *aqueous acid* such as hydrochloric acid (HCl) can

be dissolved. DBS is well-known to gel a variety of polar solvents, including ethylene glycol (EG), polyethylene glycol (PEG), and aliphatic alcohols like butanol and hexanol. Note that the gel in Figures 3.2 and 3.3 was that of DBS in butanol. As a model system for this study, we have chosen a PEG of molecular weight 200 Da. This PEG is non-volatile and miscible with water, making it a convenient solvent for our work. Moreover, PEGs are biocompatible solvents that are used in drug and vaccine formulations and even as electrolytes for rechargeable batteries.^{52,86} Hence, self-degrading gels of PEG could be of wide interest.

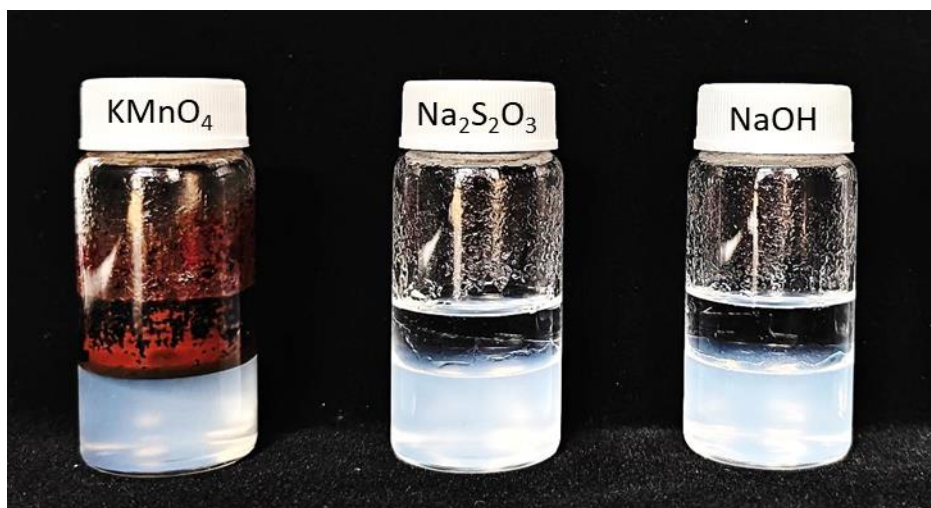


Figure 3.5. Stability of DBS gels to strong chemicals. Each vial contains 5 g of a 1% DBS gel in hexanol. Above the gel in each vial, 5 g of various aqueous solutions were added: left to right: 1 M of potassium permanganate (KMnO_4 ; strong oxidizing agent), 1 M of sodium thiosulfate ($\text{Na}_2\text{S}_2\text{O}_3$; strong reducing agent), and 1 M of sodium hydroxide (NaOH ; strong base). The photo taken two weeks later shows that the gels remain intact and unaffected by the chemicals in all three cases.

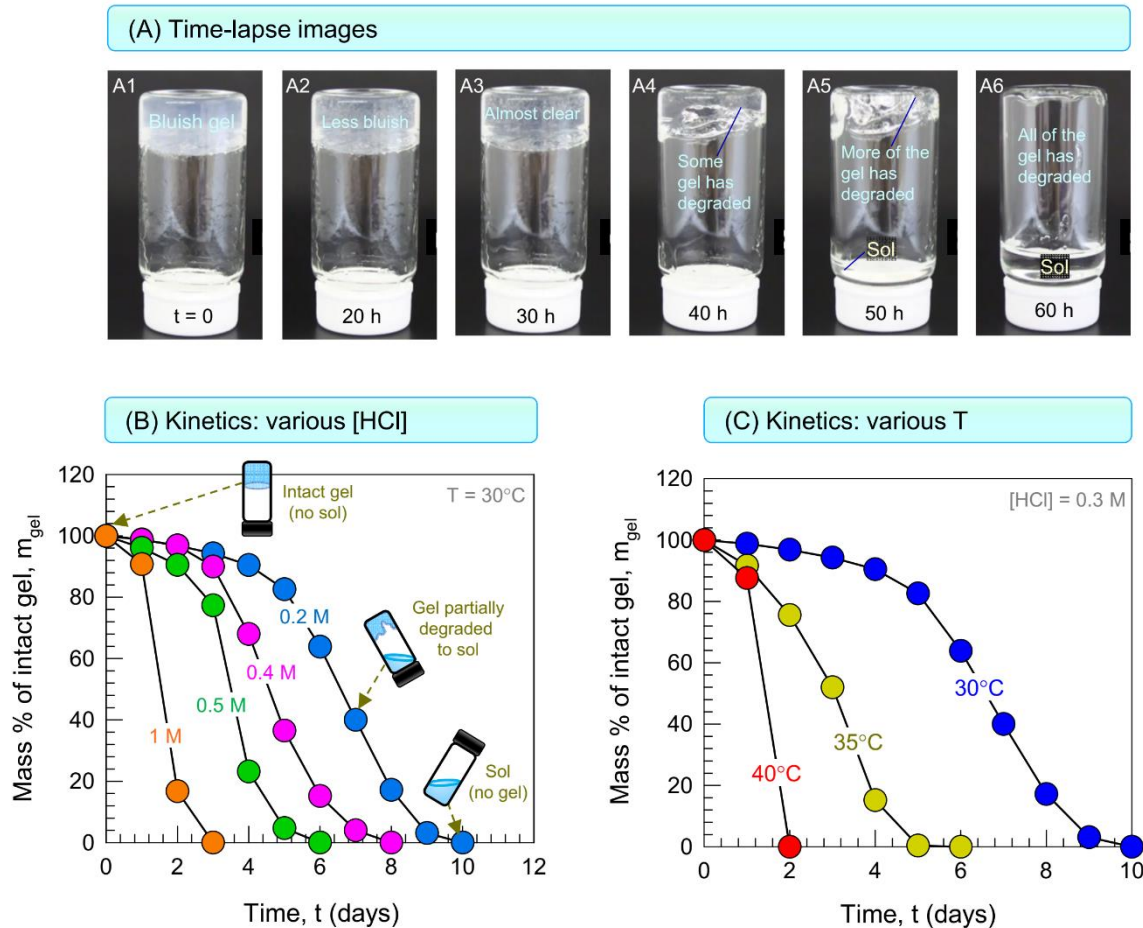


Figure 3.6. Self-degradation of DBS gels over time. (A) Time-lapse images showing the self-degradation of a gel over 60 h at room temperature. The gel is made with 2% DBS in a 80/20 mixture of PEG and acidic water (1 M HCl). With increasing time t , the gel liquefies and the mass fraction of intact gel (m_{gel}) at the top of the inverted vial decreases with t . By the end of the 60 h period, the gel has completely liquefied to a sol, i.e., m_{gel} drops to zero. (B) Plots of m_{gel} vs. t for varying [HCl] (0.2 to 1 M) at a constant temperature T of 30°C. (C) Plots of m_{gel} vs. t for varying T (30 to 40°C) at a fixed [HCl] of 0.3 M.

Initial results demonstrating self-degradation of PEG-based gels are shown visually in Figure 3.6A. We first combined PEG with aqueous HCl (1 M) in an 80/20 weight ratio. The combined liquids formed a homogeneous solution. We then converted this solution into an organogel using 2% DBS through our simple no-heat method. This gel was then left undisturbed and monitored over time at room temperature. The sample was placed in

an inverted vial, which allows us to assess whether it is in the gel state. Initially, at $t = 0$, the gel holds its weight upon vial inversion (A1), indicating that the gel modulus is high and its yield stress exceeds gravity.^{44,53} Note also the bluish tinge of the gel. Around the 20 h mark, we begin to see some visual differences (A2): the gel is still intact and holding its weight, but it is noticeably less bluish. The same trend is evident at the 30 h mark (A3) as the gel appears rather colorless. The loss of bluish tinge indicates weaker scattering of light, and it implies that either there are fewer nano-fibrils in the gel or the fibrils are smaller in diameter or length.⁸⁹ At the 40 h mark (A4), we see a reduction in the gel volume at the top of the inverted vial. This clearly means that some of the gel has degraded — and indeed this degraded gel has converted to a thin sol, which collects at the bottom of the vial (not evident in the photo because its volume is small). At the 50 h mark (A5), there is a further reduction in the gel volume. Finally, after 60 h (A6), all the remaining gel has converted to a sol and now this clear liquid has sufficient volume to be seen at the bottom of the vial.

Figure 3.6A shows that the gel spontaneously degrades over a period of 60 h. Importantly, in the initial stages (over the first 20 h), the gel is strong and indistinguishable from a regular non-degrading DBS gel. But over the next 40 h, the gel slowly liquefies until at the end, we have a clear, homogeneous sol. During the intermediate stages (40 to 60 h), the intact gel coexists with the sol. We can thus measure the mass fraction of intact gel (m_{gel}) over time t to monitor the kinetics of gel degradation. Details on how we do these measurements are discussed in the Experimental Section. The key variables that impact the rate of degradation are: (a) the acid concentration; (b) the acid amount (weight fraction); and (c) the temperature. We focus on (a) and (c) while keeping the acid weight fraction at

20%, i.e., a 80/20 mixture of PEG/acidic water. One reason for this is that DBS is insoluble in water on its own and thus the weight fraction of acid cannot be increased indefinitely.

First, we discuss the effect of acid concentration (Figure 3.6B). The data are for 2% DBS gels in 80/20 PEG/acid, with the molarity of the acid (HCl) ranging from $[HCl] = 0.3$ to 1 M. The temperature was held constant at 30°C. Figure 3.6B shows that m_{gel} drops from 100% (all gel) to 0% (all sol) over a period of days for each acid concentration, with a faster decrease at higher $[HCl]$. All curves exhibit an inverse-sigmoidal shape, with an initial lag in m_{gel} followed by a sharp drop and eventually a plateau at zero. The degradation time t_{degr} can be defined as the time for the gel to degrade completely (i.e., when $m_{gel} = 0$) or the time at the mid-point of the sigmoidal curve (i.e., when $m_{gel} = 50\%$). In either case, t_{degr} decreases as $[HCl]$ increases. For example, if $[HCl] = 0.3$ M, t_{degr} (for $m_{gel} = 0$) is 10 days, whereas t_{degr} is reduced to just 3 days when $[HCl] = 1$ M.

Next, we discuss the effect of temperature T on gel degradation (Figure 3.6C). We prepared gels of 2% DBS in 80/20 PEG/acid ($[HCl] = 0.3$ M). The gels were then subjected to different T : 30°C, 35°C, and 40°C, and in each case, we measured m_{gel} over time. As before, m_{gel} gradually decays to zero over a span of several days, with all curves having an inverse-sigmoidal shape. The higher the T , the faster the decay. This can be quantified via the decrease in t_{degr} (for $m_{gel} = 0$) as T increases. Specifically, t_{degr} decreases from 10 days at 30°C to 6 days at 35°C and further to 2 days at 40°C. Similar decrease in t_{degr} with T is reported in Incidentally, we have also tried higher temperatures: for $[HCl] = 0.3$ M at 70°C, the gel degrades in just 2 h (data not shown).

As the gel spontaneously degrades, how does its rheology change? To probe this, we conducted dynamic rheology on the intact portion of the gel at different time points as it underwent degradation. From the data, the gel modulus G' is plotted vs. t in Figure 3.7. The experiments were done in two ways, much like those in the previous figure. First, we held the temperature constant at 30°C and varied the acid content. The data in Figure 3.7A are for 2% DBS gels in 80/20 PEG/acid, with the [HCl] ranging from 0.2 to 1 M. The acid sets the initial value of G' — the more the acid, the lower this G' . Thereafter, G' decays exponentially, and the decay is also faster at higher acid content. The exponential nature of the decay is shown clearly by the semilog plot in the inset, where the G' axis is on a log scale while t is on a linear scale. The straight lines on this plot confirm the exponential form of the decay and the slope of the line is steeper when the [HCl] is higher. We also measured the rheology at various T while holding [HCl] constant. The data for 2% DBS gels in 80/20 PEG/0.2 M [HCl] at three T are shown in Figure 3.7B. Note that the initial gel modulus G' is insensitive to T — thus, all three curves start from the same value of G' . However, the decay in G' is faster at higher T , and this is evident from the inset semilog plot, where a steeper slope is observed at higher T .

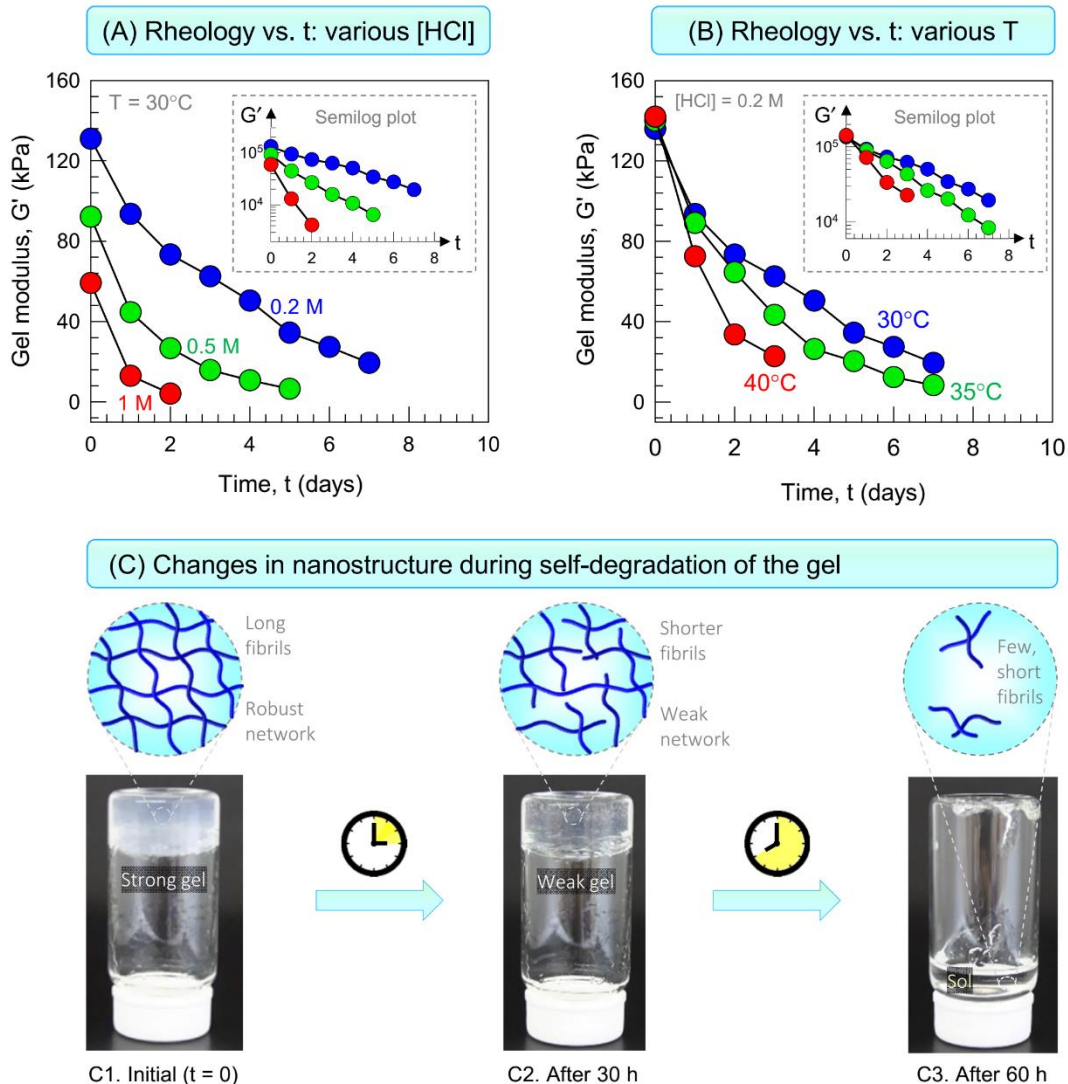


Figure 3.7. Self-degradation of DBS gels over time. Changes in rheology and nanostructure during the self-degradation of DBS gels over time. The intact portion of the gel remaining at a given time t is studied by dynamic rheology and the gel modulus G' is extracted and plotted vs. t . Gel compositions are same as in Figure 3.6. (A) Plots of G' vs. t for different [HCl] at a constant temperature T of 30°C . (B) Plots of G' vs. t for different T at a fixed [HCl] of 0.2 M. The plots show an exponential decrease in G' over time. Consistent with the exponential decay, semilog plots (insets) of the data fall on straight lines. (C) Based on the rheology, the nanostructure of the gel is postulated to change as depicted. As the gel degrades, some of the DBS nano-fibrils disappear and thereby the network becomes less dense and hence weaker (i.e., G' drops). Eventually, only short fibrils remain (i.e., the network ceases to exist) and the gel becomes a sol.

Collectively, the data in Figures 3.6 and 3.7 reveal the nanostructural transition depicted in Figure 3.7C. As DBS reacts with the acid, we can hypothesize that the molecule is being transformed to a form that cannot assemble into nano-fibrils. It is well-known that the G' of DBS gels increases with DBS concentration c in a power-law with a slope around 2, i.e., $G' \sim c^2$.^{52,53} This is also reflected in our own data; see Figure 2.4. Thus, the decrease in G' with t reflects a lowering of the DBS concentration that is part of the fibrillar network. This is shown in Panel C2 of Figure 3.7 as a network that is less dense than the initial network in Panel C1 (in other words, the mesh size ξ of the network increases with t). Note also that, during the initial period of the degradation, although G' drops with t , the gel has sufficient integrity to entrap all the solvent and retain its weight in the inverted vial. This explains why we see the ‘lag phase’ in the m_{gel} vs. t plots in Figures 3.6B and 3.6C. During this lag period, m_{gel} is close to 100%, i.e., there is negligible sol fraction coexisting with the intact gel. As G' drops further with t , a point is finally reached when the fibrillar network no longer spans the sample volume, and at that stage, some of the gel converts to a viscous sol. The sol fraction keeps growing with t until at the end, only the sol is left behind. In the sol, we expect to find only small fibrillar clusters, as shown in Panel C3.

3.2.3 Mechanism for Self-Degradation

What exactly is the chemical reaction between DBS and acid? Why does this reaction lead to gel degradation? To elucidate the mechanism, we turned to Nuclear Magnetic Resonance (NMR) spectroscopy and Mass Spectrometry (MS).

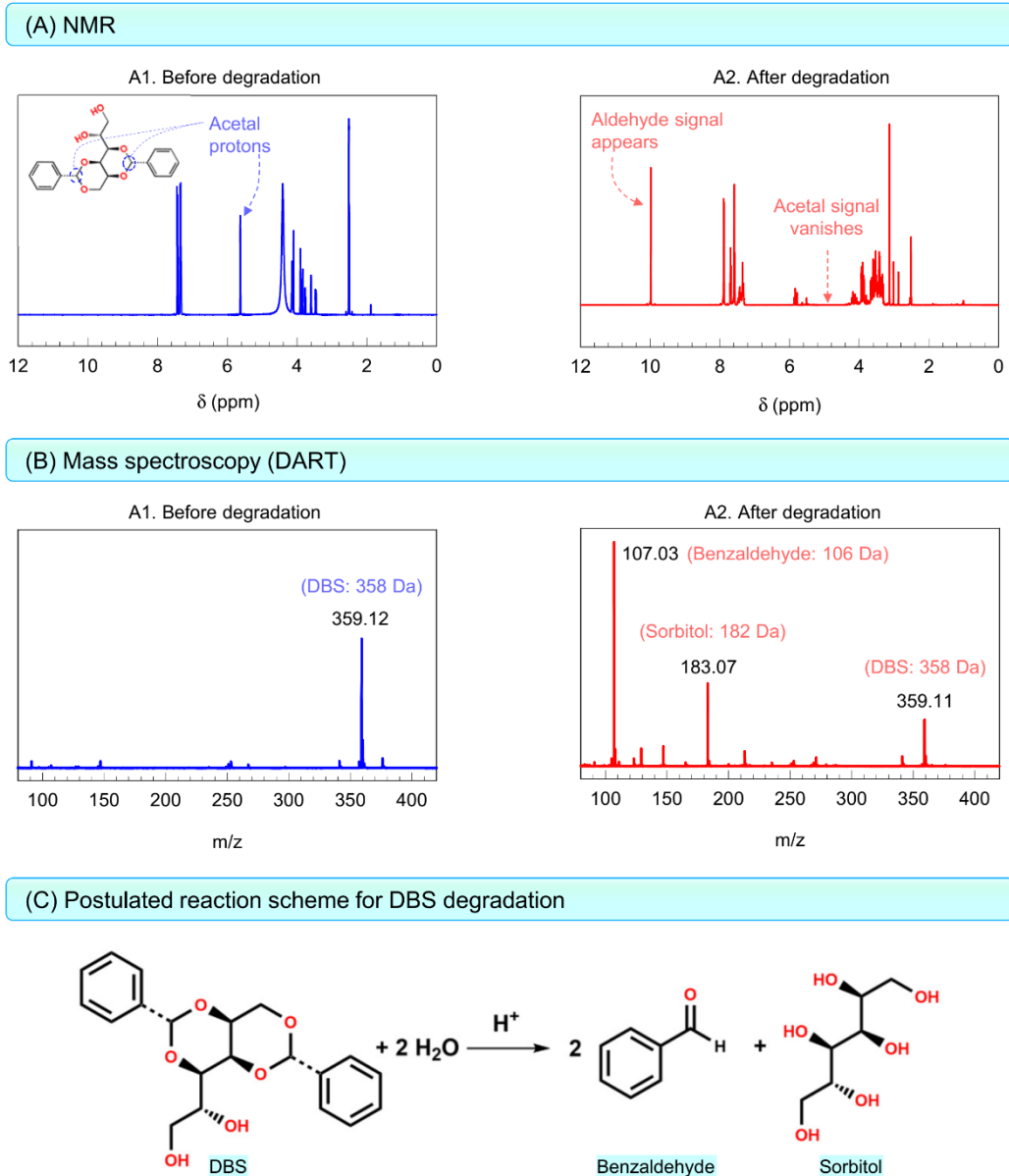


Figure 3.8. Deciphering the mechanism for self-degradation of acid-containing DBS gels. (A) ¹H NMR spectra of 1% DBS in 95/5 d-DMSO/1 M HCl in D₂O. The initial (undegraded) sample shows signals corresponding to the acetal protons whereas in the degraded sample, the acetal signals vanish and an aldehyde signal appears. (B) Mass spectroscopy (DART) of a 2% DBS gel in 80/20 PEG/0.3 M HCl. Before degradation, a DBS peak is seen. After degradation, additional peaks corresponding to benzaldehyde and sorbitol appear. (C) The data imply the reaction scheme shown, where the acetals in DBS are slowly hydrolyzed in the presence of the acid, leading to the formation of benzaldehyde and sorbitol.

First, we present data from ^1H NMR in Figure 3.8A. We analyzed two samples, each containing 1% DBS in 95/5 DMSO/HCl. The DMSO was deuterated (DMSO- d_6) and the acid (1 M HCl) was also prepared using deuterated water (D_2O). One sample was analyzed right after preparation (before the DBS degraded), while the other sample was incubated at 40°C for a week before analysis (to allow the DBS to degrade). The NMR spectra reveal significant differences between the two samples. Notably, the signals corresponding to the acetal protons of DBS are present in the initial sample (A1), but these signals vanish in the degraded sample (A2). In the latter, a new signal indicative of an aldehyde proton emerges. This observation suggests that the acid hydrolyzes the two acetal groups in DBS to form a product containing an aldehyde. We will show presently that this product is benzaldehyde.

To further investigate the degradation products, the DBS samples were subjected to MS, specifically via the Direct Analysis in Real Time (DART) technique.⁹⁰ In this technique, the sample is ionized by the addition of a proton, resulting in a +1 charge and an increase in the mass of the molecule by one. Thus, the mass-to-charge ratio (m/z) corresponds to the molecular weight (MW) of the species plus one. DART was used on a 2% DBS gel in 80/20 PEG/0.3 M [HCl] before and after degradation (Figure 3.8B). The DART spectrum of the initial gel (B1) primarily exhibits a single peak at 359, corresponding to the MW (+1) of DBS. In the spectrum of the degraded sample (B2), one peak still corresponds to unreacted DBS at 359, but two other peaks are observed at 183 and 107. These must be the reaction products and their MWs must then be 182 and 106. Such products can be accounted for by the reaction scheme shown in Figure 3.8C. Here,

hydrolysis of DBS is catalyzed by the acid, resulting in the formation of benzaldehyde (MW = 182) and sorbitol (MW = 106). Thus, our studies conclusively prove that the self-degradation of the gel is due to the acid-induced hydrolysis of the acetal groups on DBS. Such hydrolysis is well-known and is documented in textbooks.^{89,91}

We can also explicitly make the connection between the reaction scheme in Figure 3.8C and the nanostructural transition in Figure 3.7C. The key point is that the reaction products, benzaldehyde and sorbitol, cannot assemble into nano-fibrils. As noted earlier, DBS self-assembles into fibrils through non-covalent interactions: a combination of hydrogen-bonding of the hydroxyls and pi-pi stacking of the aromatic rings. Removal of either the hydroxyls or the aromatic rings from a DBS molecule would eliminate its ability to associate with its neighbors. In other words, the hydrolysis of DBS will remove molecules from the fibrils, which will either create gaps or breaks in the fibrils or make the fibrils shorter. The net result would be to make the fibrillar network less dense over time, as shown in Figure 3.7C, which explains the drop in G' with t and the eventual transition of the gel to a sol.

Additional evidence supporting the proposed reaction mechanism is shown in Figure 3.9. Here, we combine 5 g of DBS powder with 5 g of 2 M HCl in water. Note that DBS is insoluble in water and so the powder initially sits atop the acidic solution (Photo 1 in Figure 3.9A). With time (over a few days), the DBS powder disappears, leaving two immiscible liquid phases: a top oily phase and a bottom aqueous phase (Photo 2 in Figure 3.9A). NMR analysis (Figure 3.9B) confirms that the top layer is benzaldehyde, which has

limited solubility in water. The other reaction product, sorbitol, is water-soluble and partitions into the aqueous phase. Thus, the observations in Figure 3.9 are again consistent with the reaction in Figure 3.8C.

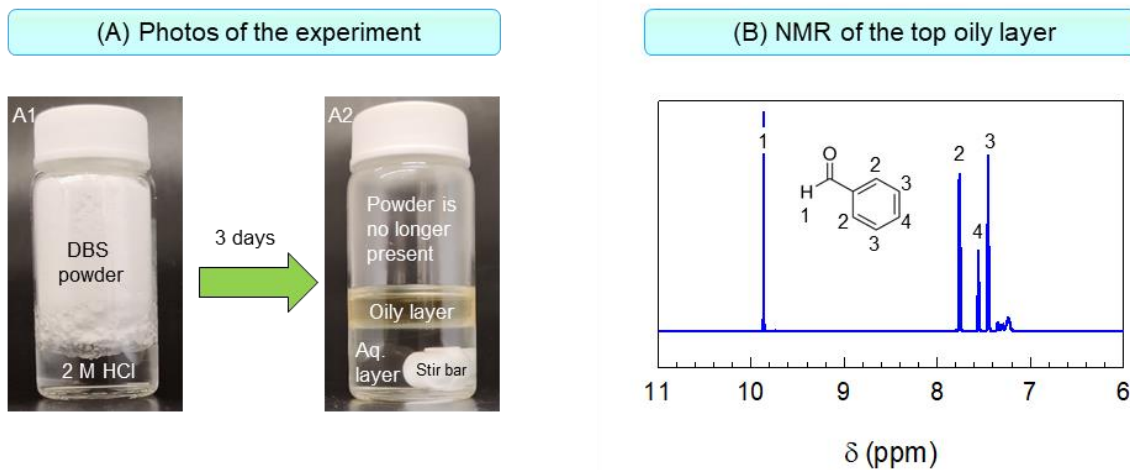


Figure 3.9. Confirming the mechanism for self-degradation of acid-containing DBS gels. (A) 5 g of solid DBS powder is added to an aqueous solution of 2 M HCl (5 g). Initially (A1), the DBS is insoluble in the acid solution. Over several days, the DBS powder disappears, leaving an oily liquid atop an aqueous layer (A2). (B) NMR analysis of the oily layer confirms that it contains benzaldehyde, which is a water-insoluble product of DBS hydrolysis (see Figure 3.8C). This supports the mechanism in Figure 3.8C.

3.2.4 Applications for Self-Degrading Gels

Self-degrading DBS gels could be useful in a range of scenarios and we now explore a couple of the possibilities indicated by Figure 3.1. The first is a valve that opens after a set time (Figure 3.10). For this, we start with a gel of 2% DBS in 80/20 PEG/acid (3 M). The acid molarity is kept high so that the gel degrades at room temperature in a reasonably short time, i.e., in ~ 12 h. 5 mL of the gel is introduced into an open syringe at $t = 0$. The bottom end of this syringe (below the gel) has an orifice with a diameter of 2 mm. Because the gel (dyed blue) is solid, it does not flow out of the orifice when the syringe is vertical (Figure 3.10A). Next, in the headspace above the gel, we add 8 mL

of mineral oil (dyed red). Although the oil is a liquid, it cannot flow out of the syringe because its path is blocked by the gel (Figure 3.10A). As long as the gel maintains its structural integrity, this situation will continue, meaning that the valve will remain closed.

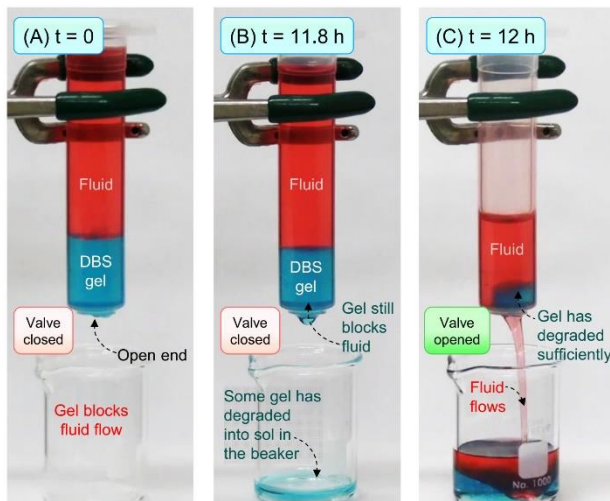


Figure 3.10. Confirming the mechanism for self-degradation of acid-containing DBS gels. Valve based on a self-degrading DBS gel that opens after a set time. (A) At $t = 0$, a gel of 2% DBS in 80/20 PEG/3 M HCl is placed at the bottom of a syringe with an open end, and 8 mL of mineral oil is added above the gel. The gel blocks the flow of the oil. (B) After 11.8 h, a small amount of degraded gel is observed in the beaker. (C) At the 12 h mark, the gel has degraded sufficiently so that the valve opens and the red fluid flows into the beaker.

We leave the syringe undisturbed at room temperature and monitor it. By the 12 h mark, the gel is degraded considerably. A few minutes before this mark, a small amount of sol (i.e., liquefied gel) is seen to drop down into the beaker (Figure 3.10B). Just a few minutes later, the entire gel is liquefied and flows out of the orifice (Figure 3.10C). In turn, the red liquid is no longer blocked (i.e., the valve is now opened) and this liquid flows out too. On the whole, using the self-degrading DBS gel, we have

demonstrated a valve that remains closed for the first 12 h and thereafter spontaneously opens. Such a valve could be integrated into a variety of devices for timed delivery of fluids and thereby of solutes in them (e.g., agrochemicals or cosmetics).

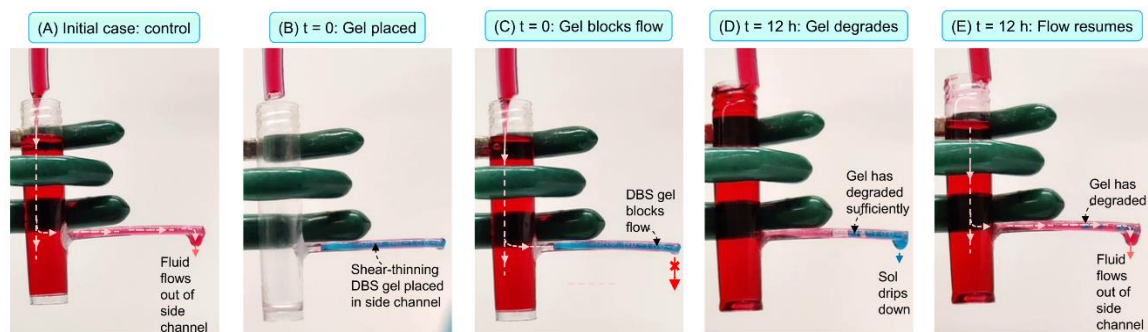


Figure 3.11. Flow diversion for a set time using a self-degrading DBS gel. (A) The setup involves a vertical main tube with a side channel. When fluid (mineral oil) is introduced from the top, it flows out of the side channel. (B) A gel of 2% DBS in 80/20 PEG/3 M HCl is injected into the side channel. (C) When fluid is now added to the tube, it cannot flow through the side channel because of the blocking gel. Thus, the gel diverts flow away from this channel. (D) At the 12 h mark, the gel is sufficiently degraded to a sol, which is forced out of the channel by the hydrostatic pressure of the fluid. (E) As a result, the block in the channel is removed, and fluid flows out through it.

Our second demonstration shows how a self-degrading gel could be used as a flow-diverting agent for a set time (Figure 3.11). For our demonstration, we use a plastic tube with a closed bottom end and an open side channel (Figure 3.11A). Details on how this setup was made are given in the Experimental Section. Initially, when mineral oil is introduced from the top into the vertical tube, it flows through the side channel and drips out. Thus, in this initial ‘control’ state, the side channel is *open*. We then introduce the self-degrading DBS gel into the side channel. The gel composition is the same as in Figure 3.10: it is made with 2% DBS in 80/20 PEG/acid (3 M), and it is designed to self-degrade in ~ 12 h.

To place the DBS gel in the side channel, we exploit its shear-thinning rheology, which is shown in Figure 2.5. The shear-thinning rheology allows us to take the above DBS gel (dyed blue) and liquefy it by imposing high shear. The liquid can thus be loaded into a syringe and we inject it into the side channel. Within seconds, the liquid sets into a gel in the channel (Figure 3.11B). With this gel in place, we introduce mineral oil into the tube from the top. Now, the oil cannot flow out through the side channel because the gel acts as a plug and blocks the flow (Figure 3.11C) — so, the channel is in a *closed* state. After 12 h at room temperature, the DBS gel self-degrades, and in the process, it liquefies (Figure 3.11D). The hydrostatic pressure of the red liquid column then activates the flow of this liquefied gel and blue liquid drips out of the side channel. In turn, because there is no longer a blocking gel, the side channel now flips from a *closed* to an *open* state. As a result, the red liquid also follows suit and flows out of the side channel. To summarize Figure 3.11, the presence of intact DBS gel in a side channel diverts the flow away from that channel. Once the gel self-degrades, flow through that channel resumes.

For various applications, the gels can be based on either polar or nonpolar liquids. Examples of the latter are mineral oil (or other aliphatic hydrocarbons) and toluene (or other aromatic hydrocarbons). We can formulate self-degrading DBS organogels with such nonpolar liquids as well. To induce such gels to degrade, aqueous acid (such as HCl, acetic acid, formic acid, etc.) can be incorporated as droplets, i.e., as an emulsion, in the nonpolar matrix.

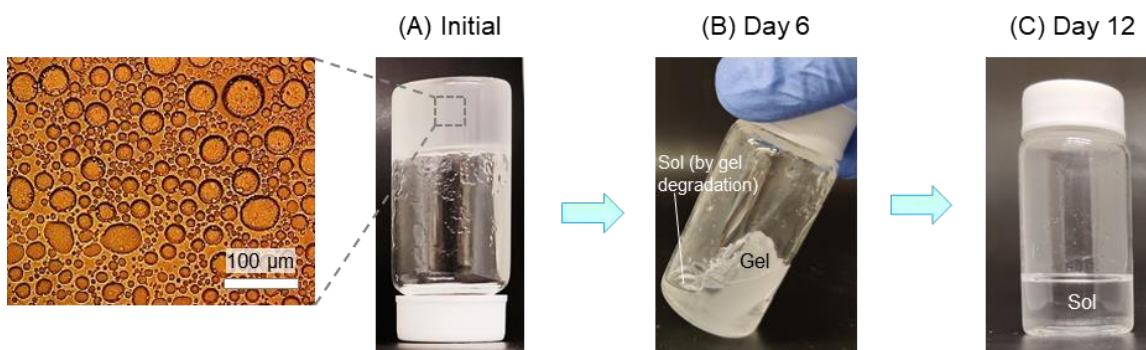


Figure 3.12. Self-degrading DBS gels in nonpolar organic liquids (emulsion gels). The gel is made with 1% DBS in 90/10 mineral oil/hexanol with 5% of 1 M HCl emulsified into it. (A) At $t = 0$, the gel is robust and supports its weight in the inverted vial. Note that the gel is turbid due to the aqueous droplets in it. The microscale droplets can be seen in the optical micrograph. (B) After day 6, the gel is partly degraded and co-exists with a thin sol. (C) After day 12, the gel is completely degraded into a thin solution.

Figure 3.12 shows an example of such an ‘emulsion gel’ using mineral oil as the nonpolar solvent. Acid (1 M HCl) is emulsified into the gel at a 5 wt% concentration. The gel was made by the simple method from Figure 3.2. First, the aqueous acid was added to the oil and then the DBS stock solution in DMSO was added, followed by vortex mixing. Right away, a stable emulsion gel is obtained (Figure 3.12A). No other surfactant or stabilizer is needed to create the emulsion. Optical microscopy shows that the gel contains stable aqueous droplets (with diameters of 5 to 50 μm). The gel is turbid due to the microscale droplets. It is robust and retains its weight in the inverted vial. Over a period of days at room temperature, the gel self-degrades (Figure 3.12B, 3.12C). By day 12, the degradation is complete and the entire sample has transformed into a sol. Thus, the concept shown in this paper of a self-degrading DBS gel can be applied to a variety of liquid matrices, both polar and nonpolar.

3.3 Conclusions

We have presented the first examples of self-degrading molecular organogels using DBS as the gelator. DBS readily self-assembles into a 3-D network of nanoscale fibrils in a variety of organic solvents, thereby converting the liquids into robust, free-standing gels. The incorporation of an acid such as HCl into the gel makes the gel degrade spontaneously over time into a sol. Because the rate of degradation is slow, the initial gel is strong and robust despite having the degrading agent embedded in it. The degradation time t_{degr} of the gels can be tailored, ranging from hours to days to weeks, depending on the acid concentration and the external temperature. Self-degradation occurs because the acid hydrolyzes DBS into benzaldehyde and sorbitol. These hydrolysis products lack the ability to self-assemble into fibrils, and thereby the gel gradually transforms into a thin solution. We have highlighted the utility of DBS-based self-degrading gels for applications in time-activated valves (i.e., valves that open after a set time) and as flow diverting agents that block flow through specific channels for a set time. The latter application is highly relevant for oil drilling operations, where these self-degrading gels present a novel solution to the long-standing problem of ‘lost circulation’.

3.4 Experimental Section

Materials. DBS was purchased from Alfa Chemistry. DMSO was obtained from Alfa Aesar. All other chemicals were from Sigma-Aldrich, including the solvents butanol, hexanol, ethylene glycol, polyethylene glycol (PEG, 200 Da), and hydrochloric acid (HCl).

Gel Preparation. DBS gels were typically prepared using the simple method discussed under Figure 3.2. The gelling solution (15% w/w DBS in DMSO) was added to the solvent of interest (e.g., butanol, hexanol, or PEG), followed by hand-shaking or vortex-mixing for 30 s. At the end of this process, a robust gel of DBS in the solvent was obtained. For comparison, the conventional method (Figure 2.3) was also used to make DBS gels. In that case, DBS powder was added to the solvent, followed by heating the mixture up to $> 100^{\circ}\text{C}$. Within about an hour, the DBS dissolved in the solvent, giving a sol. As this sol was cooled to room temperature, it transformed into a gel.

Degradation Studies. For the studies described in Figures 3.6 and 3.7, the following protocol was used. First, a given gel, e.g., of 2% DBS in a 80/20 mixture of PEG and acidic water (HCl of a given molarity) was made in a 20 mL glass vial. The vial was broken and the gel cylinder (2.5 cm diameter and 5 cm height) was taken out. This gel was then placed vertically in a larger glass bottle (100 mL volume, with a base of 6 cm diameter). The bottle was capped and then placed upright in a water bath, with the water level reaching three-quarters up to the top of the bottle (leaving the cap untouched). The temperature of the water bath was controlled by an immersion heater (Julabo). As the gel in the bottle degraded, some of the gel transformed into a sol, and this sol remained at the bottom of the

bottle. To measure the mass of intact gel at any given time, the gel-cylinder was taken out of the bottle and weighed. Thereafter, it was promptly returned to the bottle for the rest of the experiment. The above protocol was repeated for gels of different composition and for different temperatures (data in Figure 3.6). For the rheological studies during gel degradation (Figure 3.7), at a given time point, a thin slice of the gel was cut from the cylinder and was characterized by rheology. The rest of the gel-cylinder was returned to the bottle as before.

Rheology. Rheological experiments were performed on an AR2000 stress-controlled rheometer (TA Instruments). Samples were run on a parallel plate geometry (20 mm diameter). Dynamic frequency spectra were conducted in the linear viscoelastic regime of the samples, as determined previously from dynamic stress sweeps. In addition, steady-shear rheology (viscosity vs. shear-stress) as well as time-sweeps to study the recovery of structure after shear were also conducted.

Transmission Electron Microscopy (TEM). TEM was conducted on a JEOL JEM 2100 microscope at 100 keV. The gel of 1% DBS in butanol was formed on carbon/Formvar-coated copper grids using our simple method (Figure 3.3). The grids were then dried at room temperature. The dried grids were then stained with a 1% aqueous solution of uranyl acetate (UA) (from Sigma-Aldrich). The grids were air-dried before imaging.

Nuclear Magnetic Resonance (NMR) Spectroscopy. ^1H NMR spectra were recorded on either a 600 MHz Bruker Advance III NMR spectrometer equipped with a room temperature TXI probe or a 800 MHz Bruker Advance III HD NMR spectrometer equipped

with a Cryo-QCI probe at a sample temperature of 298.2 K. The data shown in Figure 3.8 are for 1% DBS in a 95/5 mixture of deuterated-DMSO/1 M HCl in D₂O.

DART-MS. A time-of-flight mass spectrometer (JEOL AccuTOF), equipped with a direct analysis in real time (DART) ion source, was used. Mass spectra were acquired at a rate of one spectrum per second, with a mass/charge (m/z) range of 50–600. An inverted melting point capillary was used to introduce the sample (gel or sol) into the DART source region. The DART ion source was operated in the positive mode with helium gas. The glow discharge needle potential was set at 3.5 kV and the grid voltage was 250 V.

Valve Experiment. For the experiment in Figure 3.10, the DBS gel was formed at the bottom of a 10 mL syringe. After the gel was formed, a 2 mm orifice (hole) was made at the syringe's end using a razor blade. 8 mL of red-dyed mineral oil was added into the headspace above the gel within the syringe. The setup was monitored until the gel degraded, as shown in the figure.

Flow-Diversion Experiment. For the experiment in Figure 3.11, two transparent plastic tubes were connected together. The larger tube (5.5 cm length, 1 cm diameter) was closed at one end. A small hole was created in the side-wall of this tube, and the smaller tube (3.5 cm length, 2 mm diameter) was inserted into this hole and affixed using epoxy resin. Thereby, the small tube became a side branch from the large tube. The DBS gel was used to block flow through this side channel for a duration of time until it degraded.

Chapter 4

Organogels that Degrade Slowly at High Temperature

4.1 Introduction

Lost circulation represents one of the most severe, costly, and time-consuming challenges in oil and gas drilling operations.^{92,93} The process of oil extraction requires drilling a well from the surface through various rock formations to reach underground hydrocarbon reserves (Figure 4.1). Throughout the drilling operation, a specialized fluid, known as drilling fluid, is continuously circulated down through the drill pipe and back up the wellbore.⁹² This fluid performs several critical functions: it lubricates and cools the drill bit, maintains wellbore stability through hydrostatic pressure, and carries rock cuttings to the surface where the fluid is filtered and recirculated.^{94,95} However, when the drill encounters fractured formations, substantial volumes of this fluid can be lost into the rock fractures, disrupting the circulation system.⁹² These fluid losses pose serious operational, economic, and safety risks, including drilling delays, resource waste, potential well control issues, and in extreme cases, catastrophic events such as blowouts or borehole collapse.^{92,93} Given these severe consequences, the oilfield industry has prioritized developing effective solutions to combat lost circulation.^{93,96,97}

Various approaches have been developed to combat lost circulation. Traditional solutions include using lost circulation materials (LCMs) such as fibrous, flaky, or granular materials that can plug the fractures.^{98,99} More recently, crosslinked polymer systems and cement squeezes have been employed to seal large voids and fractures.^{18,96,100} However,

these conventional methods have significant drawbacks.^{101,102} Conventional LCMs provide unreliable sealing that may fail during drilling operations and can damage the formation. Cement squeezes are permanent but can harm formation productivity. Crosslinked polymers may be difficult to remove once their job is complete. Additionally, most current solutions require multiple treatments and extensive waiting periods, further increasing operational costs.

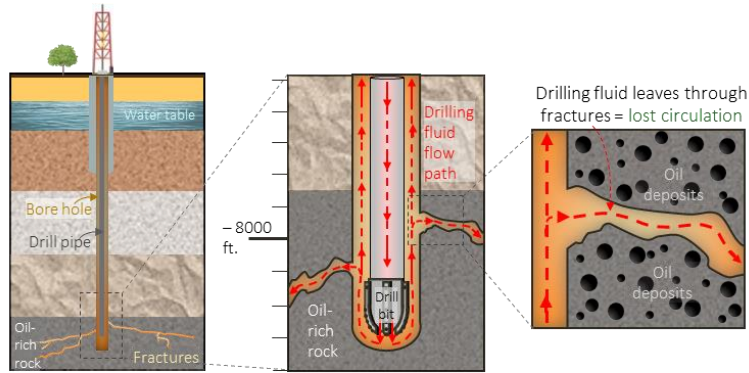
Here, we report the first self-degrading molecular organogel system that functions completely in non-aqueous environments. This represents a significant breakthrough, as self-degrading gels have traditionally been limited to water-based systems where water provides the reactive environment necessary for degradation.^{96,101} While polymer-based self-degrading gels exist, they are typically hydrogels that require water for both their formation and degradation. This water-free design is particularly advantageous for oilfield applications, where water-based systems can be problematic due to formation damage, clay swelling, and incompatibility with water-sensitive formations.^{103,104} Additionally, water-based systems may be unsuitable in high-temperature, high-salinity reservoir conditions where water can promote unwanted reactions or cause scaling issues.

Our approach uses (1,3:2,4)-dibenzylidene sorbitol (DBS) as the gelator, forming robust gels in a range of organic liquids, including both polar and non-polar ones.¹⁰⁵ Gelation occurs because DBS self-assembles into nanoscale fibrils, which connect to form a 3D network.^{38,53,54,105} A key innovation in our approach is the use of a molecular gel rather than a conventional polymer-based system. While polymer gels have been widely

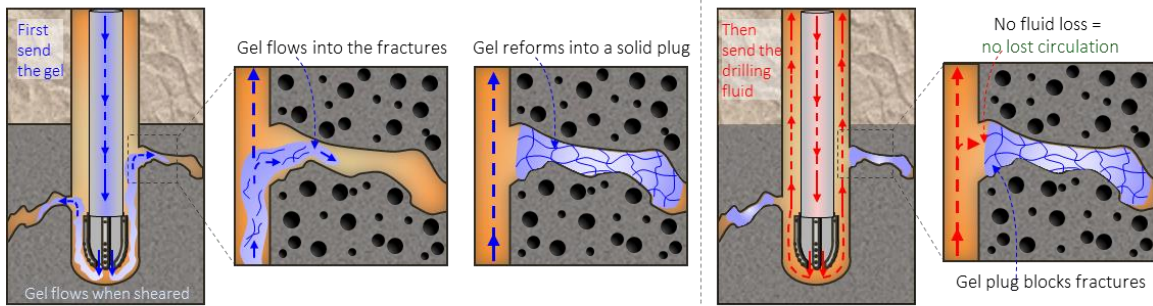
studied for similar applications, they have inherent limitations. When polymer gels degrade, the residue consists of long polymer chains, resulting in solutions that remain viscous.¹⁰⁵ In contrast, our molecular gel is designed to degrade completely into its small constituent molecules, yielding a solution with very low viscosity. These DBS-based gels exhibit two crucial properties that make them uniquely suited for lost circulation control. First, they are extremely strong, maintaining a high gel modulus ($G' > 10,000$ Pa).^{38,105} Second, they possess the ability to degrade spontaneously into low-viscosity sols ($G' \sim 0$) after a pre-determined period when left undisturbed. Additionally, molecular gels offer superior flow properties because their fibrillar network is held together by non-covalent bonds, making them inherently shear-thinning.^{47,106} Under shear stress, these non-covalent bonds break temporarily, allowing the gel to flow like a liquid - a crucial property for pumping the material down an oil well. This behavior contrasts sharply with polymer gels, which, being held by covalent bonds, tend to splinter into pieces when sheared rather than flow smoothly.

The proposed mechanism for lost circulation control is as follows (Figure 4.1B): when pumped down the well, the DBS gel would flow easily due to its shear-thinning nature (See Figure 2.5). Upon entering the fractures, it should quickly recover to form a robust gel structure with high modulus, potentially providing an effective seal against fluid loss. Most importantly, this gel is designed to transform autonomously into a low-viscosity solution after a predetermined period, without requiring any external stimuli or chemical agents.

(A) Problem of lost circulation during oil well drilling



(B) Shear-thinning gel plugs fractures and prevents fluid loss



(C) Self-degrading gel allows oil to be extracted through the fractures

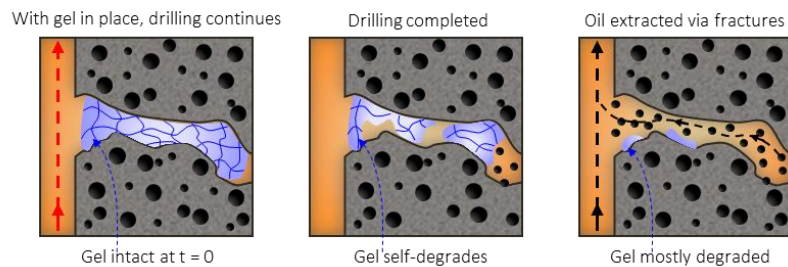


Figure 4.1. Self-degrading gels as a solution to the ‘lost circulation’ problem in the oilfield. (A) Lost circulation refers to the loss of drilling fluid into fractures during the drilling of an oil well. (B) Placing a gel in the fractures reduces this problem. (C) A self-degrading gel such as the DBS gels in this study can be particularly beneficial. The gel stays in place until the drilling is completed (e.g., for days to weeks) and thereafter it spontaneously degrades. Oil can then be extracted through the permeable fractures.

The challenge of lost circulation extends beyond the initial sealing of fractures. In permeable formations, these same fractures serve as crucial pathways for oil and gas extraction (Figure 4.1C). Therefore, while the fractures must be sealed during drilling, they need to be reopened for subsequent production. Current approaches to address this challenge have significant limitations. Some researchers have developed gels that degrade in response to external stimuli like temperature^{11,107} or light¹⁰⁸, but applying such stimuli is often impractical several thousand feet underground. Others use chemical degrading agents such as acids,¹³ bases,¹⁴ or enzymes,⁷⁸ but these present their own challenges. Degrading agents may only contact the gel's exterior, resulting in incomplete degradation. Moreover, harsh chemicals can have undesired environmental impacts on the surrounding formation.

The key to achieving controlled self-degradation lies in incorporating an organic acid (e.g., fatty acids such as hexanoic acid) into the DBS gel. The choice of acid and its concentration sets the kinetics of gel degradation and thereby the degradation time at a given temperature. Through NMR and mass spectrometry, we have identified that the degradation process involves slow conversion of alcohol groups in DBS into DBS-esters through esterification. These DBS-esters are unable to self-assemble, leading to the controlled breakdown of the gel structure. The degradation period can be tailored from days to weeks based on two key factors: (a) the expected temperature conditions in the target formation, and (b) the anticipated duration of the drilling operation.

Being low-cost and environmentally benign, these self-degrading DBS gels could potentially transform oil recovery operations, enabling safer, more efficient, and sustainable drilling practices. The combination of reliable temporary sealing and autonomous degradation in a completely non-aqueous environment represents a significant advancement over conventional lost circulation materials, potentially providing both effective wellbore integrity during drilling and autonomous restoration of formation permeability for subsequent production.

4.2 Results and Discussion

4.2.1 Self Degradation of DBS Gels

DBS organogels exhibit remarkable stability under normal conditions, remaining intact and unchanged for extended periods (more than a year) at ambient temperature.¹⁰⁵ These gels show robust resistance to various chemical environments, withstanding exposure to strong bases, oxidizing agents, and reducing agents without degradation (See Figure 3.5). In our previous work, we demonstrated that while these gels are generally stable, they could be degraded using strong aqueous acids such as hydrochloric acid (HCl), particularly in gels formed with polar organic solvents like ethylene glycol. The mechanism involved acid-catalyzed hydrolysis of acetal groups in DBS, producing benzaldehyde and sorbitol – compounds that cannot self-assemble, thus leading to gel degradation.

However, this aqueous acid-based approach has significant limitations. First, aqueous acids are insoluble in non-polar solvents such as mineral oil, restricting their use to polar systems. While aqueous acids could theoretically be incorporated into non-polar solvents as emulsions, this approach would result in inhomogeneous gels with unpredictable degradation times, heavily dependent on droplet size distribution and preparation methods. Moreover, for many applications, particularly in oilfield operations, the presence of water is undesirable due to potential formation damage and limitations in high-temperature environments ($>100^{\circ}\text{C}$). These constraints necessitated the development of a completely non-aqueous self-degrading gel system.

In this work, we demonstrate that DBS gels can be effectively degraded through the incorporation of various organic acids, including butanoic acid, hexanoic acid, and octanoic acid. Crucially, we found that the degradation rate with these organic acids is sufficiently slow to enable controlled self-degradation – where a robust gel gradually transforms into a low-viscosity solution over a predetermined period. For this study, we selected mineral oil as our model solvent system, given its non-polar nature and widespread use as a major component in oil-based drilling fluids. This choice makes our findings particularly relevant for oilfield applications.¹⁰⁹

The self-degrading behavior of our DBS organogels was initially demonstrated using a mineral oil/hexanoic acid system (Figure 4.2A). We prepared the gel by first combining mineral oil with hexanoic acid in an 80/20 weight ratio to form a homogeneous solution. This solution was then converted into an organogel using 1 wt% DBS through our previously reported no-heat method (described in Chapter 3). The gel's degradation was monitored over time at 70°C in a petri dish, where the progressive conversion of gel to sol could be clearly observed. Initially robust and transparent gel gradually degraded over several days, with complete conversion to sol occurring by day 5. The temporal evolution of the gel clearly demonstrates its controlled degradation (Figure 4.2A). At $t = 0$ (A1), the freshly prepared gel is robust and self-supporting, and exhibits a characteristic bluish tinge. After 24 hours (A2), the first signs of degradation become apparent, manifested as a reduction in gel volume. This partial degradation results in the formation of a thin sol that collects in the petri dish, though its small volume is not clearly visible in the photograph at this stage. By day 2 (A3), the degradation has progressed significantly,

evidenced by a further reduction in gel volume and the accumulation of sufficient clear sol in the petri dish to be visibly apparent. By day 3 (A4), the degradation continues with increased sol formation. At day 4 (A5), the gel volume has decreased substantially; the remaining small gel piece is shown lifted by spatula from the surrounding sol. The degradation process completes by day 5, at which point the entire sample has converted to a sol state (not shown).

The visual observations reveal that during intermediate stages of degradation, intact gel coexists with the sol phase, ultimately transforming into a clear, homogeneous sol over 5 days. This characteristic allows us to quantitatively track the degradation process by measuring the mass fraction of intact gel (m_{gel}) as a function of time (t). The degradation kinetics are influenced by four key variables: (a) acid concentration (weight fraction), (b) temperature, (c) acid type, and (d) gelator (DBS) concentration. We first investigated the effect of acid concentration while maintaining constant conditions for other variables (1% DBS in mineral oil/hexanoic acid at 70°C).

The influence of acid concentration on degradation kinetics was studied using 1% DBS gels in mineral oil/hexanoic acid mixtures, with hexanoic acid weight fractions ranging from 20% to 80% at 70°C (Figure 4.2B). The data reveal that m_{gel} decreases linearly from 100% (complete gel) to 0% (complete sol) for all acid concentrations, with higher acid fractions producing faster degradation rates. Notably, the degradation rate remains approximately constant throughout the process, as evidenced by the linear decay profiles. The degradation time (t_{degr}) can be defined either as the time for complete

degradation ($m_{gel} = 0$) or the time to reach the midpoint ($m_{gel} = 50\%$). Using either definition, t_{degr} shows an inverse relationship with hexanoic acid concentration. For instance, at 20 wt% hexanoic acid, complete degradation requires 5 days, while at 80 wt% hexanoic acid, this time reduces to less than a day.

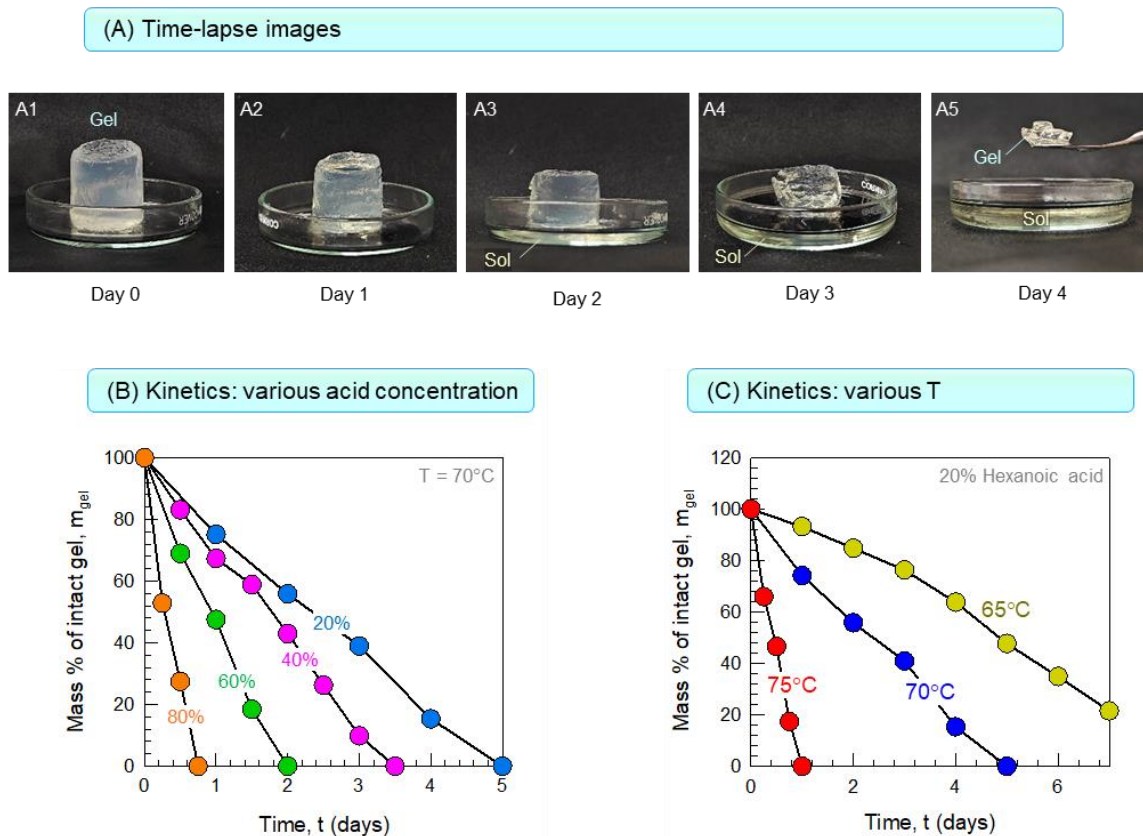


Figure 4.2: Self-degrading behavior of DBS organogels. (A) Photographs documenting degradation of 1% DBS gel in 80/20 mineral oil/hexanoic acid at 70°C. Initially robust gel (A1, Day 0) gradually degrades, with sol formation evident at edges (A2-A4). By Day 4 (A5), a small piece of gel remains (shown lifted by spatula) surrounded by sol; complete conversion to sol occurs by Day 5 (not shown). (B) Degradation kinetics at 70°C with varying hexanoic acid concentrations in mineral oil. (C) Temperature dependence of degradation for gels containing 20% hexanoic acid, showing accelerated degradation at higher temperatures (65-75°C).

A particularly intriguing aspect of our findings is the linear nature of the gel degradation process (Figure 4.2B). This linear decay of gel mass fraction (m_{gel}) with time is both unexpected and mechanistically significant. In typical degradation processes, whether in polymers, biomaterials, or other systems, one typically observes either exponential decay (first-order kinetics) or more complex degradation profiles.^{80,105,110,111} Such non-linear profiles are expected because as degradation progresses, the remaining material usually becomes either more resistant to further degradation (leading to a slowdown) or more susceptible (leading to acceleration). The observed linear degradation in our DBS system suggests a unique and remarkably controlled process where the rate of gel-to-sol conversion remains constant throughout the entire degradation period. This implies, the degradation rate appears independent of how much gel remains, meaning that the last portion of the gel degrades at the same rate as the first portion. This behavior is particularly advantageous for applications requiring predictable degradation profiles, as it allows for precise estimation of the remaining gel fraction at any given time.

Next, we discuss the effect of temperature T on gel degradation (Figure 4.2C) using gels containing 1% DBS in an 80/20 mineral oil/hexanoic acid mixture. The degradation behavior was studied at three temperatures: 65°C, 70°C, and 75°C. At all temperatures, m_{gel} exhibits the same characteristic linear decay observed in our concentration studies (Figure 4.2B). However, temperature has a dramatic effect on the degradation rate, with higher temperatures significantly accelerating the process while maintaining the linear degradation profile. The temperature dependence is quantitatively reflected in the degradation time (t_{degr}). At 65°C, degradation occurs within 10 days, which decreases to 6

days at 70°C, and further reduces to just 1 day at 75°C. This strong temperature sensitivity suggests a thermally activated process.

These findings have important practical implications for oilfield applications, where formation temperatures vary with depth.¹¹² Temperature and acid concentration provide two independent parameters for controlling the degradation time. At a given temperature, reducing acid concentration increases degradation time, while at a fixed acid concentration, temperature changes can accelerate or slow the degradation. This dual-parameter control enables precise tuning of the gel system to match specific downhole temperatures and drilling operation timeframes.

We next investigated how the type of acid affects the degradation kinetics of DBS gels. DBS gels (1 wt%) were prepared in mineral oil containing 20 wt% of different fatty acids: butanoic (C4), hexanoic (C6), and octanoic (C8) acids. All experiments were conducted at 70°C (Figure 4.3A). The normalized gel mass (m_{gel}) exhibited the same characteristic linear decay profile observed in our previous studies (Figure 4.2), but the degradation rate varied with acid chain length. Specifically, shorter-chain acids promoted faster degradation, with complete degradation times (t_{degr}) of 2, 5, and 10 days for butanoic, hexanoic, and octanoic acids, respectively. This chain-length dependence can be attributed to two factors. First, since all acids were incorporated at the same weight fraction (20 wt%), shorter-chain acids provided a higher molar concentration of reactive species. Second, shorter-chain acids generally exhibit higher reactivity due to their smaller molecular size.

These results demonstrate that acid selection provides a straightforward way to control the gel degradation time, offering flexibility for different drilling operation requirements.

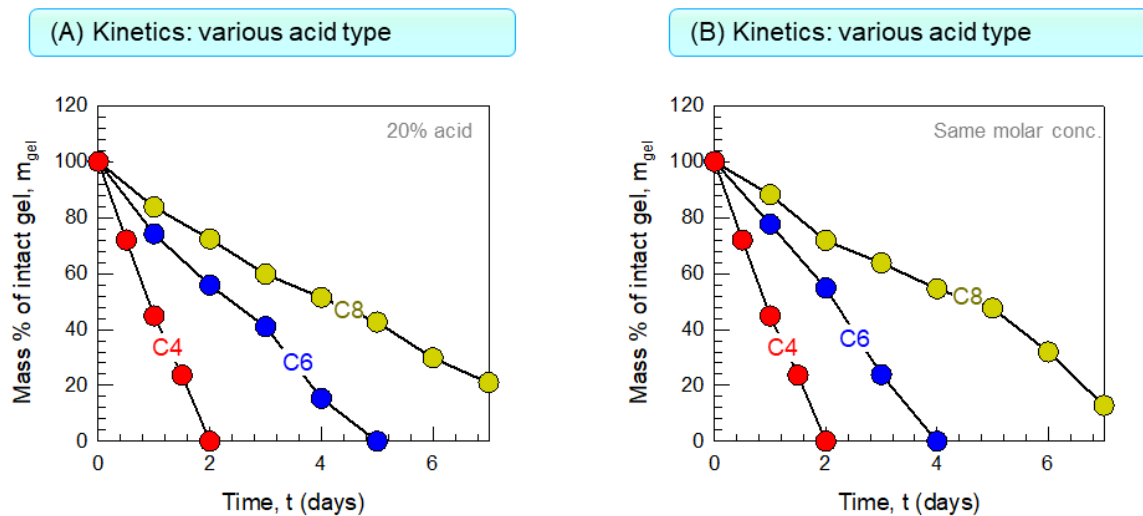


Figure 4.3: Effect of acid chain length on DBS gel degradation kinetics at 70°C. (A) Degradation profiles using different acids (C4: butanoic, C6: hexanoic, and C8: octanoic) at fixed weight fraction (20% acid). (B) Degradation profiles at equivalent molar concentrations (20 wt% butanoic acid, 26.4 wt% hexanoic acid, and 32.7 wt% octanoic acid).

To probe further, we prepared gels with different acids (butanoic, hexanoic, and octanoic) while keeping the molar concentration of the acids the same (Figure 4.3B). We prepared 20 wt% butanoic acid, 26.4 wt% hexanoic acid, and 32.7 wt% octanoic acid. Yet, we still observed that the sample with butanoic acid degraded fastest (2 days), followed by hexanoic acid (4 days), and then octanoic acid (9 days). This systematic increase in degradation time with acid chain length suggests that molecular size plays a crucial role in the degradation mechanism, even when the acid concentration is held constant on a molar basis.

DBS concentration also strongly influences the degradation time (Figure 4.4). We prepared gels with 0.5%, 1%, and 2% DBS in 80/20 mineral oil/hexanoic acid mixtures and found that increasing DBS concentration lengthens the degradation time. The 0.5% DBS gel degraded completely in 3 days, the 1% DBS gel took 5 days, and the 2% DBS gel underwent 92% degradation after 7 days. This clear dependence on DBS concentration points to the importance of the acid-to-gelator molecular ratio in controlling degradation kinetics.

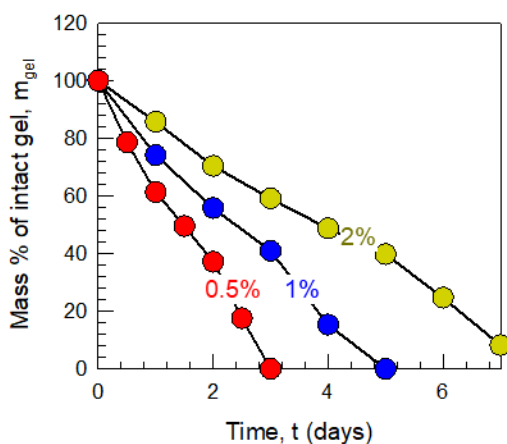


Figure 4.4: Effect of DBS concentration on gel degradation kinetics at 70°C in 80/20 mineral oil/hexanoic acid. DBS concentrations: 0.5%, 1%, and 2%.

4.2.2 Rheological Properties During Gel Degradation

We next investigated how the rheological properties of the gel evolve during the degradation process by conducting dynamic rheology measurements on the intact portion of the gel at various time points. The elastic modulus (G') was monitored over time under different conditions (Figure 4.5). Two sets of experiments were performed to understand the effects of gelator concentration and temperature. In the first set, we maintained a constant temperature of 70°C while varying the DBS concentration (0.5%, 1%, and 2%) in

an 80/20 mixture of mineral oil and hexanoic acid (Figure 4.5A). As expected, the initial value of G' increased with higher gelator concentration, ranging from $\sim 8,000$ Pa at 0.5% DBS to $\sim 100,000$ Pa at 2% DBS. Strikingly, for each concentration, G' remained essentially constant throughout the degradation process. This remarkable observation indicates that while portions of the gel are being converted into a thin sol, the remaining intact gel maintains its mechanical strength.

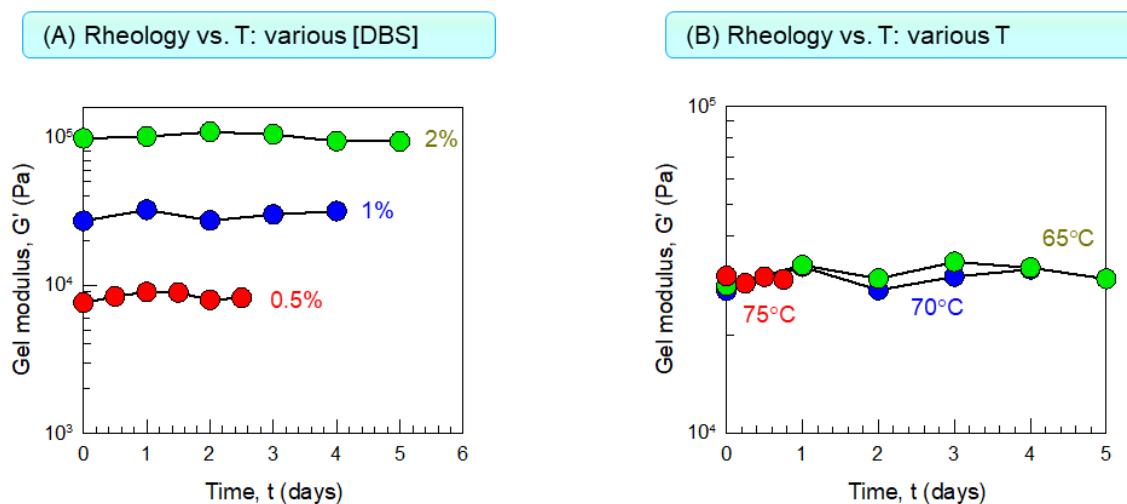


Figure 4.5: Evolution of gel modulus (G') during degradation. (A) Effect of DBS concentration (0.5%, 1%, and 2%) at 70°C. (B) Effect of temperature (65°C, 70°C, and 75°C) for 1% DBS gels. All samples prepared in 80/20 mineral oil/hexanoic acid.

In the second set of experiments, we examined temperature effects by testing 1% DBS gels in 80/20 mineral oil/hexanoic acid at three different temperatures (Figure 4.5B). Notably, G' showed minimal sensitivity to temperature, with the curves for different temperatures essentially overlapping. This temperature independence of gel strength, combined with the maintenance of G' during degradation, suggests that the degradation

process affects the amount of intact gel but not its fundamental network structure or mechanical properties.

4.2.3 Mechanism of Degradation

To elucidate the chemical mechanism underlying gel degradation in organic acid systems, we employed Nuclear Magnetic Resonance (NMR) spectroscopy and Mass Spectrometry (MS). Our investigation began with ^1H NMR analysis (Figure 4.6) comparing two samples of 1% DBS in a mixture of deuterated solvents (80/20 DMSO- d_6 /Hexanoic- d_{11} acid): one analyzed immediately after preparation (before degradation) and another after incubation at 70°C for one week (after degradation). Figure 4.6 presents the ^1H NMR spectra, with the top panels showing the full spectral range (0-14 ppm) before degradation (A) and after degradation (B). Most notably, the acetal proton signals in the 5-6 ppm region are present in both spectra, indicating that the acetal groups remain intact throughout the degradation process. This observation marks a significant departure from the aqueous acid degradation mechanism (Chapter 3), where these signals disappeared upon degradation. While several differences can be observed in the 2-5 ppm region (bottom panels) between the before degradation and after degradation samples, the most striking change is the substantial decrease in intensity of the peak at $\delta = 3.2$ ppm. This selective change in the NMR spectrum suggests a specific chemical transformation is occurring during the degradation process.

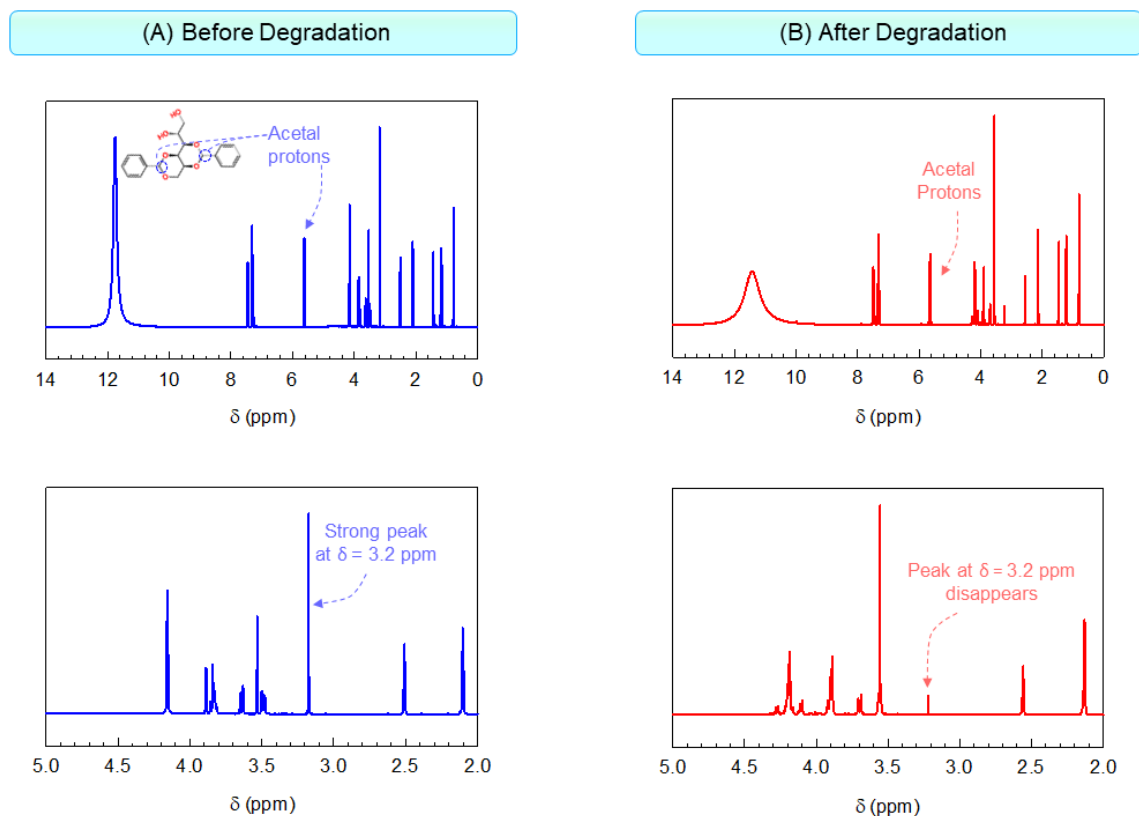


Figure 4.6: ^1H NMR spectra of DBS in 80/20 DMSO- d_6 /Hexanoic- d_{11} acid (1% DBS): (A) Before degradation and (B) After degradation at 70°C for one week. Top panels show the full spectral range (0-14 ppm), with acetal protons highlighted. Bottom panels show the expanded region (2-5 ppm), highlighting the peak at $\delta = 3.2$ ppm that disappears upon degradation. The persistence of acetal proton signals in both spectra indicates that, unlike aqueous acid degradation, the acetal groups remain intact during degradation in organic acid.

To further investigate the degradation products, the DBS samples were subjected to MS, specifically via the Direct Analysis in Real Time (DART) technique. In DART-MS, the sample is ionized by the addition of a proton, resulting in a +1 charge and an increase in the mass of the molecule by one.⁹⁰ Thus, the mass-to-charge ratio (m/z) corresponds to the molecular weight (MW) of the species plus one. We analyzed 1% DBS gel in hexanoic acid before and after degradation (Figure 4.7). The DART spectrum of the initial gel (Figure 4.7A) exhibits peaks at $m/z = 117$, corresponding to hexanoic acid (MW

+ 1), and $m/z = 359$, corresponding to DBS (MW + 1). After degradation (Figure 4.7B), while these peaks remain, two new peaks appear at $m/z = 457$ and 555 , with 457 being the major peak. These new peaks correspond to molecular weights of 456 and 554 , respectively. The reaction scheme shown in Figure 4.7C accounts for these products: the major product (MW = 456) results from esterification of one alcohol group in DBS with hexanoic acid ($358 + 116 - 18 = 456$), while the minor product (MW = 554) forms when both alcohol groups undergo esterification ($358 + 2 \times 116 - 2 \times 18 = 554$). These MS results align with our NMR observations, conclusively demonstrating that gel degradation occurs through esterification of DBS with the organic acid. The critical insight is that these DBS esters are unable to self-assemble into the nano-fibrils necessary for gel formation. DBS normally self-assembles through hydrogen-bonding involving the hydroxyl groups. Esterification of the hydroxyl groups eliminates these crucial hydrogen-bonding capabilities. Additionally, the introduction of ester groups alters the molecular shape needed for self-assembly. Consequently, these modified molecules cannot maintain the fibrillar network structure, leading to the gradual degradation of the gel into a sol, as observed in our time-dependent studies (Figure 4.2).

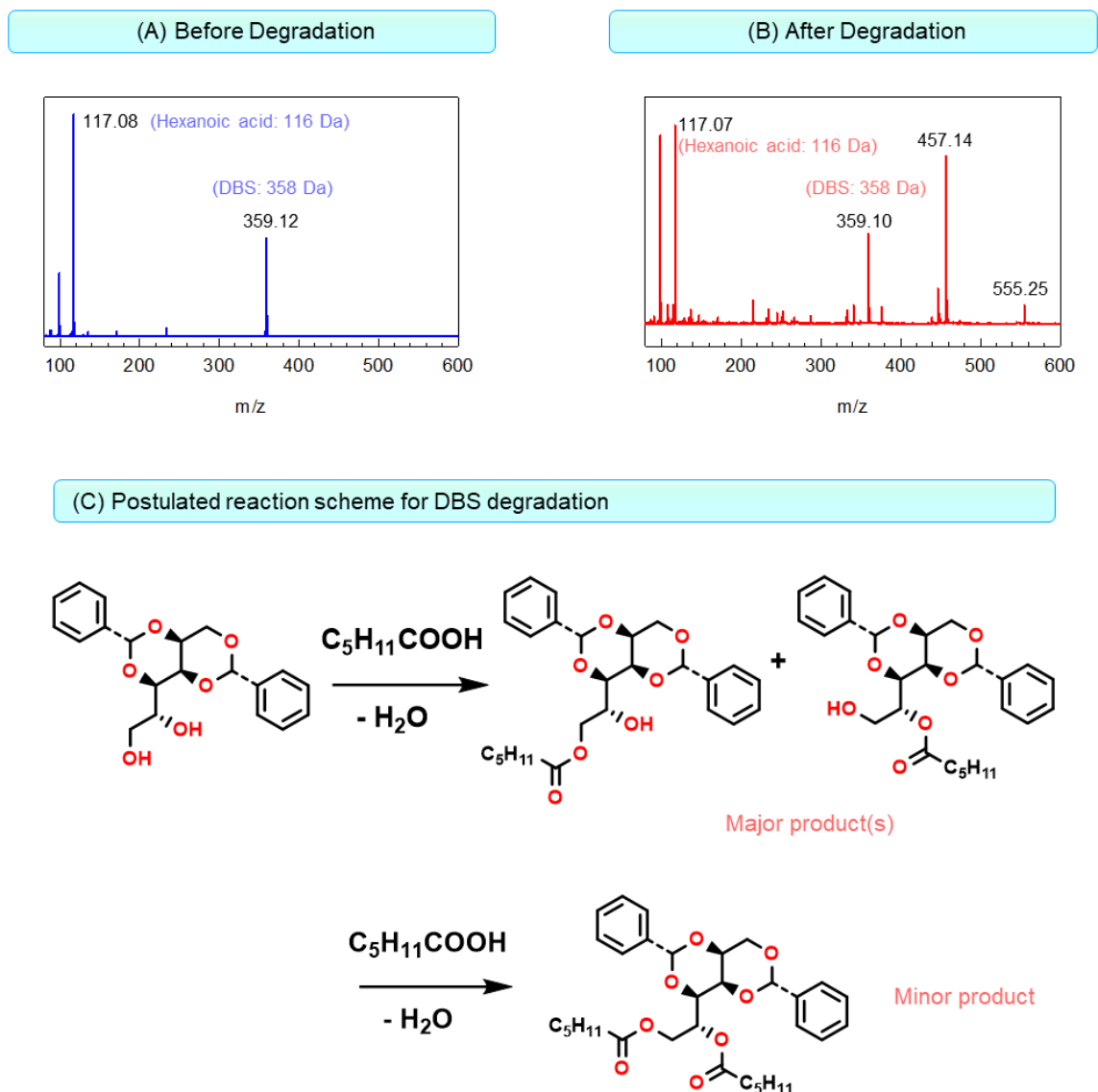


Figure 4.7: Mass spectrometry analysis and proposed reaction mechanism for DBS degradation in organic acid. (A) MS spectrum before degradation showing DBS peak at 358 Da. (B) MS spectrum after degradation at 70°C showing new peaks corresponding to esterification products. (C) Postulated reaction scheme showing esterification of DBS hydroxyl groups by hexanoic acid. DBS contains two hydroxyl groups that can undergo esterification: either hydroxyl group can be esterified (leading to two possible mono-ester products) or both hydroxyl groups can be esterified (di-ester product, minor product).

4.2.4 Mechanistic Insights from Comparative Degradation Behavior

Finally, we gain deeper insights into our DBS-organic acid system by comparing its degradation behavior with two other self-degrading gels (Figure 4.8). Most remarkably, our DBS gel with organic acid maintains constant G' throughout degradation (A1) while exhibiting linear mass loss (B1) - a unique combination that suggests an elegant "shrinking core" degradation mechanism. This synchronized release of solvent upon gelator (DBS) degradation maintains a constant network density in the remaining gel, explaining why G' remains unchanged throughout the degradation process. The behavior of the polymer hydrogel (to be discussed in Chapter 5) represents a different extreme (A3, B3). As degradation proceeds, the network becomes progressively weaker but retains all its solvent, resulting in a dramatic decrease in G' while mass remains constant. The degradation continues until the material crosses a critical threshold where it can no longer maintain a gel state and transitions to a sol. The DBS-aqueous acid system (A2, B2) presents an intermediate case. During degradation, some solvent is expelled but not enough to maintain the original network density. This partial solvent retention coupled with network degradation leads to an exponential decay in G' and sigmoidal mass loss. These comparisons reveal a fundamental advantage of our DBS-organic acid system: its ability to maintain consistent mechanical properties even as it degrades. Such predictable, well-controlled degradation behavior is particularly valuable for applications requiring reliable performance throughout the degradation period.

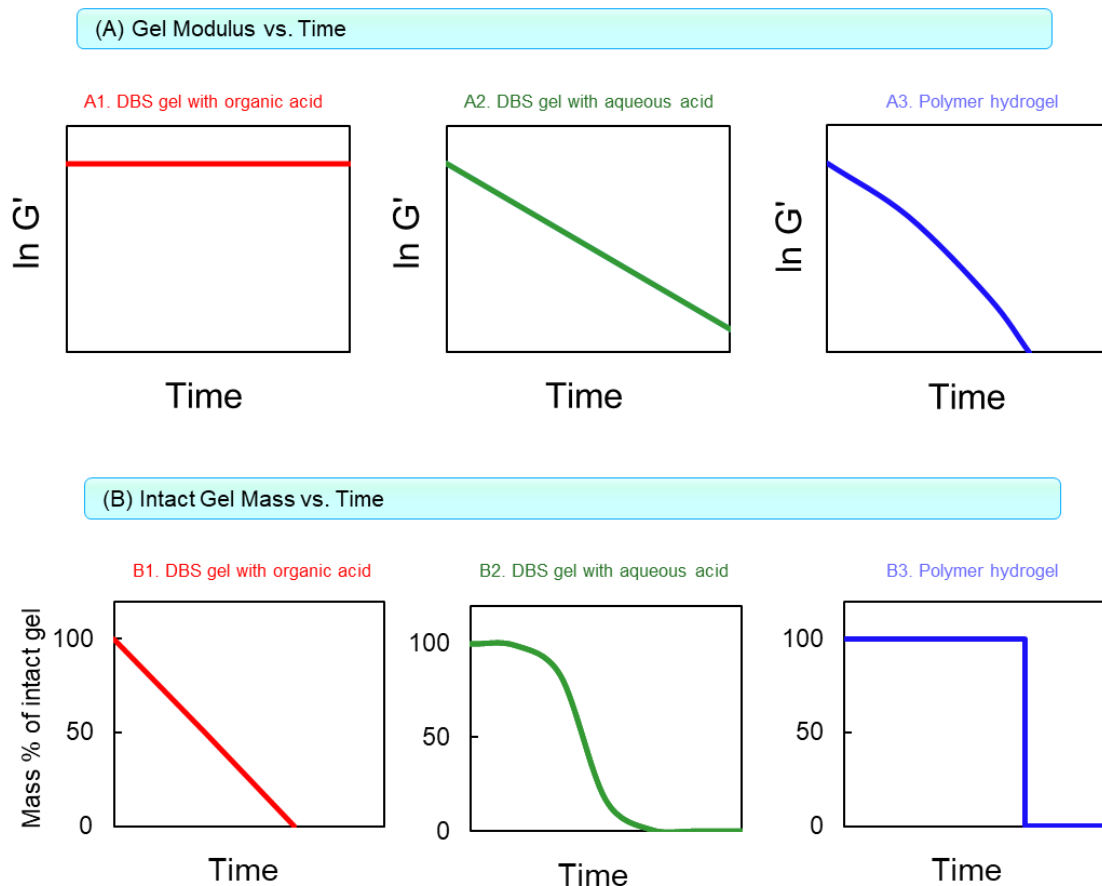


Figure 4.8: Comparison of degradation behavior in different self-degrading gels. (A) Evolution of gel modulus (G') over time for: A1. DBS gel with organic acid showing constant G' , A2. DBS gel with aqueous acid exhibiting exponential decay in G' , A3. Self-degrading polymer hydrogel (discussed in Chapter 5) showing dramatic decrease in G' . (B) Corresponding mass loss profiles of intact gel: B1. Linear mass loss for DBS gel with organic acid, B2. Sigmoidal mass loss for DBS gel with aqueous acid, B3. Constant mass maintained in polymer hydrogel with no sol expelled until gel-to-sol transition.

4.3 Conclusions

In this work, we have developed a novel class of self-degrading organogels based on DBS that function entirely in non-aqueous environments. Our system demonstrates several unique and advantageous characteristics. First, the gels exhibit controlled degradation through a simple acid-catalyzed reaction, eliminating the need for external stimuli or harsh chemical treatments. Second, the degradation kinetics follow a remarkably

linear profile, allowing precise prediction of gel lifetime. This degradation time can be systematically tuned from hours to weeks by adjusting various parameters including acid concentration, temperature, acid chain length, and DBS concentration. Perhaps most notably, these gels maintain constant mechanical strength throughout the degradation process, even as their mass decreases linearly with time. This unique "shrinking core" behavior, where the remaining gel network maintains its integrity while gradually decreasing in size, represents a significant advancement over conventional degradable systems. Such predictable mechanical properties are particularly valuable for applications requiring reliable performance throughout the degradation period. The combination of controlled degradation in non-aqueous environments, tunable lifetimes, and consistent mechanical properties makes these self-degrading DBS gels promising candidates for lost circulation prevention in oil drilling operations. More broadly, this work establishes a new paradigm for designing self-degrading soft materials with predictable properties and controlled lifetimes.

4.4 Experimental Section

Materials. DBS was purchased from Alfa Chemistry. DMSO was obtained from Alfa Aesar. Mineral oil, butanoic acid, hexanoic acid, and octanoic acid were purchased from Sigma-Aldrich.

Gel Preparation. DBS gels were prepared by first combining mineral oil with the desired organic acid (e.g., hexanoic acid) at specified weight ratios. DBS powder was then dissolved in this mixture using our previously reported no-heat method (described in Chapter 3). Briefly, a gelling solution (15% w/w DBS in DMSO) was added to the mineral oil/acid mixture, followed by hand-shaking or vortex-mixing to form the gel.

Degradation Studies. Gels were initially prepared in 20 mL glass vials. The vial was carefully broken and the gel cylinder was removed. This gel was then placed in a larger glass bottle (100 mL volume, with a base of 6 cm diameter). The bottle was capped and placed upright in a temperature-controlled water bath, with the water level reaching three-quarters up to the top of the bottle (leaving the cap untouched). For each study, a gel of specified composition (e.g., 1% DBS in 80/20 mineral oil/hexanoic acid) was monitored at the desired temperature (typically 65-75°C). To measure the mass of intact gel at any given time, the gel cylinder was taken out of the bottle and weighed. Thereafter, it was promptly returned to the bottle for the rest of the experiment. The process was repeated until complete degradation occurred or the experiment was terminated.

Rheology. Rheological experiments were performed on an AR2000 stress-controlled rheometer (TA Instruments) using a parallel plate geometry (20 mm diameter). To monitor gel properties during degradation, samples of the intact gel portion were carefully extracted at various time points and characterized by dynamic rheology. Measurements were conducted in the linear viscoelastic regime, as determined from dynamic stress sweeps.

DART-MS. Mass spectrometry analysis was performed using a JEOL AccuTOF time-of-flight mass spectrometer equipped with a direct analysis in real time (DART) ion source. Mass spectra were acquired at a rate of one spectrum per second, with a mass/charge (m/z) range of 50–600. Samples were introduced using an inverted melting point capillary. The DART ion source was operated in positive mode with helium gas, using a glow discharge needle potential of 3.5 kV and grid voltage of 250 V.

Nuclear Magnetic Resonance (NMR) Spectroscopy. ^1H NMR spectra were recorded on either a 600 MHz Bruker Advance III NMR spectrometer equipped with a room temperature TXI probe or a 800 MHz Bruker Advance III HD NMR spectrometer equipped with a Cryo-QCI probe at 298.2 K. The data shown in Figure 4.6 are for samples containing 1% DBS in 80/20 DMSO- d_6 /Hexanoic- d_{11} acid.

Chapter 5

Self-Degrading Gel-Foams

5.1 Introduction

Foams are a fascinating class of materials that are ubiquitous in our daily lives, from the foam in our morning cappuccino to firefighting foams and home insulation.^{56,59,60,113,114} These materials consist of gas bubbles dispersed in a continuous phase, which can be either a liquid (liquid foams) or a solid (solid foams).^{59,60,113} While liquid foams are inherently unstable due to drainage and coarsening, their stability can be enhanced by introducing surfactants, polymers, or particles in the continuous phase.^{62-64,115} However, these stabilized foams still eventually collapse (minutes to hours). To create permanent foam structures, the continuous phase can be transformed into a solid through gelation or crosslinking reactions. A familiar example is bread-making, where CO₂ bubbles from yeast create a ‘foam’ in dough that is then permanently set during baking as gluten proteins form a crosslinked network and starch undergoes gelatinization.¹¹⁶ Similarly, in mattress manufacturing, polyurethane liquid foams are converted to permanent structures through chemical crosslinking of the continuous phase.^{117,118} The resulting gel foams combine the advantages of both foams (high surface area, low density) and gels (structural integrity, elastic properties) into a single material system.

In typical cases where solid/gelled foams are used, such as in home insulation and structural packaging materials, the solid state is critical for the success of the application or product. However, there are instances where it is advantageous for the solid foam to

transform into a liquid of low viscosity (i.e., a sol) after a certain period. Three such cases are illustrated in Figure 5.1.

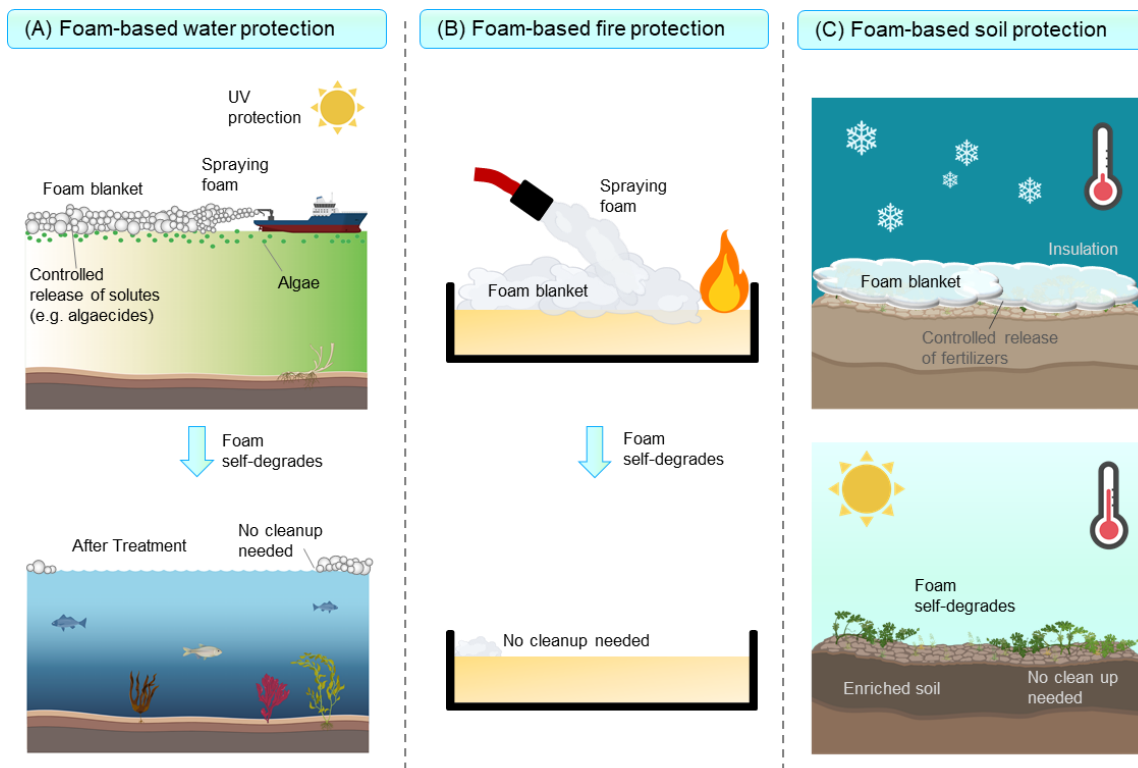


Figure 5.1: Applications of self-degrading gel foams. (A) Water body protection: Foam blanket sprayed on water surface for algae control. foam creates a protective barrier that prevents UV-induced byproduct formation and evaporation while enabling controlled release of treatment agents (e.g., algaecides). After treatment, the foam degrades completely, eliminating cleanup needs. (B) Fire prevention: Foam creates a protective barrier against fire. Post-application, the foam self-degrades without requiring manual removal. (C) Soil/crop protection: Foam provides insulation against extreme weather conditions while delivering nutrients. Upon degradation, it enriches the soil without leaving residue for cleanup.

First, consider a foam that is sprayed onto a water body (e.g., lakes, ponds, reservoirs). The gelling of the foam is important to prevent mixing with the water below, and the covering offers multiple environmental benefits including algae growth prevention, evaporation reduction, and prevention of harmful UV-induced byproduct formation.¹¹⁹⁻¹²¹

When loaded with specific payloads, these foams can actively target harmful algae near the surface or provide nutrients for marine life (Figure 5.1A). Crucially, the foam's ability to degrade eliminates the need for post-treatment cleanup. In a different context, these degradable foams could serve in fire fighting applications (Figure 5.1B), where the solid foam initially forms an effective protective blanket before degrading into a thin sol, again minimizing cleanup requirements.¹²² Similarly, when applied as a temporary protective layer over crops and soil (Figure 5.1C), the foam can shield against extreme weather conditions while carrying nutrients that enrich the soil upon degradation.¹²³ In this case, the foam serves a dual purpose - providing temporary protection while its degradation products help improve soil quality.

Faced with the challenges depicted in Figure 5.1, we have developed a strategy to take a liquid and foam it, allowing it to be sprayed and cover a large surface area (a small volume of precursor solution expands significantly during application). The liquid foam is then gelled to create a stable structure that maintains its coverage and prevents mixing with underlying fluids. Following the treatment period, we desire the solid foam to degrade back into a thin sol, which could be achieved by degrading the gel network in the continuous medium. Traditional approaches to gel degradation rely on external stimuli like temperature^{11,107} or light¹⁰⁸. For instance, gels can be induced to degrade when exposed to UV light or when heated above a critical temperature. However, applying such stimuli may be impractical in many scenarios, such as large water bodies or agricultural fields. Another possibility is using chemical 'degrading agents' to convert gels to sols. In this approach, the gel remains intact until it contacts degrading moieties, which can include acids, bases, or

enzymes.^{13,14,78} However, degrading agents can be problematic as they may harm aquatic organisms, affect soil pH, or interfere with crop growth. Moreover, their application requires an additional treatment step, which increases operational complexity and cost. Thus, both external stimuli and chemical triggers may not be deployable in some real-world applications. The concept explored in this chapter is that of *self-degrading* gel foams, which will degrade even if left undisturbed under ambient conditions, i.e., without contact with either external stimuli or chemicals in the external medium.

Our goal in this work is to create a self-degrading gel foam. To our knowledge, gelled foams with the ability to self-degrade have not been reported thus far. Here, we report a class of self-degrading gel foams based on the gelation of polyethylene glycol diacrylate (PEGDA) and polyethyleneimine (PEI).¹²⁴⁻¹²⁶ This system exploits the Michael addition reaction between PEGDA's acrylate groups and PEI's amine groups, which occurs spontaneously under mild conditions without requiring initiators or catalysts.^{80,124-126} This is particularly advantageous as traditional crosslinking methods often require radical initiators that can be problematic due to their cytotoxicity and narrow processing windows. Both PEGDA and PEI are well-established polymers with proven biocompatibility - PEGDA has been widely used in hydrogels for various applications, while PEI is commonly employed in gene delivery systems.¹²⁷⁻¹³⁰ The resulting gel network undergoes controlled degradation through hydrolysis of the ester linkages under ambient conditions. Importantly, the mechanical properties and degradation kinetics can be tuned by adjusting the concentrations of both polymers, allowing optimization of the foam properties for specific applications while maintaining the desired self-degrading behavior.

5.2 Results and Discussion

5.2.1 PEGDA/PEI Gel System

The self-degrading gel is synthesized by mixing two precursor solutions: polyethyleneimine (PEI) and polyethylene glycol diacrylate (PEGDA) (Figure 5.2A). Both precursors are water-soluble and form clear solutions - a 5 wt% PEI solution and a 5 wt% PEGDA solution. The gel network forms through Michael addition reaction between the acrylate groups of PEGDA and the primary/secondary amines of PEI.^{80,124-126} In this reaction, the amine groups of PEI act as nucleophiles, attacking the electron-deficient β -carbon of the acrylate groups in PEGDA. This creates a covalent bond between the nitrogen of PEI and the β -carbon of the former acrylate group, with the proton from the amine transferring to the α -carbon.^{80,124-126} The reaction proceeds spontaneously under ambient conditions without requiring any initiators or catalysts due to the strong nucleophilicity of the primary and secondary amines in PEI. When these solutions are mixed together, they rapidly form a crosslinked network, with PEI serving as a multifunctional crosslinker due to its numerous amine groups (Figure 5.2B). The network formation is evident from the transparent gel that maintains its shape upon vial inversion. The schematic illustrates how the PEGDA-PEI gel network is structured, with PEI chains (blue) connected by PEGDA crosslinks (red) through newly formed bonds (green) throughout the aqueous medium (light blue background). Importantly, this Michael addition forms linkages involving ester groups already present in PEGDA, which are susceptible to hydrolysis and will later enable the self-degrading behavior of our system.

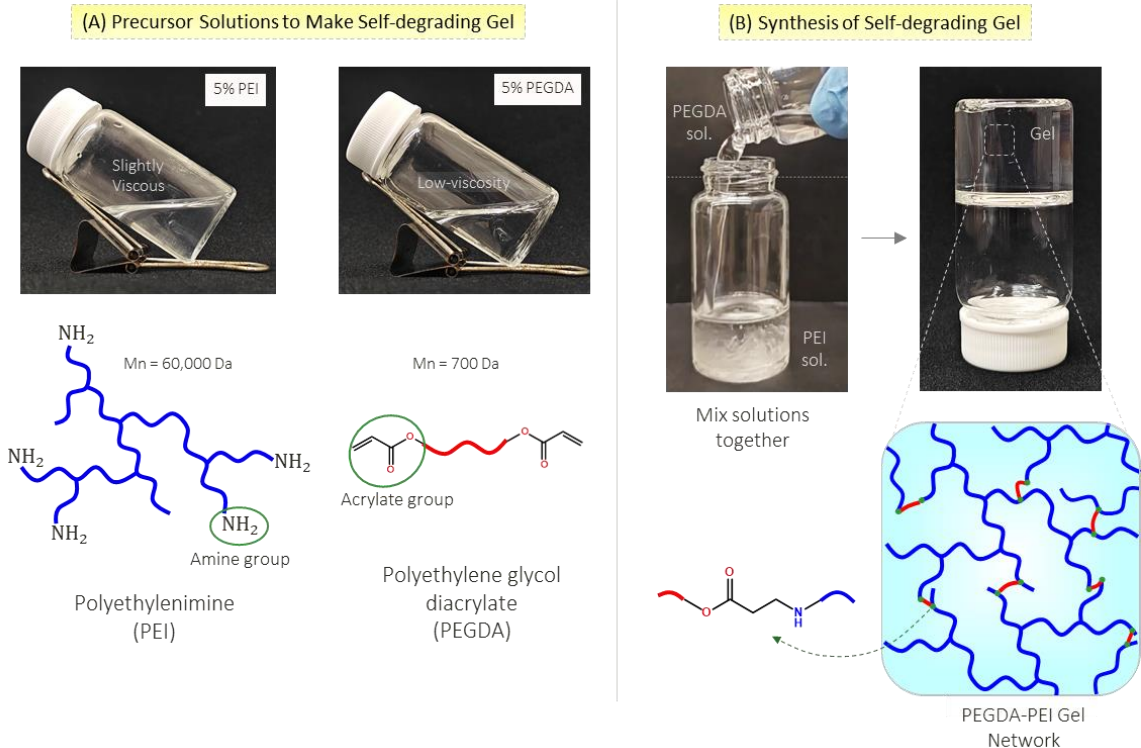


Figure 5.2: Synthesis and chemical structure of self-degrading PEGDA-PEI gel. (A) Precursor solutions showing water-soluble polyethyleneimine (PEI, 5 wt%) and polyethylene glycol diacrylate (PEGDA, 5 wt%). Chemical structures show the reactive amine groups of PEI (blue) and acrylate groups of PEGDA (red) that participate in network formation. (B) Gel synthesis demonstrated through mixing of precursor solutions and subsequent network formation, evidenced by the inverted vial test. The schematic illustrates the resulting PEGDA-PEI gel network structure where PEI chains (blue) are connected by PEGDA crosslinks (red) through newly formed bonds (green) in an aqueous environment (light blue background).

Upon mixing the two solutions, the crosslinking reaction leads to rapid gel formation, which we characterized rheologically (Figure 5.3). The dynamic time sweep measurements (Figure 5.3A) reveal the evolution of viscoelastic properties during network formation. Initially, the loss modulus (G'') exceeds the storage modulus (G'), indicating liquid-like behavior of the mixed solution. However, within few seconds (~ 30 s including the time to load the sample on the rheometer) of mixing, G' surpasses G'' , signifying the

sol-to-gel transition. This rapid gelation is advantageous for our intended applications as it allows quick solidification after deployment. The crossover point of G' and G'' represents the gel point, where the system transitions from a viscous liquid to an elastic solid. The rheological properties of the fully formed gel were examined through frequency sweep measurements conducted 5 minutes after mixing (Figure 5.3B). The frequency-independent behavior of both moduli, with G' (~50,000 Pa) consistently higher than G'' across all frequencies, is characteristic of a well-developed crosslinked network. This mechanical signature confirms the formation of a robust gel structure through the Michael addition crosslinking reaction.

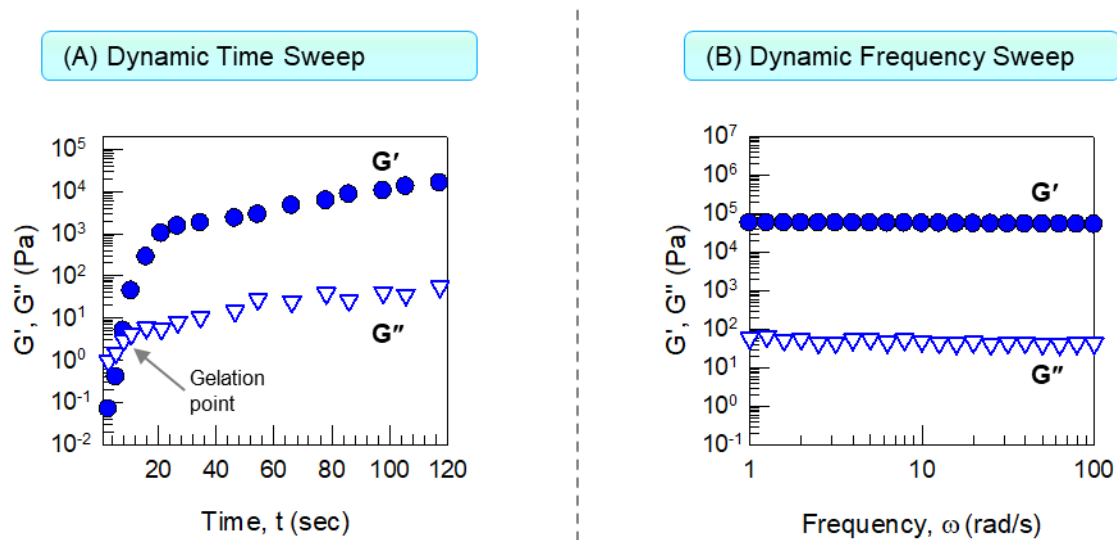


Figure 5.3: Rheological characterization of PEGDA-PEI gel formation. (A) Dynamic time sweep showing evolution of storage modulus (G' , filled circles) and loss modulus (G'' , open triangles) during gel formation. The gelation point occurs when G' crosses over G'' . (B) Dynamic frequency sweep of the formed gel showing frequency-independent behavior with G' (~50,000 Pa) consistently higher than G'' , confirming the formation of a robust crosslinked network.

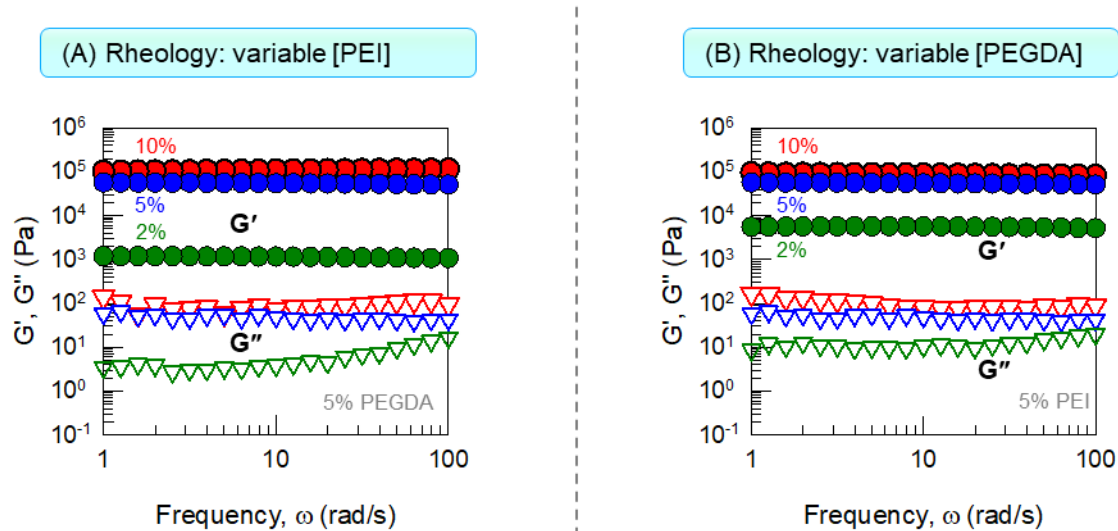


Figure 5.4: Effect of composition on gel rheology. (A) Dynamic frequency sweeps at fixed PEGDA concentration (5 wt%) with varying PEI concentration (2, 5, and 10 wt%) showing increase in storage modulus (G' , filled symbols) and loss modulus (G'' , open symbols) with increasing PEI content. (B) Dynamic frequency sweeps at fixed PEI concentration (5 wt%) with varying PEGDA concentration (2, 5, and 10 wt%) showing similar increase in moduli with increasing PEGDA content. The frequency-independent behavior of G' and G'' indicates formation of well-structured gel networks across all compositions tested.

Next, we systematically explored the effect of composition on the gel properties (Figure 5.4). First, we maintained a constant PEGDA concentration at 5 wt% while varying the PEI concentration from 2 to 10 wt% (Figure 5.4A). Dynamic frequency sweeps show that increasing PEI concentration results in significant increases in the gel elastic modulus (G'), from $\sim 1,000$ Pa at 2 wt% PEI to $\sim 50,000$ Pa at 5 wt% PEI, and further to $\sim 100,000$ Pa at 10 wt% PEI. We then examined the effect of PEGDA concentration by maintaining PEI at 5 wt% while varying PEGDA from 2 to 10 wt% (Figure 5.4B). A similar trend was observed, with the gel modulus increasing from 5,000 Pa to 50,000 Pa to 90,000 Pa as PEGDA concentration increased from 2 to 5 to 10 wt%. The increase in modulus with higher concentrations of either component can be attributed to greater crosslink density in

the network. Higher PEI concentration provides more amine groups available for crosslinking, while higher PEGDA concentration increases the number of acrylate groups that can form crosslinks. In both cases, more crosslinks lead to a more rigid network structure with higher elastic modulus. These results suggest that the mechanical properties of the gel network can be tuned over two orders of magnitude through composition control.

5.2.2 Self-Degrading Behavior of PEGDA/PEI Gel System

The PEGDA/PEI gel system undergoes spontaneous degradation under ambient conditions due to the presence of hydrolyzable ester groups in the PEGDA crosslinks. This degradation process was monitored both visually and rheologically over time (Figure 5.5). Photographs taken over 6 hours show the evolution of gel degradation (Figure 5.5A). Initially, a robust rigid gel maintains its shape. As time progresses, the gel gradually begins to sag, indicating progressive network breakdown. By 4.5 hours, it becomes difficult for the gel to maintain its shape, and at 6 hours, it completely reverts to a liquid state (sol).

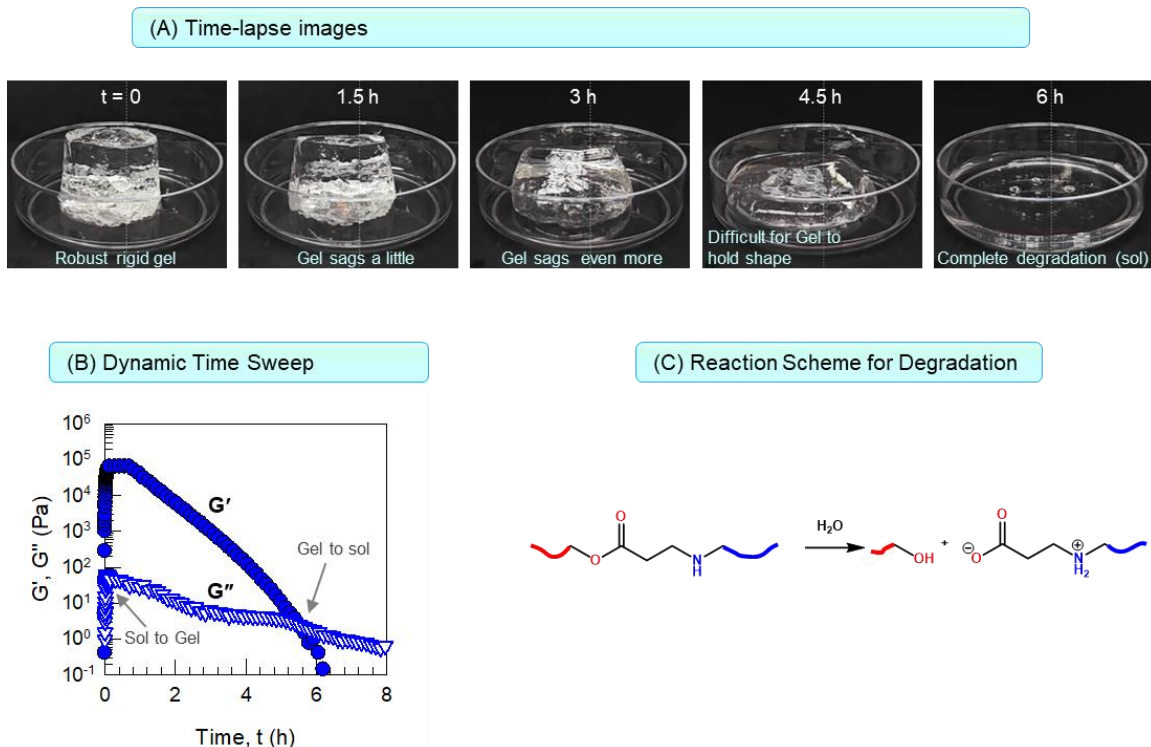


Figure 5.5: Characterization of PEGDA/PEI gel degradation. (A) Photographs showing evolution of gel degradation over 6 hours. Initially rigid gel progressively loses structural integrity and completely reverts to sol state. (B) Dynamic time sweep rheology showing rapid initial gelation ($G' > G''$ within 30s), followed by gradual degradation over 6 hours. The gel-to-sol transition occurs at 5.8h when G' crosses G'' . (C) Reaction scheme showing hydrolysis of ester linkages in PEGDA segments responsible for network degradation.

This degradation process was quantitatively tracked through dynamic time sweep rheology (Figure 5.5B). Upon mixing, the sample quickly gels (within 30 seconds) as G' exceeds G'' . The storage modulus continues to increase, reaching a maximum value of approximately 50,000 Pa, indicating formation of a well-structured elastic network. Over time, both moduli decrease, with G' showing a more dramatic drop, indicating progressive network degradation. At 5.8 hours, G' and G'' cross over, signifying the gel-to-sol transition where the material loses its elastic character and becomes predominantly viscous. This degradation occurs through hydrolysis of the ester linkages in the PEGDA segments of the

network (Figure 5.5C). Water molecules attack these ester bonds, breaking the PEGDA crosslinks and ultimately leading to network disintegration. Notably, this degradation occurs spontaneously under ambient conditions without requiring any external triggers or stimuli.

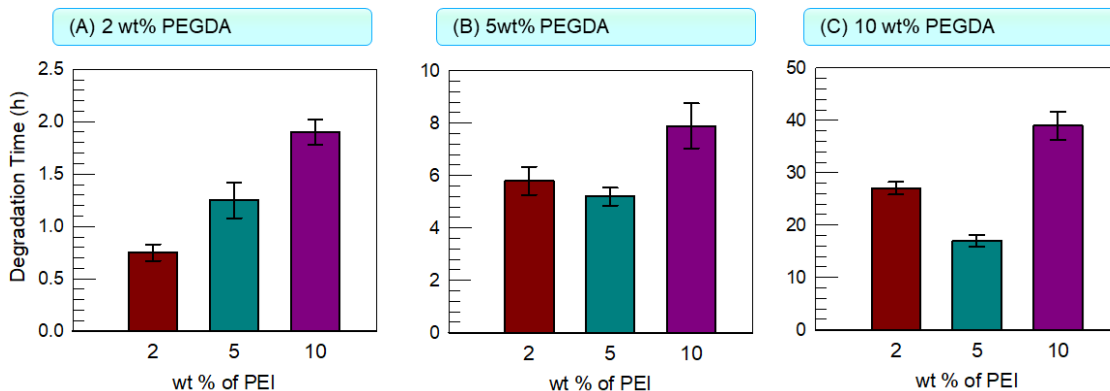


Figure 5.6: Effect of composition on gel degradation time. Degradation times for gels with different compositions: (A) 2 wt% PEGDA (B) 5 wt% PEGDA and (C) 10 wt% PEGDA, each with varying PEI concentrations (2, 5, and 10 wt%). Error bars represent standard deviation from three independent measurements.

We next investigated how the gel composition affects degradation kinetics (Figure 5.6). First, at 2 wt% PEGDA, varying PEI concentration from 2 to 10 wt% shows that degradation time increases monotonically with PEI content (Figure 5.6A). The average degradation times were 0.75, 1.25, and 1.9 hours for 2, 5, and 10 wt% PEI, respectively. Increasing PEGDA concentration to 5 wt% (Figure 5.6B) dramatically extended degradation times to several hours and, interestingly, changed how PEI concentration affected degradation. At 5 wt% PEGDA, we observed a non-monotonic dependence on PEI concentration: samples with 5 wt% PEI degraded fastest (5.2 hours), while those with 2 wt% and 10 wt% PEI took longer (5.8 and 7.9 hours, respectively). This non-monotonic

trend persisted at 10 wt% PEGDA (Figure 5.6C), where degradation times were further extended: 17 hours for 5 wt% PEI, 27 hours for 2 wt% PEI, and 39 hours for 10 wt% PEI. This non-monotonic effect of PEI concentration likely results from two competing mechanisms. On one hand, the amine groups in PEI catalyze the hydrolysis of ester groups, which should accelerate degradation. On the other hand, increasing PEI concentration raises the system's viscosity, potentially slowing the degradation reaction kinetics. The interplay between these opposing effects may explain the observed non-monotonic dependence on PEI concentration.

To test our hypothesis about viscosity effects, we conducted experiments using lower molecular weight PEI ($M_n = 2,000$ Da) and compared it to our previous results with higher molecular weight PEI ($M_n = 60,000$ Da). We prepared samples with 5 and 10 wt% PEGDA, each at varying PEI concentrations (2, 5, and 10 wt%). Note that gels did not form with 2 wt% PEGDA using the lower molecular weight PEI. Using 5 wt% PEGDA (Figure 5.7A), the degradation times decreased monotonically with increasing PEI concentration: 25, 14, and 8 minutes for 2, 5, and 10 wt% PEI, respectively. This trend starkly contrasts with our previous results using high molecular weight PEI, where the 5 wt% PEI showed fastest degradation (5.2 hours) compared to 2 wt% (5.8 hours) and 10 wt% (7.9 hours). Notably, the degradation times with low molecular weight PEI are significantly shorter - minutes rather than hours. Similarly, with 10 wt% PEGDA (Figure 5.7B), degradation times with low molecular weight PEI decreased monotonically from 300 to 67 to 22 minutes as PEI increased from 2 to 5 to 10 wt%. This again contrasts with the non-monotonic behavior observed with high molecular weight PEI (27, 17, and 39

hours for 2, 5, and 10 wt% PEI), and again shows much faster overall degradation. The dramatic differences in both the trend and timescale can be attributed to viscosity effects: the lower molecular weight PEI (2,000 Da) contributes minimally to system viscosity compared to the higher molecular weight PEI (60,000 Da).

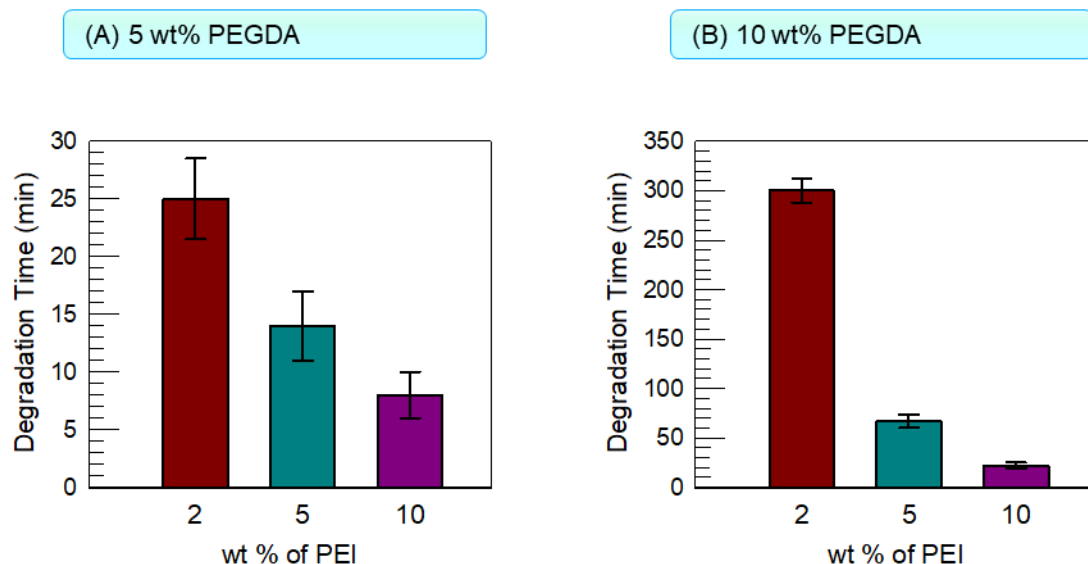


Figure 5.7: Effect of low molecular weight PEI ($M_n = 2,000$ Da) on gel degradation time. Degradation times for gels with (A) 5 wt% PEGDA and (B) 10 wt% PEGDA, each with varying PEI concentrations (2, 5, and 10 wt%). Error bars represent standard deviation from three independent measurements.

To further validate our hypothesis about viscosity effects, we modified the system viscosity independently of the reactive components. We added sodium alginate, a high molecular weight biopolymer that is chemically inert in our system, to alter the solution viscosity without affecting the reaction chemistry. Sodium alginate was chosen because it does not participate in the Michael addition reaction between PEGDA and PEI, nor does it affect the ester hydrolysis mechanism. Furthermore, at the pH of our system, alginate's

carboxylate groups remain deprotonated and do not catalyze ester hydrolysis. Using our base composition of 5 wt% PEGDA and 5 wt% PEI ($M_n = 2,000$ Da), we varied the alginate concentration from 0 to 1 wt% (Figure 5.8). The degradation time increased systematically with alginate content: 14, 20, and 28 minutes for 0, 0.5, and 1 wt% alginate, respectively. This clear correlation between increased viscosity and longer degradation times provides strong support for our hypothesis about the role of viscosity in controlling gel degradation kinetics.

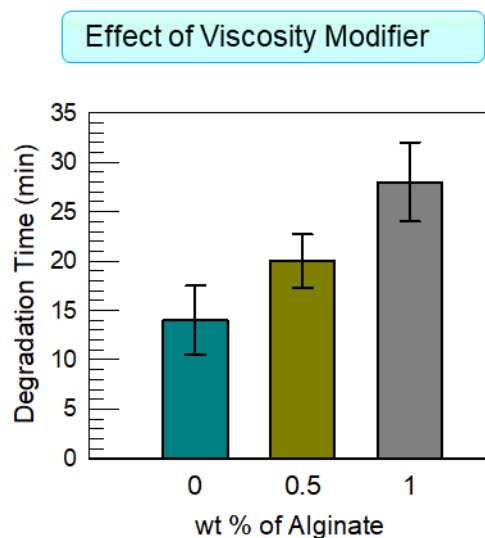


Figure 5.8: Effect of viscosity modifier on gel degradation. Degradation times for gels containing 5 wt% PEGDA and 5 wt% PEI ($M_n = 2,000$ Da) with varying concentrations of sodium alginate (0, 0.5, and 1 wt%). Error bars represent standard deviation from three independent measurements.

5.2.3 Self-Degrading Gel Foams

We next investigated the formation of self-degrading foams. Our strategy involves first generating foam from the liquid precursor solution, which subsequently gels to form a solid foam structure that can later degrade. Two approaches can be used to incorporate gas into a liquid to generate foams (Figure 5.9): mechanical shear and in-situ gas generation. While mechanical shear can directly incorporate air (Figure 5.9A), in-situ gas generation relies on chemical reactions to produce gas bubbles within the liquid (Figure 5.9B). We chose to use in-situ gas generation, specifically the enzymatic decomposition of hydrogen peroxide (H_2O_2) to oxygen gas using catalase. This approach offers two key advantages: (1) precise control over foam expansion through reactant concentrations, and (2) elimination of high-shear mixing requirements.

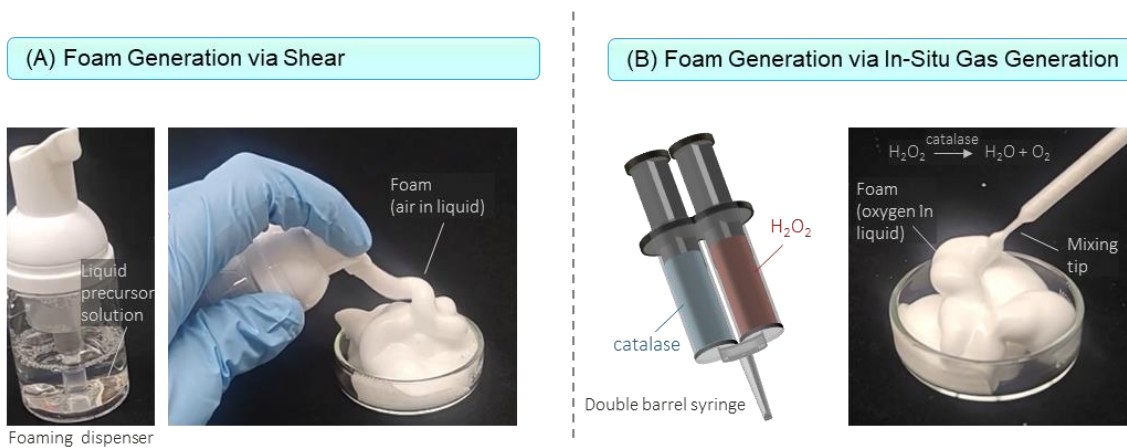


Figure 5.9: Methods for foam generation. (A) Mechanical shear method using a foaming dispenser to incorporate air into the liquid precursor solution. (B) In-situ gas generation method using a double-barrel syringe system where H_2O_2 decomposition by catalase generates oxygen bubbles.

The extent of foam expansion can be systematically controlled through H_2O_2 concentration (Figure 5.10). As H_2O_2 concentration increased from 1 to 10 wt. %, the expansion ratio increased from 6 to 28, meaning the initial precursor solution expanded to 6-28 times its original volume. The expansion ratio shows a nearly linear relationship with H_2O_2 concentration, suggesting that oxygen generation is the limiting factor in foam expansion. Typically, surfactants or particle stabilizers are required to prevent rapid foam collapse through mechanisms such as drainage and coalescence. However, in our system, the quick gelation (within seconds) combined with PEI's inherent stabilizing properties enables foam stability without additional stabilizers, making it particularly suitable for applications where surfactants or particles are undesirable.

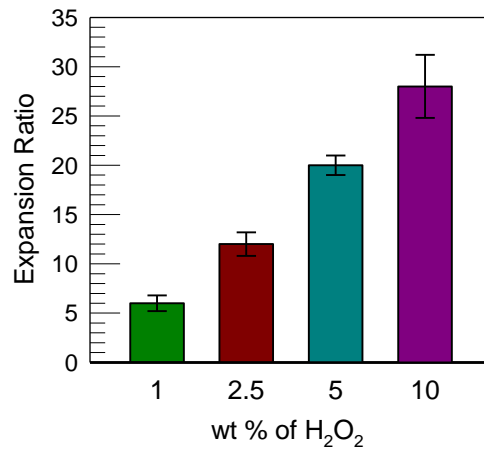


Figure 5.10: Control of foam expansion through H_2O_2 concentration. Expansion ratio (final volume/initial volume) increases with H_2O_2 concentration from 6-fold at 1 wt.% to 28-fold at 10 wt.% H_2O_2 . Error bars represent standard deviation from three independent measurements.

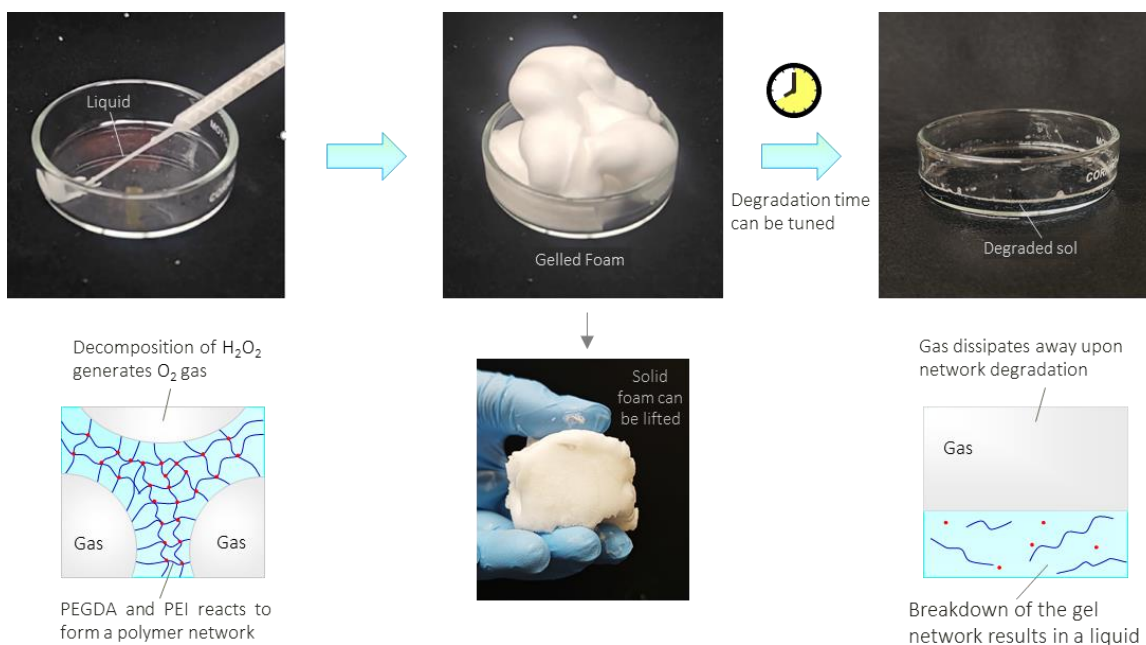


Figure 5.11: Formation, gelation, and degradation of self-degrading foam. Photographs and schematics showing the transformation sequence: liquid precursor solution expands due to O_2 generation from H_2O_2 decomposition while simultaneously gelling through PEGDA-PEI reaction to form a robust solid foam. The foam eventually degrades back to a liquid state with a tunable degradation time.

We implemented this foaming approach using a double-barrel syringe system (Figure 5.11). One compartment contains PEGDA (5 wt%) and H_2O_2 (10 wt%), while the other contains PEI (5 wt%) and catalase (0.1 wt%). When injected, these solutions combine in the static mixing tip, triggering a sequence of rapid transformations. The gas generation is instantaneous as catalase immediately decomposes H_2O_2 into O_2 , creating bubbles throughout the liquid medium. Concurrent with gas generation, the Michael addition between PEGDA and PEI forms a crosslinked network within seconds, stabilizing the foam structure. The rapid foam generation and gelation ensure that the foam structure is captured before any significant bubble coalescence or drainage can occur. The solid foam formed is sufficiently robust that it can be lifted, demonstrating the structural integrity provided by

the gel network. What makes this system particularly interesting is its complete transformation cycle: starting as a low-volume liquid, expanding into a large-volume solid foam, and finally reverting to a low-volume liquid through network degradation. The degradation time can be controlled from minutes to days by adjusting composition, as demonstrated in our earlier studies.

5.2.4 Demonstration of Self-degrading Foams

To illustrate the controlled release and automatic cleanup capabilities of our self-degrading foam system, we conducted dye release experiments using Rhodamine B as a model solute (Figure 5.12). When a dye solution is directly added to water (Figure 5.12A), it immediately mixes with the bulk liquid below. We then compared two foam-based delivery approaches. First, using a conventional liquid foam stabilized by 2 wt% Tween 80 surfactant (Figure 5.12B), the foam initially stays at the surface due to its low density. However, rapid drainage occurs - within 1 minute, significant liquid has drained, and by 2 minutes, most of the dye-containing liquid has transferred to the bulk solution, resulting in intense pink coloration. In contrast, our self-degrading PEGDA/PEI gel foam (5 wt% each) demonstrates controlled release behavior (Figure 5.12C). The foam, dispensed via double-barrel syringe, expands and maintains its structure at the water surface. As the gel network gradually degrades, it releases the dye in a controlled manner - by 2 hours, the light pink color of the solution indicates initial dye release. The color intensity increases by 4 hours as degradation continues, and by 6 hours, the foam has completely degraded, leaving a clean surface with uniform dye distribution in the solution below.



Figure 5.12: Demonstration of controlled release using self-degrading foam. (A) Direct addition of dye solution shows immediate mixing. (B) Conventional liquid foam (2 wt% Tween 80) shows rapid drainage within minutes. (C) Self-degrading gel foam (5 wt% PEGDA/PEI) demonstrates controlled release over 6 hours with eventual complete degradation.

The tunable degradation kinetics of our PEGDA/PEI system enables control over solute release rates from the foam. We quantified the release profiles by measuring dye concentration in the solution below the foam using UV/VIS spectrophotometry (Figure

5.13). The non-gelling liquid foam releases its entire payload within 3 minutes due to rapid drainage. In contrast, our gel foams show dramatically different release profiles depending on composition. A foam containing 5 wt% PEGDA and 5 wt% PEI exhibits complete release over approximately 6 hours. Increasing PEI concentration to 10 wt% (with 5 wt% PEGDA) extends the release time to nearly 24 hours. Further modification using 10 wt% PEGDA and 2 wt% PEI results in the slowest release, with only 60% of the dye released after 30 hours. This ability to tune release profiles over such a wide time range makes these foams particularly versatile for various controlled release applications.

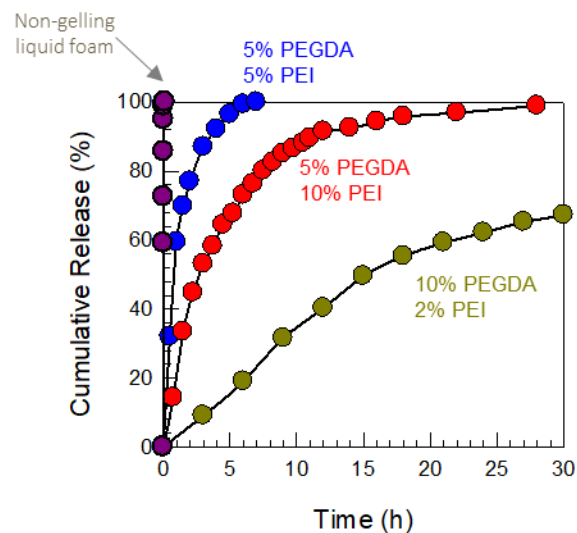


Figure 5.13: Controlled release profiles from self-degrading foams. Cumulative dye release over time for different foam compositions. Non-gelling liquid foam shows immediate release (< 3 min), while gel foams demonstrate tunable extended release: 5 wt% PEGDA/5 wt% PEI (6h), 5 wt% PEGDA/10 wt% PEI (24h), and 10 wt% PEGDA/2 wt% PEI (>30h).

Our self-degrading foam system offers a promising solution for treating harmful algal blooms (HABs), which pose significant environmental and economic challenges in

coastal regions.^{131,132} Figure 5.14 illustrates the application concept: the algaecide-containing foam is sprayed onto water surfaces affected by HABs. Due to the foam's low density, it remains localized at the surface where the algae are concentrated. As the foam gradually degrades, it releases algaecide specifically into the surface layer where it's needed, while marine life below remains protected. The controlled release profiles demonstrated in our dye studies (Figure 5.13) suggest that treatment duration can be tuned based on specific application needs. After treatment, the foam completely degrades, requiring no cleanup and leaving behind only treated water with neutralized algae.

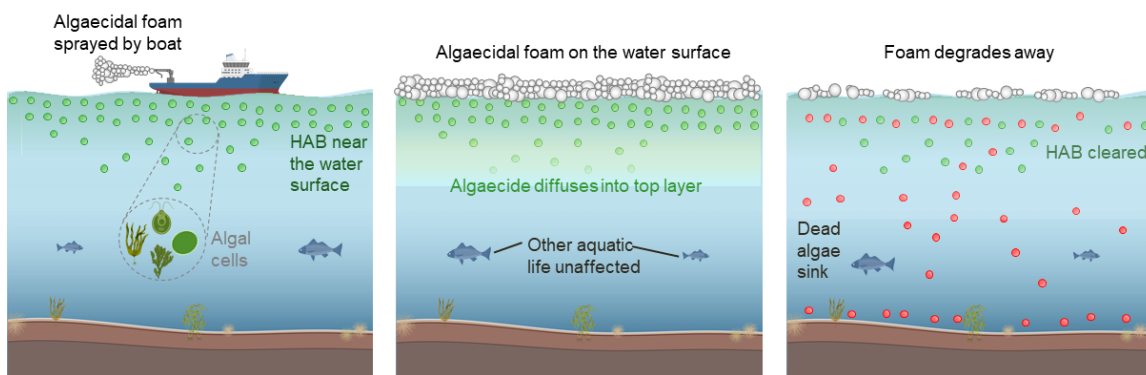


Figure 5.14: Application of self-degrading foam for HAB treatment. Schematic showing: (left) initial application of algaecidal foam over HAB-affected water, (middle) controlled release of algaecide into surface layer while protecting aquatic life below, and (right) complete foam degradation after treatment with dead algae sinking to bottom.

5.3 Conclusions

In this work, we have developed a new class of self-degrading gel foams based on the reaction between PEGDA and PEI. The system exhibits several unique features: (1) rapid gelation that enables foam stabilization without requiring additional surfactants, (2) tunable degradation times from minutes to days through composition control, and (3) complete degradation back to a low-viscosity liquid state. We demonstrated that foam expansion can be precisely controlled through H_2O_2 concentration. Through composition studies, we showed that both PEGDA and PEI concentrations significantly influence degradation time, with lower molecular weight PEI providing faster degradation. Using model dye studies, we demonstrated that these foams can provide controlled release of compounds over predetermined time periods, in contrast to conventional liquid foams that release their contents almost immediately. This combination of controlled expansion, tunable degradation, and programmed release makes these materials particularly promising for applications requiring temporary surface coverage with automatic cleanup, such as treatment of harmful algal blooms.

5.4 Experimental Section

Materials. Polyethylene glycol diacrylate (PEGDA, $M_n = 700$), polyethyleneimine (PEI, $M_n = 60,000$ and $M_n = 2,000$), hydrogen peroxide solution (30 wt% in H₂O), catalase from bovine liver, sodium alginate (medium viscosity), and Rhodamine B were purchased from Sigma-Aldrich and used as received. Deionized (DI) water was used in all experiments.

Preparation of Self-degrading Gels. Self-degrading gels were prepared by mixing equal volumes of PEGDA (4-20 wt%) and PEI (4-20 wt%) solutions to achieve final concentrations of 2-10 wt% for each component. The solutions were mixed thoroughly and allowed to gel at room temperature.

Preparation of Self-degrading Gel Foams. Self-degrading gel foams were prepared using a double-barrel syringe system. One compartment contained PEGDA (2-10 wt%) and H₂O₂ (1-10 wt%) in DI water, while the other contained PEI (2-10 wt%) and catalase (0.1 wt%) in DI water. For dye release studies, Rhodamine B was added to the PEGDA solution.

Expansion Ratio Measurements. Expansion ratios were determined in a graduated cylinder. A fixed volume (2 mL) of the precursor solutions was added to the cylinder and quickly mixed with a long spatula. The final volume was recorded immediately after mixing, and the expansion ratio was calculated as final volume/initial volume.

Rheological Characterization. Rheological measurements were performed on an AR2000 stress-controlled rheometer (TA Instruments) using a parallel plate geometry (40

mm diameter) at 25°C. Dynamic frequency sweeps were conducted in the linear viscoelastic regime from 1-100 rad/s at 1% strain. Dynamic time sweeps were performed at 10 Hz frequency and 1% strain to monitor gel formation and degradation.

Degradation Time Measurements. Degradation times were determined through vial inversion tests. Samples were prepared in glass vials and inverted at regular time intervals. The degradation time was recorded as the point when the gel could no longer maintain its shape upon inversion and flowed like a liquid.

Dye Release Studies. UV-vis spectrophotometry measurements were performed using a Varian Cary 50 spectrophotometer. The absorbance of Rhodamine B was monitored at 555 nm using a 1 cm path length cuvette at room temperature. Samples were diluted as needed to maintain absorbance readings within the linear range.

Chapter 6

Recommendations and Future Work

6.1 Project Summary

In this dissertation, we have introduced a fundamentally new concept in materials science: soft materials that can be programmed to transform from solid-like gels to flowing liquids after a predetermined time without any external intervention. Through three interconnected studies, we have demonstrated that this concept of autonomous degradation can be realized across distinctly different material platforms: (1) molecular organogels containing acid in polar solvents, where degradation occurs through hydrolysis, (2) completely non-aqueous molecular organogels based on organic acids, where esterification drives the degradation, and (3) polymeric gel foams formed through Michael addition chemistry, where controlled hydrolysis of network crosslinks enables both spatial and temporal control over degradation. Together, these studies establish self-degradation as a versatile approach that can be implemented across multiple chemical platforms and length scales.

In Chapter 3, we introduced self-degrading molecular organogels based on (1,3:2,4)-dibenzylidene sorbitol (DBS) in various organic solvents. These gels exhibit controlled degradation through acid-catalyzed hydrolysis of acetal groups in DBS, transforming from robust gels ($G' > 10,000$ Pa) to thin sols over a period that can be tuned from hours to days. The system allows remarkable control over the degradation process - at time $t = 0$, the gel is extremely strong and indistinguishable from a non-degrading DBS

gel, yet it completely liquefies after a predetermined time. The degradation time can be precisely controlled through two key parameters: acid concentration and temperature. For example, at 30°C, increasing the HCl concentration from 0.3 M to 1.0 M reduces the degradation time from 10 days to 3 days. Similarly, at a fixed acid concentration of 0.3 M, raising the temperature from 30°C to 40°C decreases the degradation time from 10 days to 2 days. Through NMR and mass spectrometry studies, we conclusively showed that degradation occurs through acid-catalyzed hydrolysis of the acetal groups in DBS, producing benzaldehyde and sorbitol as degradation products. These small molecules cannot self-assemble into the nanofibrillar network required for gelation, explaining the complete conversion to a flowing liquid. We demonstrated practical applications of these self-degrading gels in time-activated valves (where the valve opens after a set time) and flow diversion (where flow through a channel is blocked for a predetermined period).

In Chapter 4, we expanded upon our self-degrading gel concept to develop completely non-aqueous organogels specifically designed for lost circulation control in oil drilling. While our previous work with aqueous acids demonstrated the feasibility of self-degrading gels, oilfield applications require water-free systems that can function at elevated temperatures (> 70°C). By incorporating organic acids like hexanoic acid into DBS gels in mineral oil, we achieved controlled degradation through esterification rather than hydrolysis. The system exhibits several remarkable properties: First, the degradation follows a strictly linear profile, where the mass fraction of intact gel decreases at a constant rate until complete liquefaction. Second, the gel maintains its initial mechanical strength (G' remains constant) throughout the degradation process, even as its volume decreases - a

unique "shrinking core" behavior that distinguishes it from conventional degradable materials. The degradation time can be systematically tuned through multiple parameters: increasing the acid concentration from 20 to 80 wt% reduces degradation time from 5 days to less than 1 day at 70°C; shorter-chain acids promote faster degradation (2, 5, and 10 days for butanoic, hexanoic, and octanoic acids respectively); and temperature strongly accelerates the process (from 10 days at 30°C to 2 days at 40°C). Through detailed NMR and mass spectrometry studies, we established that degradation occurs through esterification of DBS hydroxyl groups by the organic acid, producing DBS-esters that cannot self-assemble into fibrils. These properties make these gels particularly suitable for lost circulation control, where they can temporarily seal rock fractures during drilling operations before autonomously degrading to restore formation permeability.

In Chapter 5, we created a new class of self-degrading gel foams based on the Michael addition reaction between polyethylene glycol diacrylate (PEGDA) and polyethyleneimine (PEI). These materials uniquely combine spatial control through foam expansion with temporal control through programmed degradation. The gel network forms rapidly through the reaction between PEGDA's acrylate groups and PEI's primary/secondary amines, achieving high mechanical strength ($G' \sim 50,000$ Pa) within seconds. Foam generation is accomplished through the enzymatic decomposition of H₂O₂ by catalase, which produces oxygen bubbles in situ. This approach offers precise control over foam expansion - increasing H₂O₂ concentration from 1 to 10 wt% systematically increases the expansion ratio from 6-fold to 28-fold. The gel's degradation occurs through hydrolysis of ester linkages in the network and can be tuned from minutes to days through

composition. For example, with 5 wt% PEGDA, increasing PEI molecular weight from 2,000 to 60,000 Da extends degradation time from minutes to days. Interestingly, the degradation kinetics show a non-monotonic dependence on PEI concentration due to competing effects of catalytic activity and solution viscosity. Using rhodamine B as a model compound, we demonstrated that these foams enable controlled release over predetermined periods - from immediate release for non-gelling liquid foams to sustained release over 30 hours for optimized gel compositions. This combination of controlled expansion, tunable degradation, and programmed release makes these materials particularly promising for environmental applications such as treatment of harmful algal blooms, where the foam can deliver treatment agents to the water surface and then autonomously degrade without requiring cleanup.

6.2 Recommendations for Future Work

6.2.1 Triggered and Delayed Degradation Systems

An intriguing direction would be controlling the start of the degradation timer. Currently, the degradation 'clock' starts as soon as the material is prepared. We propose engineering materials where a 'trigger' can be used to start the degradation clock. As illustrated in Figure 6.1, one potential approach involves encapsulating the degrading agent (e.g., acid) and dispersing it throughout the material. The capsules would have a hermetic seal (e.g., wax shell) that prevents the degrading agent from interacting with the material structure. When a trigger is applied (e.g., temperature above the wax melting point), the capsule shells disintegrate (melt), releasing the degrading agent throughout the material and initiating the degradation clock. This technique would allow our materials to have an indefinite shelf-life, only beginning the degradation cycle once the trigger is applied.

Another fascinating aspect to explore would be 'delaying' the start of degradation clock without any external trigger. After the material is prepared, the onset of degradation could be automatically delayed through internal mechanisms. This could be achieved by incorporating systems that release healing agents during early stages of degradation, effectively counteracting initial degradation processes until the healing agents are depleted. Such self-regulating systems could provide more precise control over when degradation begins.

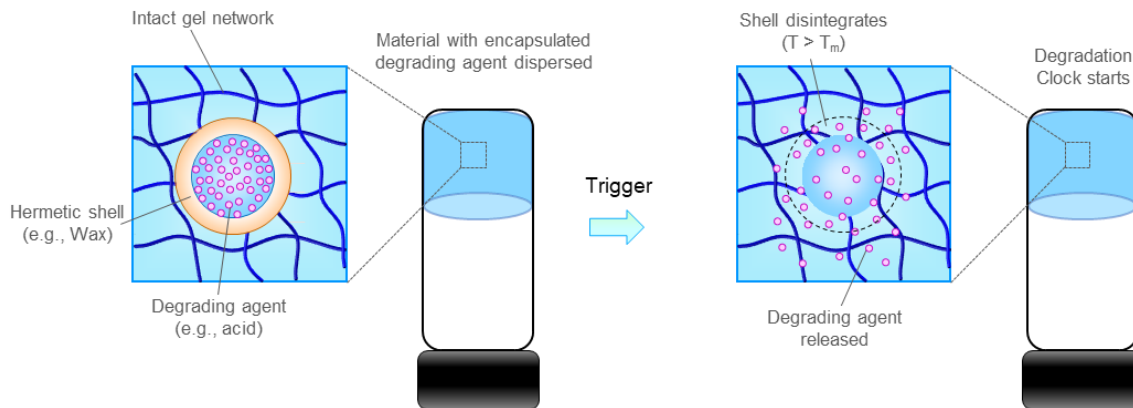


Figure 6.1. Concept for triggered initiation of self-degrading materials. A degrading agent (e.g., acid) is initially encapsulated within a hermetic shell (e.g., wax) and dispersed throughout an intact gel network. When an external trigger is applied (e.g., temperature above the wax melting point), the shell disintegrates, releasing the degrading agent. This starts the degradation "clock", causing controlled breakdown of the surrounding network. This approach would enable indefinite storage until degradation is deliberately initiated.

6.2.2 Extension to New Chemical Platforms

While we have demonstrated self-degrading materials based on DBS, PEGDA-PEI, and related chemistries, the concept could be extended to many other chemical platforms. Investigation of alternative molecular gelators with different self-assembly mechanisms could provide access to new mechanical properties or compatibility with different solvents. For instance, gelators based on peptide self-assembly or metal-coordination could offer unique degradation mechanisms while maintaining autonomous behavior. Development of new polymer backbones with programmed degradation triggers could enable better control over degradation products and kinetics. Similarly, exploration of alternative catalytic systems beyond acid catalysis could provide new routes to controlled network breakdown. The creation of hybrid materials combining multiple degradation mechanisms might allow

for more precise control over the degradation timeline. This expansion would enable new applications where current systems are limited by their chemical composition.

6.2.3 Development of Temperature-Independent Degradation Systems

While our current systems exhibit controlled degradation, their strong temperature dependence can limit practical applications. In oilfield applications, temperature variations with well depth can cause unpredictable degradation times. Similarly, for surface treatment applications, day/night temperature cycles could lead to inconsistent performance. Future work could explore the incorporation of temperature-responsive buffer systems that modulate local pH or catalytic activity to compensate for temperature effects. The key challenge will be maintaining autonomous degradation while achieving temperature independence. This might be accomplished through careful molecular design of the degradation triggers, perhaps incorporating competing reactions with opposite temperature dependencies to achieve a net temperature-neutral effect. Success in this area would dramatically improve the reliability of self-degrading materials in real-world applications.

6.2.4. Sequential Release from a Multi-Compartment Self-Degrading System

Building on our work with self-degrading gels, we propose developing smart delivery systems that combine controlled degradation with targeted release. Our self-degrading systems could be modified to incorporate different functional payloads (e.g., drugs, agrochemicals, or growth factors) that are released as the gel degrades. By carefully

engineering the gel composition and degradation kinetics, sequential release of multiple agents could be achieved. This would enable new therapeutic approaches where different drugs need to be delivered in a specific sequence, as well as engineering new materials (e.g., multicompartiment capsules) to carry out cascade reactions that wouldn't be otherwise possible.

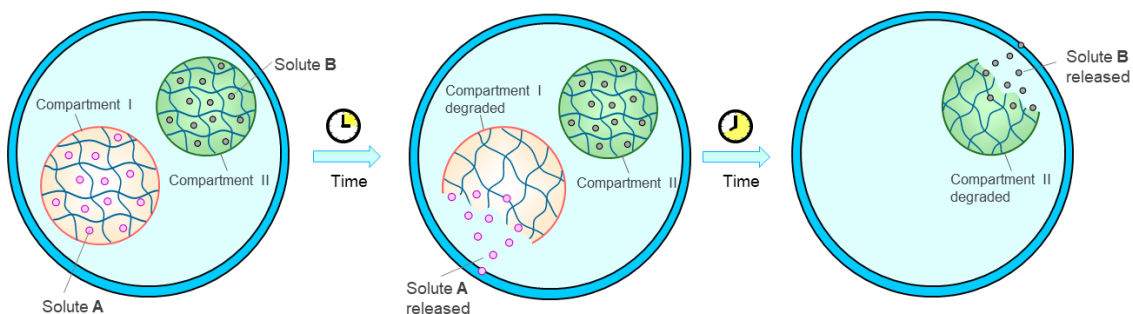


Figure 6.2. Sequential release from a multi-compartment self-degrading system. The system contains two compartments loaded with different solutes (A and B), each programmed to degrade at different times. Initially (left), both solutes are trapped within their respective gel networks. As time progresses (middle), Compartment I degrades first, releasing Solute A while Compartment II remains intact. After additional time (right), Compartment II degrades and releases Solute B. This design enables programmed sequential delivery of multiple agents.

As shown in Figure 6.2, a multi-compartment system could be designed where each compartment contains different solutes and is programmed to degrade at different times. Initially, both compartments contain their respective solutes (A and B) trapped within the gel network. As time progresses, Compartment I degrades first, releasing Solute A while Compartment II remains intact. After additional time, Compartment II degrades, releasing

Solute B. This sequential release could enable complex therapeutic regimens or multi-step chemical processes to be carried out in a pre-programmed sequence.

The successful implementation of these recommendations would significantly advance the field of self-degrading materials. These advances could enable applications in fields ranging from medicine to environmental remediation to advanced manufacturing. However, achieving these goals will require careful molecular design, creative synthetic approaches, and thorough characterization of both degradation mechanisms and material properties.

List of Publications

Publications:

- [1] LK Border, MG Nader, FA Burni, SM Grasso, IO Ortega, M Saruwatari, A Sandler, M Erdi, P Kofinas, SR Raghavan. “Switchable Adhesion of Hydrogels to Plant and Animal Tissues.” *Advanced Science* **Accepted**.
- [2] FA Burni, W Xu, R Spencer, E Bergstrom, D Chappell, J Wee, SR Raghavan. “Self-degrading molecular organogels: Self-assembled gels programmed to spontaneously liquefy after a set time.” *Advanced Functional Materials* **2024**. 2403617.
- [3] FA Burni, NR Agrawal, M Walker, H Ali, SR Raghavan. “Complexity in a Simple Self-Assembling System: Lecithin-Water-Ethanol Mixtures Exhibit a Re-Entrant Phase Transition and a Vesicle-Micelle Transition (VMT) on Heating.” *Langmuir* **2024**.
- [4] W Xu, FA Burni, SR Raghavan. “Reversibly Sticking Metals and Graphite to Hydrogels and Tissues.” *ACS Central Science* **2024**. 10 (3), 695-707.
- [5] SN Subraveti, SM Peters, MG Nader, FA Burni, SR Raghavan. “A Smart Skin for Hydrogels That Enables Switchable Solute Release.” *ACS Applied Materials & Interfaces* **2024**. 16 (7), 9201-9209.
- [6] S Nikfarjam, R Gibbons, FA Burni, SR Raghavan, A Mikhail, T Woehl. “Chemically Fueled Dissipative Assembly of Protein Hydrogels Mediated by Protein Unfolding.” *Biomacromolecules* **2023**. 24 (3), 1131-1140.
- [7] NR Agrawal, M Omarova, FA Burni, VT John, SR Raghavan. “Spontaneous Formation of Stable Vesicles and Vesicle Gels in Polar Organic Solvents.” *Langmuir* **2021**. 37 (26), 7955-7965.

Manuscripts in preparation:

- [1] FA Burni, SR Raghavan. “Organogels that Degrade Spontaneously Over Weeks: A Solution to the ‘Lost Circulation’ Problem in Oil Drilling.” *Manuscript in preparation*. To be submitted by Dec. 2024.

- [2] FA Burni, E Utlu, H Cho, R Spencer, SR Raghavan. “Sustained Release of Hydrophilic Solutes Over Weeks from Hydrogels: A Simple Solution to a Hard Problem.” *Manuscript in preparation*. To be submitted by Dec. 2024.
- [3] FA Burni, A Malhotra, VT John, SR Raghavan. “Self-Degrading Polymer Foams Loaded with Algaecides for Eliminating Algal Blooms.” *Manuscript in preparation*. To be submitted by Jan. 2025.
- [4] FA Burni, W Chu, S Raghavan. “Mimicking the nucleus: Stimuli-responsive coacervate formation and dissolution in a microcapsule.” *Manuscript in preparation*. To be submitted by Jan. 2025
- [5] FA Burni, IM Philip, M Walker, SR Raghavan. “A Fast and Efficient Way to Remove Pollutants from Water Using Porous Hydrogels.” *Manuscript in preparation*. To be submitted by Feb. 2025.

Patent:

- [1] FA Burni, SR Raghavan, J Wee, D Chappell. “Self-degrading Organogels.” *U.S. Patent Application No. 18/173,550. (2024)*.

List of Presentations

Invited Talk:

- [1] “Self-degrading gels: Solids that transform into liquids after a set time.” **Oral presentation** at *Burgers Program for Fluid Dynamics* (2024), College Park, Maryland.

Conference Presentations:

- [1] “Complexity in a Simple Self-Assembling System: Lecithin-Water-Ethanol Mixtures Exhibit a Re-Entrant Phase Transition.” **Oral presentation** at *AICHE Annual Meeting* (2024), San Diego, California.
- [2] “Reversibly Sticking Metals and Graphite to Hydrogels and Tissues.” **Oral presentation** at *AICHE Annual Meeting* (2024), San Diego, California.
- [3] “Self-Degrading Molecular Organogels: Self-Assembled Gels Programmed to Spontaneously Liquefy after a Set Time.” **Oral presentation** at *AICHE Annual Meeting* (2024), San Diego, California.
- [4] “Organogels that degrade slowly at high temperature: A solution to the ‘lost circulation’ problem in oil well drilling.” **Oral presentation** at *SoR 95th Annual Meeting* (2024), Austin, Texas.
- [5] “Creating biopolymer gels in 3D using electric fields: 3D-printing without heat or light.” **Oral presentation** at *SoR 95th Annual Meeting* (2024), Austin, Texas.
- [6] “Unique rheology of self-degrading gel foams: Transitioning from liquid to solid to liquid.” **Oral presentation** at *SoR 95th Annual Meeting* (2024), Austin, Texas.
- [7] “A Cryo-TEM Study of Phase Transition in Lecithin-Water-Ethanol Mixtures.” **Poster presentation** at *M&M Meeting* (2024), Cleveland, Ohio.
- [8] “Multicompartment capsules: Mimicking cellular architecture through ‘smart’ and responsive compartments.” **Oral presentation** at *ACS Spring* (2024), New Orleans, Louisiana.
- [9] “From nature to capsules: Crafting stimuli-responsive membraneless compartments via coacervation.” **Oral presentation** at *ACS Spring* (2024), New Orleans, Louisiana.

- [10] “A free-standing organogel that spontaneously degrades to a thin sol after a set time.” **Poster presentation** at *XIXth International Congress on Rheology* (2023), Athens, Greece.
- [11] “Mimicking colloidal phenomena in a cell’s nucleus: Formation of microcompartments by complex coacervation.” **Oral presentation** at *97th ACS Colloids and Surface Science Symposium* (2023), Raleigh, North Carolina.
- [12] “Self-assembled organogels with time-programmed rheology: Spontaneous gel-to-sol transition after a set time.” **Oral presentation** at *97th ACS Colloids and Surface Science Symposium* (2023), Raleigh, North Carolina.
- [13] “Biological surfactants provide a green way to gel organic liquids by forming dense vesicles.” **Oral presentation** at *97th ACS Colloids and Surface Science Symposium* (2023), Raleigh, North Carolina.
- [14] “A free-standing organogel that spontaneously degrades to a thin sol after a set time.” **Oral presentation** at *MRS Spring Meeting* (2023), San Francisco, California.
- [15] “Self-assembly beyond water—forming lipid vesicles and vesicle-gels in polar organic solvents.” **Oral presentation** at *MRS Spring Meeting* (2023), San Francisco, California.
- [16] “Cell-like containers with inner organelles formed by coacervation of proteins and biopolymers.” **Oral presentation** at *MRS Spring Meeting* (2023), San Francisco, California.
- [17] “A gel with an in-built clock: Spontaneous dissolution of a molecular organogel after several days.” **Oral presentation** at *SoR 93rd Annual Meeting* (2022), Chicago, Illinois.
- [18] “Vesicles as gelling agents: Close-packed lipid vesicles provide a “green” route to gel polar solvents like glycerol.” **Oral presentation** at *SoR 93rd Annual Meeting* (2022), Chicago, Illinois.
- [19] “Mimicking the cellular architecture: Stimuli responsive aqueous/aqueous phase separation in microcapsules.” **Oral presentation** at *ACS Fall* (2022), Chicago, Illinois.
- [20] “Self-degrading organogels: A novel class of lost circulation materials.” **Oral presentation** at *ACS Fall* (2022), Chicago, Illinois.
- [21] “Bio-inspired compartmentalized capsules formed by complex coacervation.” **Oral presentation** at *Polymer Networks Group* (2022), Rome, Italy.

- [22] “Reversible formation and dissolution of inner compartments in microcapsules.” **Oral presentation** at *The International Chemical Congress of Pacific Basin Societies* (2021), Virtual.
- [23] “Mimicking the nucleus: Stimuli-responsive coacervate formation and dissolution in a microcapsule.” **Poster presentation** at *AIChE Annual Meeting* (2021), Boston, Massachusetts.

References

- [1] Winter, H. H. "Polymer Gels, Materials That Combine Liquid And Solid Properties." *MRS Bull.* **1991**, *16*, 44-47.
- [2] Burratti, L.; Proposito, P.; Venditti, I. "Functionalized Gels for Environmental Applications." *Gels* **2023**, *9*, 9100818.
- [3] Malkin, A. Y.; Derkach, S. R.; Kulichikhin, V. G. "Rheology of Gels and Yielding Liquids." *Gels* **2023**, *9*, 9090715.
- [4] Raghavan, S. R.; Douglas, J. F. "The conundrum of gel formation by molecular nanofibers, wormlike micelles, and filamentous proteins: gelation without cross-links?" *Soft Matter* **2012**, *8*, 8539-8546.
- [5] Nath, P. C.; Debnath, S.; Sridhar, K.; Inbaraj, B. S.; Nayak, P. K.; Sharma, M. "A Comprehensive Review of Food Hydrogels: Principles, Formation Mechanisms, Microstructure, and Its Applications." *Gels* **2023**, *9*, 9010001.
- [6] Burey, P.; Bhandari, B. R.; Howes, T.; Gidley, M. J. "Hydrocolloid gel particles: Formation, characterization, and application." *Crit. Rev. Food Sci. Nutr.* **2008**, *48*, 361-377.
- [7] Abdullah; Liu, L.; Javed, H. U.; Xiao, J. "Engineering Emulsion Gels as Functional Colloids Emphasizing Food Applications: A Review." *Front. Nutr.* **2022**, *9*, 890188.
- [8] Skilling, K. J.; Citossi, F.; Bradshaw, T. D.; Ashford, M.; Kellam, B.; Marlow, M. "Insights into low molecular mass organic gelators: a focus on drug delivery and tissue engineering applications." *Soft Matter* **2014**, *10*, 237-256.
- [9] Annabi, N.; Tamayol, A.; Uquillas, J. A.; Akbari, M.; Bertassoni, L. E.; Cha, C.; Camci-Unal, G.; Dokmeci, M. R.; Peppas, N. A.; Khademhosseini, A. "25th Anniversary Article: Rational Design and Applications of Hydrogels in Regenerative Medicine." *Adv. Mater.* **2014**, *26*, 85-124.
- [10] Taylor, M. J.; Tomlins, P.; Sahota, T. S. "Thermoresponsive Gels." *Gels* **2017**, *3*, 3010004.
- [11] Jia, H.; Kang, Z.; Li, S. X.; Li, Y. F.; Ge, J. R.; Feng, D. L. "Thermal degradation behavior of seawater based temporary plugging gel crosslinked by polyethyleneimine for fluid loss control in gas well: Kinetics study and degradation prediction." *J. Dispers. Sci. Technol.* **2021**, *42*, 1299-1310.

- [12] Brown, T. E.; Marozas, I. A.; Anseth, K. S. “Amplified Photodegradation of Cell-Laden Hydrogels via an Addition-Fragmentation Chain Transfer Reaction.” *Adv. Mater.* **2017**, *29*, 201605001.
- [13] Kim, Y. K.; Kwon, Y. J. “Separation and recovery of nucleic acids with improved biological activity by acid-degradable polyacrylamide gel electrophoresis.” *Electrophoresis* **2010**, *31*, 1656-1661.
- [14] Chang, R. X.; Li, N.; Qin, J. L.; Wang, H. J. “Easy degradable polymeric gel with extremely base-labile cross-linking.” *Polymer* **2015**, *60*, 62-68.
- [15] “Polymeric Gels: Characterization, Properties and Biomedical Applications.” in *Polymeric Gels: Characterization, Properties and Biomedical Applications*; Pal, K., Banerjee, I., Eds., 2018; pp 1-555.
- [16] Tanaka, T. “Gels.” *Sci.Am.* **1981**, *244*, 124-&.
- [17] Khan, F.; Atif, M.; Haseen, M.; Kamal, S.; Khan, M. S.; Shahid, S.; Nami, S. A. A. “Synthesis, classification and properties of hydrogels: their applications in drug delivery and agriculture.” *J. Mat. Chem. B* **2022**, *10*, 170-203.
- [18] Han, J.; Sun, J.; Lv, K.; Yang, J.; Li, Y. J. G. “Polymer Gels Used in Oil–Gas Drilling and Production Engineering.” *Gels* **2022**, *8*, 637.
- [19] Vernáez, O.; García, A.; Castillo, F.; Ventresca, M. L.; Müller, A. J. “Oil-based self-degradable gels as diverting agents for oil well operations.” *J. Pet. Sci. Eng.* **2016**, *146*, 874-882.
- [20] Sangeetha, N. M.; Maitra, U. “Supramolecular gels: Functions and uses.” *Chem. Soc. Rev.* **2005**, *34*, 821-836.
- [21] Dowling, M. B.; Lee, J. H.; Raghavan, S. R. “pH-Responsive Jello: Gelatin Gels Containing Fatty Acid Vesicles.” *Langmuir* **2009**, *25*, 8519-8525.
- [22] Burni, F. A.; Xu, W. H.; Spencer, R. G.; Bergstrom, E.; Chappell, D.; Wee, J. K.; Raghavan, S. R. “Self-Degrading Molecular Organogels: Self-Assembled Gels Programmed to Spontaneously Liquefy after a Set Time.” *Adv. Funct. Mater.* **2024**, *34*, 202403617.
- [23] Kuzina, M. A.; Kartsev, D. D.; Stratonovich, A. V.; Levkin, P. A. “Organogels versus Hydrogels: Advantages, Challenges, and Applications.” *Adv. Funct. Mater.* **2023**, *33*, 202301421.

- [24] Ganesh, S.; Subraveti, S. N.; Raghavan, S. R. "How a Gel Can Protect an Egg: A Flexible Hydrogel with Embedded Starch Particles Shields Fragile Objects Against Impact." *ACS Appl. Mater. Interfaces* **2022**, *14*, 20014-20022.
- [25] Zarket, B. C.; Raghavan, S. R. "Onion-like multilayered polymer capsules synthesized by a bioinspired inside-out technique." *Nat. Commun.* **2017**, *8*, 41467.
- [26] Zhou, P.; Regenstein, J. M. "Effects of alkaline and acid pretreatments on Alaska pollock skin gelatin extraction." *J. Food Sci.* **2005**, *70*, C392-C396.
- [27] Guo, L.; Colby, R. H.; Lusignan, C. P.; Whitesides, T. H. "Kinetics of triple helix formation in semidilute gelatin solutions." *Macromolecules* **2003**, *36*, 9999-10008.
- [28] Ahn, S. H.; Rath, M.; Tsao, C. Y.; Bentley, W. E.; Raghavan, S. R. "Single-Step Synthesis of Alginate Microgels Enveloped with a Covalent Polymeric Shell: A Simple Way to Protect Encapsulated Cells." *ACS Appl. Mater. Interfaces* **2021**, *13*, 18432-18442.
- [29] Hilbig, J.; Hartlieb, K.; Gibis, M.; Herrmann, K.; Weiss, J. "Rheological and mechanical properties of alginate gels and films containing different chelators." *Food Hydrocolloids* **2020**, *101*.
- [30] Hijnen, N.; Cai, D. Y.; Clegg, P. S. "Bijels stabilized using rod-like particles." *Soft Matter* **2015**, *11*, 4351-4355.
- [31] Reddy, N. K.; Zhang, Z. K.; Lettinga, M. P.; Dhont, J. K. G.; Vermant, J. "Probing structure in colloidal gels of thermoreversible rodlike virus particles: Rheology and scattering." *J. Rheol.* **2012**, *56*, 1153-1174.
- [32] Borin, D.; Odenbach, S.; Iskakova, L.; Zubarev, A. "Non-ergodic tube structures in magnetic gels and suspensions." *Soft Matter* **2018**, *14*, 8537-8544.
- [33] Arno, M. C.; Inam, M.; Weems, A. C.; Li, Z. H.; Binch, A. L. A.; Platt, C. I.; Richardson, S. M.; Hoyland, J. A.; Dove, A. P.; O'Reilly, R. K. "Exploiting the role of nanoparticle shape in enhancing hydrogel adhesive and mechanical properties." *Nat. Commun.* **2020**, *11*, 41467.
- [34] Thakur, S.; Razavi, S. "Particle Size and Rheology of Silica Particle Networks at the Air-Water Interface." *Nanomaterials* **2023**, *13*, 13142114.
- [35] Burns, N. A.; Naclerio, M. A.; Khan, S. A.; Shojaei, A.; Raghavan, S. R. "Nanodiamond gels in nonpolar media: Colloidal and rheological properties." *J. Rheol.* **2014**, *58*, 1599-1614.

- [36] Endres, S. C.; Ciacchi, L. C.; Mädler, L. “A review of contact force models between nanoparticles in agglomerates, aggregates, and films.” *J. Aerosol. Sci.* **2021**, *153*, 105719.
- [37] Dickinson, E. “Structure and rheology of colloidal particle gels: Insight from computer simulation.” *Adv. Colloid Interface Sci.* **2013**, *199*, 114-127.
- [38] Okesola, B. O.; Vieira, V. M. P.; Cornwell, D. J.; Whitelaw, N. K.; Smith, D. K. “1,3:2,4-Dibenzylidene-D-sorbitol (DBS) and its derivatives - efficient, versatile and industrially-relevant low-molecular-weight gelators with over 100 years of history and a bright future.” *Soft Matter* **2015**, *11*, 4768-4787.
- [39] Stokes, J. R.; Frith, W. J. “Rheology of gelling and yielding soft matter systems.” *Soft Matter* **2008**, *4*, 1133-1140.
- [40] Oza, A. U.; Venerus, D. C. “The dynamics of parallel-plate and cone-plate flows.” *Phys. Fluids* **2021**, *33*, 023102.
- [41] Davies, G. A.; Stokes, J. R. “On the gap error in parallel plate rheometry that arises from the presence of air when zeroing the gap.” *J. Rheol.* **2005**, *49*, 919-922.
- [42] Malkin, A. Y.; Isayev, A. I. *Rheology: Concepts, Methods, and Applications, 3rd Edition*, 2017.
- [43] “Rheology of Biological Soft Matter: Fundamentals and Applications.” in *Rheology of Biological Soft Matter: Fundamentals and Applications*; Kaneda, I., Ed., 2017; pp 1-390.
- [44] Macosko, C. W. J. M.; *Applications Rheology principles*, 1994.
- [45] Weiss, R. G. “The Past, Present, and Future of Molecular Gels. What Is the Status of the Field, and Where Is It Going?” *J. Am. Chem. Soc.* **2014**, *136*, 7519-7530.
- [46] Altay, B. N.; Lewis, C. L. “Rheological Characterization.” in *Standardized Procedures and Protocols for Starch*; Punia Bangar, S., Ed.; Springer US: New York, NY, 2024; pp 145-196.
- [47] Mallia, V. A.; Weiss, R. G. J. S. M. “Correlations between thixotropic and structural properties of molecular gels with crystalline networks.” *Soft Matter* **2016**, *12*, 3665-3676.
- [48] Raghavan, S. R.; Khan, S. A. “Shear-Induced Microstructural Changes In Flocculated Suspensions Of Fumed Silica.” *J. Rheol.* **1995**, *39*, 1311-1325.
- [49] Smith, D. K. “Lost in translation? Chirality effects in the self-assembly of nanostructured gel-phase materials.” *Chem. Soc. Rev.* **2009**, *38*, 684-694.

- [50] Liu, X. Y. “Gelation with small molecules: from formation mechanism to nanostructure architecture.” in *Low Molecular Mass Gelators: Design, Self-Assembly, Function*; Fages, F., Ed., 2005; Vol. 256; pp 1-37.
- [51] Terech, P.; Weiss, R. G. “Low molecular mass gelators of organic liquids and the properties of their gels.” *Chem. Rev.* **1997**, *97*, 3133-3159.
- [52] Wilder, E. A.; Hall, C. K.; Khan, S. A.; Spontak, R. J. “Effects of composition and matrix polarity on network development in organogels of poly(ethylene glycol) and dibenzylidene sorbitol.” *Langmuir* **2003**, *19*, 6004-6013.
- [53] Diehn, K. K.; Oh, H.; Hashemipour, R.; Weiss, R. G.; Raghavan, S. R. “Insights into organogelation and its kinetics from Hansen solubility parameters. Toward a *a priori* predictions of molecular gelation.” *Soft Matter* **2014**, *10*, 2632-2640.
- [54] Liu, S. J.; Yu, W.; Zhou, C. X. “Solvents effects in the formation and viscoelasticity of DBS organogels.” *Soft Matter* **2013**, *9*, 864-874.
- [55] Salonen, A. “Mixing bubbles and drops to make foamed emulsions.” *Curr. Opin. Colloid Interface Sci.* **2020**, *50*, 101381.
- [56] Illy, E.; Navarini, L. “Neglected Food Bubbles: The Espresso Coffee Foam.” *Food Biophys.* **2011**, *6*, 335-348.
- [57] Lovejoy, S.; Gaonac'h, H.; Schertzer, D. “Bubble distributions and dynamics: The expansion-coalescence equation.” *J. Geophys. Res.-Solid Earth* **2004**, *109*, 11203.
- [58] Chatzigiannakis, E.; Veenstra, P.; ten Bosch, D.; Vermant, J. “Mimicking coalescence using a pressure-controlled dynamic thin film balance.” *Soft Matter* **2020**, *16*, 9410-9422.
- [59] Schramm, L. L. *Emulsions, Foams, and Suspensions: Fundamentals and Applications*, 2005.
- [60] Cantat, I.; Cohen-Addad, S.; Elias, F.; Graner, F.; Höhler, R.; Pitois, O.; Rouyer, F.; Saint-Jalmes, A. *Foams: Structure and Dynamics*; Oxford University Press, 2013.
- [61] Choudhary, H.; Raghavan, S. R. “Superfast-Expanding Porous Hydrogels: Pushing New Frontiers in Converting Chemical Potential into Useful Mechanical Work.” *ACS Appl. Mater. Interfaces* **2022**, *14*, 13733-13742.
- [62] Choudhary, H.; Rudy, M. B.; Dowling, M. B.; Raghavan, S. R. “Foams with Enhanced Rheology for Stopping Bleeding.” *ACS Appl. Mater. Interfaces* **2021**, *13*, 13958-13967.

- [63] Koehler, S.; Stone, H. A.; Brenner, M.; Eggers, J. J. P. R. E. “Dynamics of foam drainage.” *Phys. Rev. E* **1998**, *58*, 2097.
- [64] Koehler, S. A.; Hilgenfeldt, S.; Stone, H. A. “A generalized view of foam drainage: Experiment and theory.” *Langmuir* **2000**, *16*, 6327-6341.
- [65] Lee, J. I.; Huh, H. S.; Park, J. Y.; Han, J. G.; Kim, J. M. “Coarsening behavior of bulk nanobubbles in water.” *Sci Rep* **2021**, *11*, 41598.
- [66] Yu, W.; Kanj, M. Y. “Review of foam stability in porous media: The effect of coarsening.” *J. Pet. Sci. Eng.* **2022**, *208*, 109698.
- [67] de Chalendar, J. A.; Garing, C.; Benson, S. M. “Pore-scale modelling of Ostwald ripening.” *J. Fluid Mech.* **2018**, *835*, 363-392.
- [68] Marrucci, G. “A theory of coalescence.” *Chem. Eng. Sci.* **1969**, *24*, 975-985.
- [69] Raut, J. S.; Stoyanov, S. D.; Duggal, C.; Pelan, E. G.; Arnaudov, L. N.; Naik, V. M. “Hydrodynamic cavitation: a bottom-up approach to liquid aeration.” *Soft Matter* **2012**, *8*, 4562-4566.
- [70] Huerre, A.; Miralles, V.; Jullien, M. C. “Bubbles and foams in microfluidics.” *Soft Matter* **2014**, *10*, 6888-6902.
- [71] Li, B.; Zhou, D.; Han, Y. L. “Assembly and phase transitions of colloidal crystals.” *Nat. Rev. Mat.* **2016**, *1*, 15011.
- [72] Cao, Y.; Mezzenga, R. J. N. F. “Design principles of food gels.” *Nat. Food* **2020**, *1*, 106-118.
- [73] Lu, P. J.; Weitz, D. A. “Colloidal Particles: Crystals, Glasses, and Gels.” in *Annual Review of Condensed Matter Physics, Vol 4*; Langer, J. S., Ed., 2013; Vol. 4; pp 217-233.
- [74] Lan, Y.; Corradini, M. G.; Weiss, R. G.; Raghavan, S. R.; Rogers, M. A. “To gel or not to gel: correlating molecular gelation with solvent parameters.” *Chem. Soc. Rev.* **2015**, *44*, 6035-6058.
- [75] Draper, E. R.; Adams, D. J. “Low-Molecular-Weight Gels: The State of the Art.” *Chem* **2017**, *3*, 390-410.
- [76] Zhu, D. Y.; Bai, B. J.; Hou, J. R. “Polymer Gel Systems for Water Management in High-Temperature Petroleum Reservoirs: A Chemical Review.” *Energy Fuels* **2017**, *31*, 13063-13087.

- [77] Hu, J. J.; Chen, Y. H.; Li, Y. Q.; Zhou, Z. J.; Cheng, Y. Y. "A thermo-degradable hydrogel with light-tunable degradation and drug release." *Biomater.* **2017**, *112*, 133-140.
- [78] Kim, U. J.; Isobe, N.; Kimura, S.; Kuga, S.; Wada, M.; Ko, J. H.; Jin, H. O. "Enzymatic degradation of oxidized cellulose hydrogels." *Polym. Degrad. Stab.* **2010**, *95*, 2277-2280.
- [79] Sawhney, A. S.; Pathak, C. P.; Hubbell, J. A. "Bioerodible Hydrogels Based On Photopolymerized Poly(Ethylene Glycol)-Co-Poly(Alpha-Hydroxy Acid) Diacrylate Macromers." *Macromolecules* **1993**, *26*, 581-587.
- [80] Metters, A.; Hubbell, J. "Network formation and degradation behavior of hydrogels formed by Michael-type addition reactions." **2005**, *6*, 290-301.
- [81] Cao, Q. C.; Sun, G. F.; Wang, X.; Yang, F.; Zhang, L. C.; Wu, D. C. "Bioinspired self-degradable hydrogels towards wound sealing." *Biomater. Sci.* **2021**, *9*, 3645-3649.
- [82] Wang, Y.; Liu, D.; Liao, R.; Zhang, G.; Zhang, M.; Li, X. J. C.; Physicochemical, S. A.; Aspects, E. "Study of adhesive self-degrading gel for wellbore sealing." *Colloids Surf A* **2022**, *651*, 129567.
- [83] Zou, C.; Dai, C.; Liu, Y.; You, Q.; Ding, F.; Huang, Y.; Sun, N. J. J. o. M. L. "A novel self-degradable gel (SDG) as liquid temporary plugging agent for high-temperature reservoirs." *J. Mol. Liq.* **2023**, *386*, 122463.
- [84] Liu, Z.; Xu, J.; Peng, W.; Yu, X.; Chen, J. J. P. "The Development and Evaluation of Novel Self-Degrading Loss-Circulation Material for Ultra-Deepwater Drilling in South China Sea." *Processes* **2023**, *11*, 1802.
- [85] Yamasaki, S.; Tsutsumi, H. "The Dependence Of The Polarity Of Solvents On 1,3/2,4-Di-O-Benzylidene-D-Sorbitol Gel." *Bull. Chem. Soc. Jpn.* **1995**, *68*, 123-127.
- [86] Basrur, V. R.; Guo, J. C.; Wang, C. S.; Raghavan, S. R. "Synergistic Gelation of Silica Nanoparticles and a Sorbitol-Based Molecular Gelator to Yield Highly-Conductive Free-Standing Gel Electrolytes." *ACS Appl. Mater. Interfaces* **2013**, *5*, 262-267.
- [87] Oh, H.; Yaraghi, N.; Raghavan, S. R. "Gelation of Oil upon Contact with Water: A Bioinspired Scheme for the Self-Repair of Oil Leaks from Underwater Tubes." *Langmuir* **2015**, *31*, 5259-5264.

- [88] Larson, R. G. *The structure and rheology of complex fluids*; Oxford university press New York, 1999; Vol. 150.
- [89] Klein, D. R. *Organic chemistry*; John Wiley & Sons, 2020.
- [90] Dong, Y. *Direct analysis in real time mass spectrometry: principles and practices of DART-MS*; John Wiley & Sons, 2017.
- [91] Wuts, P. G.; Greene, T. W. *Greene's protective groups in organic synthesis*; John Wiley & Sons, 2006.
- [92] Gaurina-Medjimurec, N.; Pasic, B. "Lost Circulation." in *Risk Analysis for Prevention of Hazardous Situations in Petroleum and Natural Gas Engineering*, 2014; pp 73-95.
- [93] Winn, C.; Dobson, P.; Ulrich, C.; Kneafsey, T.; Lowry, T. S.; Akerley, J.; Delwiche, B.; Samuel, A.; Bauer, S. "Context and mitigation of lost circulation during geothermal drilling in diverse geologic settings." *Geothermics* **2023**, 108.
- [94] Lumb, P. "Drilling and Drilling Fluids." *Eng. Geol* **1982**, 19, 74-75.
- [95] Lyons, W.; Carter, T.; Lapeyrouse, N. J.; Lyons, W.; Carter, T.; Lapeyrouse, N. J. *Drilling Fluids*, 2012.
- [96] Magzoub, M. I.; Salehi, S.; Hussein, I. A.; Nasser, M. S. "Loss circulation in drilling and well construction: The significance of applications of crosslinked polymers in wellbore strengthening: A review." *J. Pet. Sci. Eng.* **2020**, 185.
- [97] Bruton, J. R.; Ivan, C. D.; Heinz, T. J. "Lost circulation control: evolving techniques and strategies to reduce downhole mud losses"; SPE/IADC Drilling Conference and Exhibition, 2001.
- [98] Xu, C. Y.; Zhang, H. L.; Kang, Y. L.; Zhang, J. Y.; Bai, Y. R.; Zhang, J.; You, Z. J. "Physical plugging of lost circulation fractures at microscopic level." *Fuel* **2022**, 317.
- [99] Alhaidari, S. A.; Alarifi, S. A.; Bahamdan, A. "Plugging efficiency of flaky and fibrous lost circulation materials in different carrier fluid systems." *Front. Physics* **2022**, 10.
- [100] Cui, K. X.; Jiang, G. C.; Yang, L. L.; Deng, Z. Q.; Zhou, L. "Preparation and properties of magnesium oxysulfate cement and its application as lost circulation materials." *Pet. Sci.* **2021**, 18, 1492-1506.

- [101] Fang, J. W.; Zhang, X.; Li, L.; Zhang, J. J.; Shi, X.; Hu, G. Q. "Research Progress of High-Temperature Resistant Functional Gel Materials and Their Application in Oil and Gas Drilling." *Gels* **2023**, *9*.
- [102] Davoodi, S.; Al-Shargabi, M.; Wood, D. A.; Rukavishnikov, V. S.; Minaev, K. M. "Synthetic polymers: A review of applications in drilling fluids." *Pet. Sci.* **2024**, *21*, 475-518.
- [103] Halim, M. C.; Hamidi, H.; Akisanya, A. R. "Minimizing Formation Damage in Drilling Operations: A Critical Point for Optimizing Productivity in Sandstone Reservoirs Intercalated with Clay." *Energies* **2022**, *15*.
- [104] Li, Y. X.; Xia, C. Y.; Liu, X. "Water-based drilling fluids containing hydrophobic nanoparticles for minimizing shale hydration and formation damage." *Heliyon* **2023**, *9*.
- [105] Burni, F. A.; Xu, W. H.; Spencer, R. G.; Bergstrom, E.; Chappell, D.; Wee, J. K.; Raghavan, S. R. "Self-Degrading Molecular Organogels: Self-Assembled Gels Programmed to Spontaneously Liquefy after a Set Time." *Adv. Funct. Mater.* **2024**, *34*.
- [106] Yu, G. C.; Yan, X. Z.; Han, C. Y.; Huang, F. H. "Characterization of supramolecular gels." *Chem. Soc. Rev.* **2013**, *42*, 6697-6722.
- [107] Taylor, M. J.; Tomlins, P.; Sahota, T. S. "Thermoresponsive Gels." **2017**, *3*.
- [108] Brown, T. E.; Marozas, I. A.; Anseth, K. S. "Amplified Photodegradation of Cell-Laden Hydrogels via an Addition-Fragmentation Chain Transfer Reaction." *Adv. Mater.* **2017**, *29*.
- [109] Thoresen, K. M.; Hinds, A. A. "A Review of the Environmental Acceptability and the Toxicity of Diesel Oil Substitutes in Drilling Fluid Systems"; IADC/SPE Drilling Conference, 1983.
- [110] Moeinzadeh, S.; Barati, D.; Sarvestani, S. K.; Karaman, O.; Jabbari, E. "Nanostructure Formation and Transition from Surface to Bulk Degradation in Polyethylene Glycol Gels Chain-Extended with Short Hydroxy Acid Segments." *Biomacromolecules* **2013**, *14*, 2917-2928.
- [111] Metters, A. T.; Anseth, K. S.; Bowman, C. N. "A statistical kinetic model for the bulk degradation of PLA-*b*-PEG-*b*-PLA hydrogel networks:: Incorporating network non-idealities." *J. Phys. Chem. B* **2001**, *105*, 8069-8076.
- [112] Philippi, G. T. "On the depth, time and mechanism of petroleum generation." *GCA* **1965**, *29*, 1021-1049.

- [113] Weaire, D. L.; Hutzler, S. *The Physics of Foams*; Clarendon Press, 1999.
- [114] Yu, X. Y.; Jiang, N.; Miao, X. Y.; Li, F.; Wang, J. Y.; Zong, R. W.; Lu, S. X. "Comparative studies on foam stability, oil-film interaction and fire extinguishing performance for fluorine-free and fluorinated foams." *Process Saf. Environ. Protect.* **2020**, *133*, 201-215.
- [115] Yu, W.; Kanj, M. Y. "Review of foam stability in porous media: The effect of coarsening." *J. Pet. Sci. Eng.* **2022**, *208*.
- [116] Hu, X. H.; Cheng, L.; Hong, Y.; Li, Z. F.; Li, C. M.; Gu, Z. B. "An extensive review: How starch and gluten impact dough machinability and resultant bread qualities." *Crit. Rev. Food Sci. Nutr.* **2023**, *63*, 1930-1941.
- [117] Yontz, D. J. *An analysis of molecular parameters governing phase separation in a reacting polyurethane system*; University of Massachusetts Amherst, 1999.
- [118] Andrieux, S.; Quell, A.; Stubenrauch, C.; Drenckhan, W. "Liquid foam templating - A route to tailor-made polymer foams." *Adv. Colloid Interface Sci.* **2018**, *256*, 276-290.
- [119] Kemsley, J. "Bromate in Los Angeles water." *Chem. Eng. News* **2007**, *85*, 9-9.
- [120] Haghghi, E.; Madani, K.; Hoekstra, A. Y. "The water footprint of water conservation using shade balls in California." *Nat. Sustain.* **2018**, *1*, 358-360.
- [121] Anderson, D. M.; Fensin, E.; Gobler, C. J.; Hoeglund, A. E.; Hubbard, K. A.; Kulis, D. M.; Landsberg, J. H.; Lefebvre, K. A.; Provoost, P.; Richlen, M. L.; Smith, J. L.; Solow, A. R.; Trainer, V. L. "Marine harmful algal blooms (HABs) in the United States: History, current status and future trends." *Harmful Algae* **2021**, *102*.
- [122] Yu, X. Y.; Li, F.; Fang, H. S.; Miao, X. Y.; Wang, J. Y.; Zong, R. W.; Lu, S. X. "Foaming behavior of fluorocarbon surfactant used in fire-fighting: The importance of viscosity and self-assembly structure." *J. Mol. Liq.* **2021**, *327*.
- [123] Jeong, S. W.; Jeong, J.; Kim, J. "Simple surface foam application enhances bioremediation of oil-contaminated soil in cold conditions." *J. Hazard. Mater.* **2015**, *286*, 164-170.
- [124] Liang, Y. Y.; Jensen, T. W.; Roy, E. J.; Cha, C. Y.; DeVolder, R. J.; Kohman, R. E.; Zhang, B. Z.; Textor, K. B.; Rund, L. A.; Schook, L. B.; Tong, Y. W.; Kong, H. "Tuning the non-equilibrium state of a drug-encapsulated poly(ethylene glycol) hydrogel for stem and progenitor cell mobilization." *Biomaterials* **2011**, *32*, 2004-2012.

- [125] Naga, N.; Sato, M.; Mori, K.; Nageh, H.; Nakano, T. "Synthesis of Network Polymers by Means of Addition Reactions of Multifunctional-Amine and Poly(ethylene glycol) Diglycidyl Ether or Diacrylate Compounds." *Polymers* **2020**, *12*.
- [126] Kim, M.; Cha, C. "Integrative control of mechanical and degradation properties of in situ crosslinkable polyamine-based hydrogels for dual-mode drug release kinetics." *Polymer* **2018**, *145*, 272-280.
- [127] Khalili, M. H.; Zhang, R. J.; Wilson, S.; Goel, S.; Impey, S. A.; Aria, A. I. "Additive Manufacturing and Physicomechanical Characteristics of PEGDA Hydrogels: Recent Advances and Perspective for Tissue Engineering." *Polymers* **2023**, *15*.
- [128] Zhu, J. M. "Bioactive modification of poly(ethylene glycol) hydrogels for tissue engineering." *Biomaterials* **2010**, *31*, 4639-4656.
- [129] Zou, Y.; Li, D.; Shen, M. W.; Shi, X. Y. "Polyethylenimine-Based Nanogels for Biomedical Applications." *Macromol. Biosci.* **2019**, *19*.
- [130] Kubilay, S.; Demirci, S.; Can, M.; Aktas, N.; Sahiner, N. "Dichromate and arsenate anion removal by PEI microgel, cryogel, and bulkgel." *J. Environ. Chem. Eng.* **2021**, *9*.
- [131] Karlson, B.; Andersen, P.; Arneborg, L.; Cembella, A.; Eikrem, W.; John, U.; West, J. J.; Klemm, K.; Kobos, J.; Lehtinen, S.; Lundholm, N.; Mazur-Marzec, H.; Naustvoll, L.; Poelman, M.; Provoost, P.; De Rijcke, M.; Suikkanen, S. "Harmful algal blooms and their effects in coastal seas of Northern Europe." *Harmful Algae* **2021**, *102*.
- [132] Brooks, B. W.; Lazorchak, J. M.; Howard, M. D.; Johnson, M. V.; Morton, S. L.; Perkins, D. A.; Reavie, E. D.; Scott, G. I.; Smith, S. A.; Steevens, J. A. "Are harmful algal blooms becoming the greatest inland water quality threat to public health and aquatic ecosystems?" *Environmental toxicology and chemistry* **2016**, *35*, 6-13.